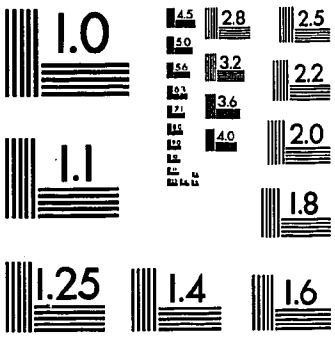

MICROCOPY RESOLUTION TEST CHART
NATIONAL BUREAU OF STANDARDS
STANDARD REFERENCE MATERIAL 1010a
(ANSI and ISO TEST CHART No. 2)

Fisher, Jean Elizabeth Clarke

A QUANTITATIVE STUDY ON THE DEVELOPMENT OF MONKEY SUBTHALAMIC NUCLEUS

City University of New York PH.D. 1985

PLEASE NOTE:

In all cases this material has been filmed in the best possible way from the available copy. Problems encountered with this document have been identified here with a check mark __✓__.

1. Glossy photographs or pages __✓__
2. Colored illustrations, paper or print _____
3. Photographs with dark background __✓__
4. Illustrations are poor copy _____
5. Pages with black marks, not original copy _____
6. Print shows through as there is text on both sides of page _____
7. Indistinct, broken or small print on several pages __✓__
8. Print exceeds margin requirements _____
9. Tightly bound copy with print lost in spine _____
10. Computer printout pages with indistinct print _____
11. Page(s) _____ lacking when material received, and not available from school or author.
12. Page(s) _____ seem to be missing in numbering only as text follows.
13. Two pages numbered _____. Text follows.
14. Curling and wrinkled pages _____
15. Dissertation contains pages with print at a slant, filmed as received _____
16. Other _____

_____

_____

University
Microfilms
International

A QUANTITATIVE STUDY ON THE DEVELOPMENT OF MONKEY SUBTHALAMIC NUCLEUS

by

JEAN ELIZABETH CLARKE FISHER

A dissertation submitted to the Graduate Faculty in Psychology in partial fulfillment of the requirements for the degree of Doctor of Philosophy, the City University of New York.

1985

This manuscript has been read and accepted for the Graduate Faculty in Psychology in satisfaction of the dissertation requirement for the degree of Doctor of Philosophy.

8/20/85
Date

Chairman of Examining Committee

9/5/85
Date

Herbert D. Saltzstein
Executive Officer

Efrain Azmitia, Ph.D.

Doreen Berman, Ph.D.

Richard Bodnar, Ph.D.

Wha Yu, Ph.D.

The City University of New York

Abstract

A QUANTITATIVE STUDY ON THE DEVELOPMENT OF THE MONKEY SUBTHALAMIC NUCLEUS

by

Jean E. Fisher

Adviser: Professor Pedro Pasik

The first four postnatal months encompass significant changes in the motor behavior of the macaque. The purpose of this study is to provide normative data on the development of the monkey subthalamic nucleus during this period. This structure is in a position to modulate the outflow of the basal ganglia which in turn exert a powerful influence on movement control. In addition, this work addresses the controversy regarding the number and distribution of subthalamic cell types.

Total volumes of subthalamic nuclei were found not to change significantly. Mean cross-sectional area of neuronal somata decreased by 33% during the period of study. Cluster analysis indicated the existence of two cells populations differing in size and location allowing the subdivision of the nucleus into a magnocellular and a parvocellular segment.

The proportion of the subthalamic nucleus occupied by neuropil decreased by 25% from birth to 17 weeks. Lengths of synaptic profiles were reconstructed by computer-assisted stereologic analysis to produce the distribution of synaptic plaque sizes. These data were used to determine

partial densities, total density and the estimated total number of synapses at each age. A significant decrease in synapses occurred for both mature and immature contacts. This synapse elimination process was particularly marked after the first month.

Results indicate that there are substantial changes in the subthalamic nucleus during the first four postnatal months. An important feature is the marked reduction of synapses. In addition, there are significant differences in size and location of two populations of cells which are found at all postnatal ages studied. This finding correlates well with known topologic differences in the extrinsic connections of the structure. It is posited that the morphological reorganization of the subthalamic nucleus during the first four months of postnatal life contributes to the maturation of movement in the macaque.

Acknowledgements

This dissertation could not have been undertaken, much less completed, without the help and support of Faculty, family, and friends. My deepest thanks go to Dr. Pedro Pasik, an outstanding teacher and scientist, who directed every aspect of this work, to Dr. Tauba Pasik who taught me the skills of light and electron microscopy and who, in addition, evaluated every synapse used in this study, and to their son, Alexander Pasik, who devised the computer program which permitted the analysis of the synapse data. In addition, I owe a debt of gratitude to Marilyn Ilvento and Victor Rodriguez for the vast amount of technical support they gave me. The latter, in particular, consistently produced micrographs of the highest quality.

Additional thanks, no less heartfelt, go to Dr. Michael Gottlieb who taught me that serious work could be done with a light heart, to Dr. Margaret Hallissy who read and commented on the literature review, to the members of my Committee who included, in addition to Dr. Pedro Pasik, Drs. Efrain Azmitia, Doreen Berman, Richard Bodnar and Wha Yu, to Frank Bednarski who devoted many evening hours to reading this work and discussing it with me, to Dr. Charline Sacks who offered encouragement at every step of the way and to members of the Research Computing Unit of the Department of Biomathematical Sciences who answered untold computing questions.

Finally, blessings on those without whose love and support this endeavour would not have been possible: Dr. Clark Fisher, Timothy Fisher, CDR James V. Clarke USNR-R, Joan Clarke, James J. Clarke and Esther Clarke.

Table of Contents

List of Tables

List of Figures

CHAPTER I

Introduction

During the early postnatal period in primate, the brain grows rapidly and is particularly susceptible to injury by toxins, infection, and metabolic factors in a way which is not true of the adult (Courville, 1971). Both the cerebral cortex and basal ganglia are especially affected by reduction in oxygenation of the blood. Among the behavioral sequelae of this type of perinatal insult are motor alterations which include a juvenile form of parkinsonism, athetosis, choreo-athetosis, rigidity and torsion spasm. The motor disabilities may change in kind and/or increase in severity into adolescence. The late appearance of movement disorders and their seeming progression may be due more to the postnatal maturation of the central nervous system, which alters the pattern of the clinical picture, than to the actual progression of the pathologic process (Marsden, 1976). Post-mortem examinations reveal a variety of lesions or anatomical abnormalities associated with the developmental motor dysfunction. Among these are cortical cysts, atrophy of cortex or basal ganglia, and/or status marmoratus, a condition characterized grossly by the appearance of marbling in the basal ganglia, and microscopically by neuronal loss and gliosis (Dekaban, 1970; Smith, 1974). These alterations have been reproduced experimentally in monkeys by induction of fetal hypoxia followed by anoxia (Myers, 1975).

Any correlation of motor dysfunction with changes in particular components of the basal ganglia during development depends upon an accurate determination of the normal maturational sequences of these structures. Such information is particularly necessary in order to assess the effect of insult upon development. Without knowledge of the normal state of components of the basal ganglia during development, neither the direct nor the indirect effects of perinatal insult can be correctly determined. Systematic quantitative information of this kind is scanty for primates. Developmental studies have centered on the telencephalic and mesencephalic nuclei, especially those which are directly involved in Parkinson's Disease in the adult, while the diencephalic component of the basal ganglia system, the subthalamic nucleus, has received comparatively little attention. This is probably because the subthalamic nucleus is a structure which, although particularly well defined in primates (Whittier and Mettler, 1949), is relatively inaccessible. It lies deep within the diencephalon and direct manipulation frequently affects the fiber bundles within which the nucleus is lodged. The results of early studies gave little impetus to further investigation despite the fact that both experimental lesions in monkey and destruction due to infarct in humans yield a highly reproducible motor defect, choreoid hyperkinesia in monkey and hemiballismus in man (Carpenter and Carpenter, 1951). Within the recent past, however,

clinical and anatomical findings have increased the interest in the subthalamic nucleus. Lesions of this structure have been implicated, for example, in rigidity associated with perinatal trauma (Courville, 1971). Moreover, anatomical studies, to be reviewed below, place this structure in a position to modulate the outflow of the entire basal ganglia system which, in turn, exerts a powerful influence on motor control.

The purpose of this study is to provide quantitative information on the development of the subthalamic nucleus in primate, obtained at both the light and electron microscopic levels. It is hoped that this will permit the correlation of the sequence of maturation with synchronous development of appropriate motor responses. In addition, this work addresses a controversy with regard to the number and distribution of cell types within the nucleus. This question is related to the recently discovered regional differences in subthalamic afferents and efferents.

CHAPTER II

Review of the Literature

The Development of Movement in the Macaque

Hines (1942) described the maturation of motor function in macaques after observation and extensive testing of 31 infant monkeys, and found that within the first three months after birth, the monkey progresses from a condition of complete dependence on its mother to one of relative freedom. This process involves the replacement of many reflexes with coordinated, purposeful movement.

Reflexes

During the first four months of life, the reaction of the infant monkey to elicitation of the superficial reflexes is quite variable. An adult response either to scratching the lateral border of the sole (plantar reflex) or of the ulnar border of the palm (palmar reflex) is not achieved until the fifth or sixth postnatal month. The grasp reflex in response to pressure on the palms is present at birth but disappears by 10 weeks; at this time, the Hoffman reflex, flexion of thumb and digits in response to tweaking of the terminal phalanges of the middle digits, also achieves its adult form. In general, during the first postnatal weeks, deep tendon reflexes exhibit a briskness and radiation to adjacent musculature which subsequently regresses. The order of this process varies between muscle groups.

Hines (1942) also tested monkeys on their ability to execute coordinated movements of the extremities after

external stimulation. Among these actions are the placing of the extremities in response to tactile or visual stimuli, stepping and hopping when the muscles of the extremities are stretched, and compensatory adjustments to dropping through the air. Adult placing occurs by the fourth week, with the response to visual stimuli preceding that to tactile stimulation. Stepping has a variable course, with forward and lateral stepping appearing within the first three weeks, but posterior stepping only after the fifth week. While the initial response to dropping is seen as early as two to three weeks postnatally, adequate preparation for landing does not occur until the monkey is between four and six months old.

Posture

The typical orientation of the newborn monkey is with its ventral surface upward, as it clings to its mother. If it is placed back down on a surface, an infant of up to six weeks of age will right itself by hyperextension of the head and trunk. However, as Harlow and Harlow (1965) indicate, an infant monkey will refuse to right itself if it is given the opportunity to grasp. In the early weeks, therefore, infantile grasping usually directed toward the mother supersedes the righting reflex. During the seventh through sixteenth weeks, the macaque placed on its back will turn over by quickly rolling to the side. By the seventeenth week, it achieves the adult pattern of righting itself by flexion of the trunk.

If the newborn monkey is placed on its stomach, it sprawls. However, within two weeks, the monkey is able to crouch (Hines, 1942). Thereafter, it develops an upright posture in which there are six contact points: the sitting pads, the heels, and the hands. Between four and eight weeks, the monkey may sit solely on the volar surfaces of the feet, occasionally with support of the tail. An adult sitting posture, on feet alone, is not completely achieved until the end of the first year.

Standing is first observed in the monkey within the first two postnatal weeks. Initially, it is wide-based and precarious. It approaches the adult pattern at 10 weeks and reaches it by 12-15 weeks.

Progression

Harlow and Harlow (1965) noted that the infant monkey is not purely a reflexive creature within the first three weeks of postnatal life. In fact, between the tenth and twentieth day, monkeys achieve purposeful locomotion, in both the horizontal and vertical planes (climbing), with progression requiring alternating flexion and extension. This appears in the young infant as reaching and grasping, supplanted during the third through fifth weeks by a relatively exaggerated reach and placement and, during the tenth to sixteenth postnatal weeks, by the adult reaching and placement.

In the vertical plane, the initial movements are reaching and grasping. This is superseded by an easy grasp

movement which can be released to allow the climbing animal to back down. Finally, by five to eight weeks of age, the monkey is able to turn around in the vertical plane. Galloping, the movement which involves simultaneous, rather than alternating, flexion and extension, occurs between six and twelve weeks. Jumping in the vertical plane begins in the fifth postnatal week, whereas its more difficult form, jumping across a gap, does not develop until the eighth week.

Spontaneous Movement

Simonds (1974) noted that the reflex grasping which ties the infant to its mother is replaced between the tenth and twentieth postnatal days by coordinated motor control which allows the infant to break contact with its mother and then to regain it. Hines (1942) observed that initial spontaneous movements are synergistic, with the movement originating proximally and proceeding invariably down to the extremity. Complex patterns of movement, as for example rhythmic movement during nursing, develop and regress in the first weeks. In its adult form, spontaneous movement requires both fixation of the trunk, which does not occur until the fourth to sixth postnatal weeks, as well as fixation of the proximal extremities. Thus, for example, manual manipulation is seen, at first, as pawing at an object. During the second to third weeks, the monkey may pick at the object, and by the eighth week is able to pick it up. Manipulation improves substantially between the

third and fifth postnatal weeks (Mason, 1965). From then until the eleventh week, as postural fixation is achieved, the monkey develops the ability to initiate an action distally, and selectively with regard to the appropriate musculature.

Table 1 summarizes the above findings on the development of movement in the macaque during the first year. It is apparent that during the first four months of postnatal life, which is the period under consideration in this study, most of the features of motor development reach maturity. Such features include stepping, placing, vertical progression and jumping, the grasp and Hoffman reflexes, spontaneous movement, standing, galloping, righting and horizontal progression. Other forms of motor function, such as hopping, palmar and plantar reflexes and sitting, achieve adult form only by six months of age. It is clear, therefore, that full maturation extends beyond the period of observation of the present investigation.

Morphologic Substratum of Motor Function

The development of motor responses is based on the morphological maturation of the various structures related to movement. The neuroanatomical pathway for voluntary movement involves the corticospinal tract which is influenced by both the cerebellum and basal ganglia system through the thalamus (Carpenter, 1985). The basal ganglia system consists of a group of subcortical nuclei the function of which may be conceptualized as focussing and

Table 1

Development of Movement in the Macaque
(data from Hines, 1942)

Postnatal Weeks

	1	2	3	4	5	6	7	8	9	10	11	12	13	14	15	16	17	18	19	20	...	26+
Reflexes:																						
Grasp										M	M	M	M	M	M	M	M	M	M	M	M	M
Hoffman										M	M	M	M	M	M	M	M	M	M	M	M	M
Palmar																						M
Plantar																						M
Tendon	(variable)																					
Stepping				M	M	M	M	M	M	M	M	M	M	M	M	M	M	M	M	M	M	M
Placing					M	M	M	M	M	M	M	M	M	M	M	M	M	M	M	M	M	M
Standing												M	M	M	M	M	M	M	M	M	M	M
Righting																	M	M	M	M	M	M
Sitting																						M
Progression:																						
Vertical								M	M	M	M	M	M	M	M	M	M	M	M	M	M	M
Jumping								M	M	M	M	M	M	M	M	M	M	M	M	M	M	M
Galloping												M	M	M	M	M	M	M	M	M	M	M
Horizontal																	M	M	M	M	M	M
Spontaneous Movement										M	M	M	M	M	M	M	M	M	M	M	M	M

M indicates mature behavior.

Vertical dotted line represents the limit of the present study.

facilitating motor behaviors generated by the cerebral cortex, and as suppressing conflicting actions (Penny and Young, 1983). These nuclei include the two striatal components, the caudate and putamen; the outflow element, the globus pallidus; and other nuclei: the subthalamic nucleus, the substantia nigra, and the pedunculopontine nucleus, which participate in loop connections with the previous structures (Carpenter, 1985). The interactions among these nuclei, as well as with the thalamus and cortex, are complex and involve several loops. At its simplest, the role of the basal ganglia may be to influence the excitatory reciprocal connections between cortex and two thalamic nuclei, the ventral anterior nucleus (VA) and the ventral lateral nucleus (VL) (Penney and Young, 1983). This is done primarily through disinhibition. The cerebral cortex excites the striatum (Purpura, 1975) which in turn inhibits the medial segment of the globus pallidus and the substantia nigra, pars reticulata (Purpura, 1975), both of which are inhibitory to the VA and VL nuclei of the thalamus (McKenzie, 1985). The subthalamic nucleus, with its reciprocal connections with the globus pallidus (van der Kooy, Hattori, Shannak and Hornykiewicz, 1981) and projection to the substantia nigra (Kanazawa, Marshall and Kelly, 1976), has the anatomical connections which would allow it to modulate the output of the system. The connectivity of the subthalamic nucleus with cortex, basal

ganglia, and other brain structures will be discussed in detail further below.

It is known that perinatal insult to the brain can produce a variety of movement disorders which apparently change with postnatal maturation of the central nervous system. Extensive studies have been made of the development of cerebral cortex and of one of the two major influences on cortical output, the cerebellum. See, for example the work of Armstrong-James and Johnson (1970), Del Cerro and Snider (1968), Gruner (1970) and Hamori and Somogyi (1983). Comparatively little attention has been paid to the development of the basal ganglia, particularly in primate. However, patterns of morphological and physiological development have been identified in some species; these will be discussed below.

Development of the Basal Ganglia System

Neostriatum

Brand and Rakic (1979) identified the time of origin of monkey neostriatal neurons by exposing monkeys in utero to tritiated thymidine on various prenatal days. The infants were sacrificed between two and five months postnatally and their brains processed for autoradiography. Heavily labelled cells were considered to have completed their final divisions by the day of injection, and lightly labelled cells to have divided at least once more thereafter. Two groups of cells were found which differ in size and time of neurogenesis. During the normal gestational period of the

monkey, which is approximately 168 days (Altman and Dittmer, 1964), production of large cells is limited to embryonic days 36-43 (E36-E43) while small cells are produced during days E36-E80. There is no evidence for postnatal neurogenesis in the primate basal ganglia.

The course of postnatal development of the monkey neostriatum has been studied systematically at the light and electron microscopic levels by DiFiglia, Pasik and Pasik (1979, 1980). They found that the cell types, identifiable in the adult monkey on the basis of size and presence of dendritic spines, are present in the first postnatal week, as are immature cells which are difficult to categorize. At this time, most neurons show signs of immaturity such as growth cones and filopodia. Of the efferent cells, those believed to be excitatory mature before those considered to be inhibitory. Further, the former show a decline whereas the latter exhibit a progressive increase in spine density during the first postnatal months. Neostriatal interneurons pass through a spiny period before reaching aspiny maturity.

At the electron microscopic level, the developmental features identified in Golgi stained material, such as growth cones and filopodia, are recognizable. Further, degenerating axons are seen in monkeys up to eight weeks of age. In addition, there are age related changes in the vesicle composition of presynaptic terminals and in the distribution of synaptic types. Quantitatively, the density of synapses within the neostriatal neuropil increases

between one week and adulthood. However, the distribution of synapses is altered in that axodendritic contacts decrease during this period whereas those between axons and dendritic spines increase.

It is apparent that the early postnatal period in monkey is one of reorganization within the neostriatum (DiFiglia et al., 1980). This is also true of other species. Electron microscopy of kitten neostriatum shows changes in the number of vesicles within terminals, in relative proportion of symmetric synapses, as well as in the number of dendritic spines (Adinolfi, 1977; Hull, McAllister, Levine and Adinolfi, 1981). Further, the distribution of the spines is altered during the first 20 postnatal weeks such that the density on distal dendrites increases while that on the proximal dendrites decreases (Hull et al., 1981). Hull et al., (1981) suggested that the anatomical maturation which they observed in kitten is related to known physiological changes during the first postnatal months. For example, only by the end of the second month, the proportion of cells responding to cortical stimulation is equivalent to that seen in the adult cat. Further, a marked decrease in latency of response has occurred as well as an increase in the ability of cells to follow electrical pulses delivered to the cortex. Finally, in puppy neostriatum, the density of corticostriatal synapses is approximately 30% of that observed in the adult dog (Tanaka, Gorska and Dutkiewicz, 1980) and, in rat,

there is an increase in asymmetric synapses by terminals containing round vesicles, particularly during the third postnatal week (Hattori and McGeer, 1973).

Globus Pallidus

Studies of postnatal development of both neurons and connectivity, similar to those done in neostriatum, have been undertaken in the pallidal complex of non-primate mammals. There are differences in the frequency of occurrence of different types of nerve endings in kitten and in cat. In addition, there are increases in the numbers of axodendritic and asoxomatic contacts during the first two postnatal weeks (Adinolfi, Levine and Hull, 1980). In kitten, 70% of pallidal neurons responding to caudate stimulation are initially excited; with increasing age, this response is replaced by excitation and inhibition, or by inhibition alone. Further, the latency of response decreases and the temporal correlation between stimulus and response increases with age (Levine, Cherubini, Novack, Hull and Buchwald, 1979). Adinolfi et al. (1980) suggested that their morphological studies support physiological evidence for a functional striopallidal pathway at birth and that physiological changes reflect increases in axodendritic connectivity.

Substantia Nigra

In a study of the substantia nigra in kitten, Phelps, Adinolfi and Levine (1983) characterized a growth process in nigral neurons. At an early stage, the neuropil contains

immature dendrites with prominent varicosities and filiform processes along the shaft as well as growth cones at the dendritic tips. As was the case with the neostriatal neurons, the nigral cells which are aspiny in the adult exhibit spines during a brief, early period of development. By 40-55 days postnatally, most dendrites within the substantia nigra are smooth. Dendritic length, measured in the pars compacta, increases by 42% from birth. Thin neostriatal axons are observed in the kitten, from birth, as are thicker axons, probably of subthalamic origin. Striatal and cortical stimulation, as well as somatosensory stimuli elicit age related nigral responses (Fisher, Levine, Hull and Buchwald, 1982). The initial response can be either excitatory or inhibitory in kitten, whereas it is inhibitory in the adult cat. These authors also noted that the response latency decreased with age.

Summary

In summary, most of the major components of the basal ganglia system display age-related changes in morphology and physiology during the early postnatal period. In the case of the subthalamic nucleus, although young animals have been studied, systematic analyses of the age-related changes in morphology and physiology of this structure have not been reported.

Anatomy of the Subthalamic Nucleus

Anatomical studies of the subthalamic nucleus have been undertaken in a wide variety of mammals and at different

ages. These include mouse and rabbit (Ramon y Cajal, 1911), rat (Ramon y Cajal, 1911; Kanazawa, Marshall and Kelly, 1976; Carter and Fibiger, 1978), kitten (Ramon y Cajal, 1911; Iwahori, 1978), cat (Nauta and Cole, 1978), adult monkey (Rafols and Fox, 1978; Yelnik and Percheron, 1980) and human (Whittier and Mettler, 1949; Yelnik and Percheron, 1980). These studies indicate that there are a number of aspects of cellular morphology and of connectivity which are similar across ages and species.

Gross Morphology of the Subthalamic Nucleus

The subthalamic nucleus is located within the diencephalon, medially adjacent to the internal capsule. The nucleus has the shape of a biconvex lens and, at its largest intersecting plane lies at a 45 degree angle to the midline of the brain (Whittier and Mettler, 1949). As Figure 1 shows, the lateral border of the subthalamic nucleus is well defined by the internal capsule, the dorsal surface by the fibers of the lenticular fasciculus and its ventral surface by the substantia nigra. The medial aspect of the nucleus is less well demarcated. Rostrally, the nucleus borders on the hypothalamus and, more caudally, on the tegmental nuclei.

Neuronal Types

With the light microscope, neurons within the subthalamic nucleus are seen to be either fusiform, triangular, or polygonal (Ramon y Cajal, 1911), are relatively large and without discrete Nissl bodies (Whittier

Figure 1. Micrographs of adult monkey brain.

Top: photograph of a coronal section from the brain of an adult monkey (Macaca mulatta) at mid-rostrocaudal extent of the subthalamic nucleus. Arrow indicates the subthalamic nucleus, ringed arrow the substantia nigra, and crossed arrow, the zona incerta. Scale: 5 mm.

Bottom: enlarged area of the right subthalamic nucleus of the same animal. Note the higher cell density in the ventromedial area. Scale: 1 mm.

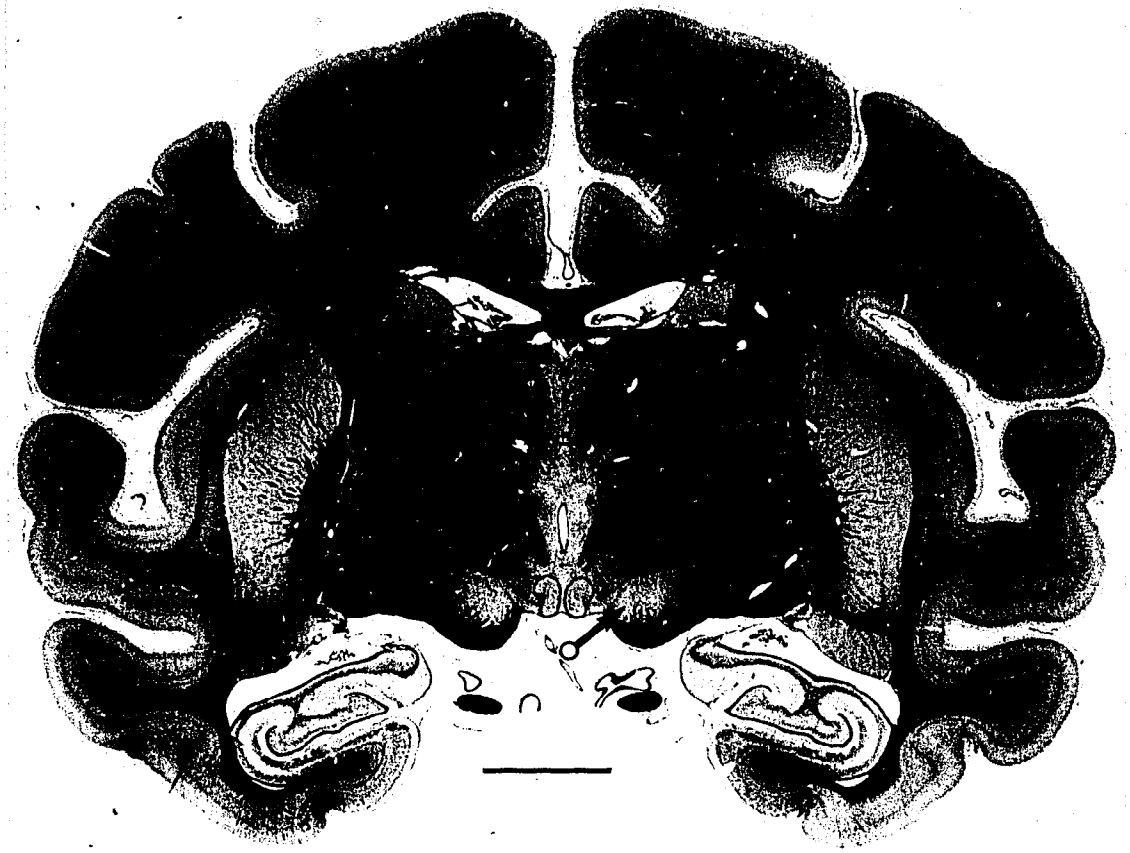

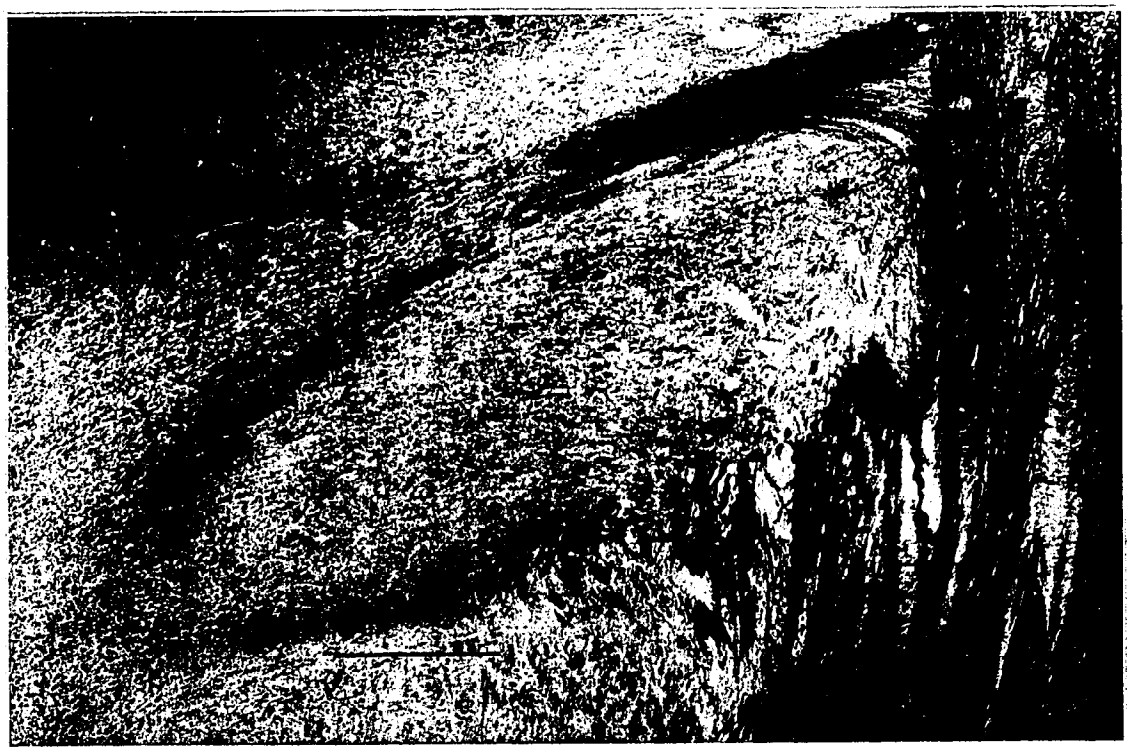

and Mettler, 1949). They have spines which are concentrated on the trunks and proximal portions of the dendrites (Rafols and Fox, 1976).

Those who distinguish several cell types within the nucleus do so on the basis of cell size, dendritic conformation and axonal morphology (Iwahori, 1978; Kita, Chang, and Kitai, 1983; Rafols and Fox, 1976; Ramon y Cajal, 1911). Yelnik and Percheron (1979) contended, however, that the size differences which have led others to report the existence of several cell types within the nucleus are artifactual. In a Golgi study of human and monkey brain, entire neurons were reconstructed from serial sections in three dimensions. Orthogonal rotation of these reconstructions revealed that the shape of the neurons with their entire dendritic trees varied with the plane of section. Thus, cells which might appear to be small cells in coronal section, may be seen to be large cells when viewed orthogonally. As a result of this study, Yelnik and Percheron (1979) concluded that there is only one cell type within the subthalamic nucleus.

At the electron microscopic level the most commonly identified cell is characterized by a pale, deeply invaginated nucleus (Rafols and Fox, 1976; Chang, Kita and Kitai, 1983). In rat and monkey, there is little rough endoplasmic reticulum; this conforms to the light microscopic observation of paucity of discrete Nissl bodies. However, formation of these organelles is observed in the

baboon (Hassler, Usunoff, Romansky and Christ, 1982). In this species, the cytoplasm contains abundant mitochondria and Golgi apparatus. There are numerous lysosomes as well and, in adult animals, lipofuscin granules. A second cell type consists of small neurons which have a thin rim of cytoplasm and few organelles (Rafols and Fox, 1976). Kita et al. (1983) distinguished the second neuronal type on the basis of axonal morphology and presence of intranuclear rodlets.

Subthalamic Neuropil

In rat, the neuropil of the subthalamic nucleus contains many thin dendrites, a few thicker dendritic stalks and a large number of myelinated axons (Chang et al., 1983). Dendrites have few spines and none are observed to contain vesicles. Hassler et al. (1982) reported the existence of nine synaptic types in the baboon, basing this attribution on the size and shape of presynaptic and postsynaptic elements as well as on vesicle shape and synaptic symmetry. Other authors are more conservative. Chang et al. (1983) reported three types of axon terminals. The first, 0.2 to 1 micrometers in diameter, are packed with round vesicles and make asymmetrical contacts with thin dendrites and spines. These correspond to three elements of Hassler's classification and are similar to cortical afferents to the striatum. The second, up to five times the size of the first, contain round and flattened vesicles and make symmetric contact with somata and thick dendrites as well as

with somal and dendritic spines. These are also shown by Hassler et al. (1982) in the baboon and are like terminals of pallidal origin (Usunoff, Hassler, Romansky, Wagner, and Christ, 1982). It should be noted that synapses of pallidal terminals form symmetric contacts with subthalamic neurons (van der Kooy et al., 1981). The third type, which were probably tangentially sectioned, are of intermediate size and vesicle morphology. The thin intrinsic collaterals of subthalamic efferent neurons have small terminals which contain oval vesicles and have not yet been definitively assigned to any of the three categories by Chang et al. (1984). These subthalamic terminals make synaptic contact with dendritic shafts of subthalamic neurons (Chang et al., 1984).

Afferentation

Lateral pallidal segment.

In primate, the main source of afferents to the subthalamic nucleus is the lateral pallidal segment (Carpenter, Fraser, and Shriver, 1968; Carpenter and Strominger, 1967; Nauta and Mehler, 1966). In carnivores and rodents, this structure is referred to as the globus pallidus, whereas the medial pallidal segment is called the entopeduncular nucleus. Autoradiographic and degeneration studies in the monkey show the pallidosubthalamic projection to be topologically organized (Carpenter, Batton, Carleton and Keller, 1981a; Carpenter et al., 1968). Figure 2 shows that this projection is such that the rostral portion of the

Figure 2. Afferents to the subthalamic nucleus in monkey (modified from Carpenter, 1968). The plane of section is horizontal. AC, anterior commissure. III, third ventricle. Cx, cerebral cortex. GPe, external segment of the globus pallidus. GPi, internal segment of the globus pallidus. IC, internal capsule. Cm-Pf, centremedian-parafascicular complex of the thalamus. H2, H2 Field of Forel. PPN, pedunculopontine nucleus. SN, substantia nigra. LG, lateral geniculate nucleus. Dashed lines within the subthalamic nucleus subdivide it into medial and lateral regions.

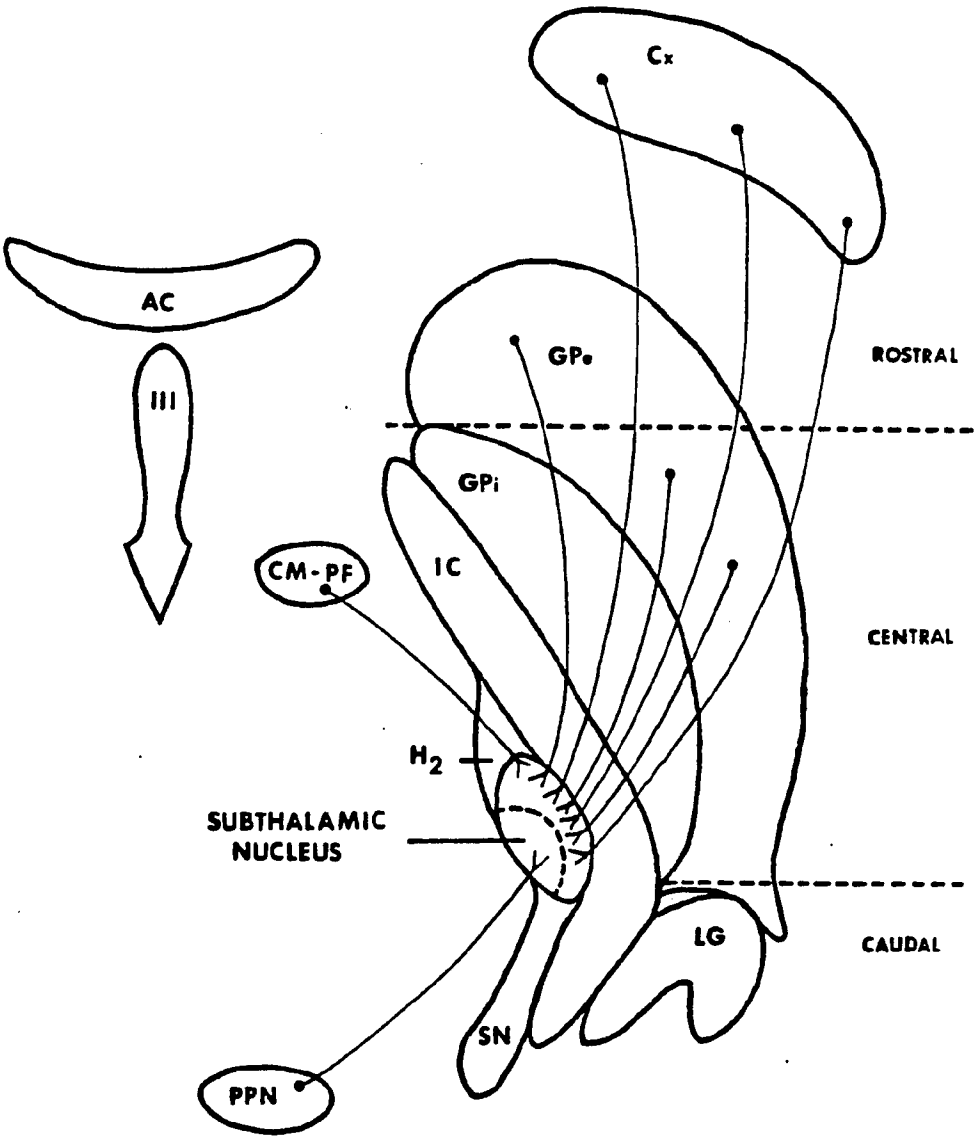
Cx
AC
III
GPe
ROSTRAL
GPi
IC
CM-PF
CENTRAL
H2
SUBTHALAMIC
NUCLEUS
LG
CAUDAL
SN
PPN

lateral pallidal segment projects to the medial two-thirds of the rostral subthalamic nucleus as well as to the middle third of that structure. The major central portion of the lateral pallidal segment projects to the lateral third of the subthalamic nucleus almost entirely along its rostrocaudal dimension. An electrophysiological study of the rat subthalamic nucleus found that stimulation of the rostromedial globus pallidus inhibits the medial subthalamic nucleus, the caudomedial pallidum affects the central region of the nucleus, and the lateral portion of the pallidum inhibits cells in the lateral part of the nucleus (Rouzaire-Dubois, Hammond, Yelnik and Feger, 1984).

Regional differences in the projection of the pallidum upon the subthalamic nucleus have also been noted biochemically. Both glycine (van der Kooy et al., 1981) and GABA (Feger, 1981; Rouzaire-duBois, Hammond, Hamon and Feger, 1980) have been suggested as possible neurotransmitters in the inhibitory pallidosubthalamic pathway. There is a mediolateral concentration gradient in the distribution of glutamic acid decarboxylase (GAD), the synthesizing enzyme for GABA, within the subthalamic nucleus, with the greatest concentration found medially (Fonnum, Grofova and Rinvik, 1978). Regional differences in afferentation may be of greater importance in primate or in cat than in rat since it is estimated that the dendritic field of the subthalamic neuron covers only one-fifth of the

nucleus in monkey whereas it encompasses the entire structure in rat (Hammond and Yelnik, 1983).

Cortex.

In monkey, primary motor cortex (area 4) projects somatotopically on the dorsal subthalamic nucleus (Hartman-von Monakow, Akert and Kunzle, 1979). The projection is organized in such a manner that the face, arm, and leg are represented sequentially from the lateral region of the subthalamic nucleus to the medial aspects of that structure. Ablation of precruciate cortex in cat (Auer, 1956), of prefrontal cortex in pig-tailed macaques (DeVito and Smith, 1964), and lesions of motor cortex, Brodmann's areas 4 and 6 in rhesus monkey (Petras, 1965), result in fiber degeneration in the subthalamic nucleus. Injection of tritiated proline into cortical area 8 in Macaca fascicularis produces a low level of labelling in the subthalamic nucleus (Kunzle and Akert, 1977). At the electron microscopic level, moderate degeneration in fibers and terminal boutons is found in the subthalamic nucleus of cat ipsilateral to ablated sensorimotor cortex (Romansky, Usunoff, Ivanov and Galabov, 1979). Cortical efferents are seen to be either thinly myelinated or unmyelinated. The small terminals contain round vesicles and make asymmetrical synapses on spines or small dendrites. Physiological support for a corticosubthalamic connection in rat is assumed by excitatory electrical activity in the subthalamic nucleus as the result of cortical stimulation (Kitai and

Deniau, 1981), and by short latency, cortically dependent responses in the lateral third of the subthalamic nucleus to contralateral vibrissal or bodily stimulation (Hammond, Deniau, Rouzaire-Dubois and Feger, 1978). In this latter study, however, topological correspondence between the body part stimulated and the location of the cells excited within the subthalamic nucleus was not observed.

Striatum.

A direct striosubthalamic pathway has been proposed on the basis of short-latency activation of the subthalamic nucleus by striatal stimulation in monkey (Ohye, LeGuyader and Feger, 1976). In cat, a study using anterograde transport of conjugates of wheat germ agglutinin and horseradish peroxidase (HRP) revealed a reciprocal axonal connection between the striatum and subthalamic nucleus (Beckstead, 1983).

Pedunculopontine nucleus.

A projection from the pedunculopontine nucleus to the subthalamic nucleus has been demonstrated by retrograde transport of HRP in monkey (Rinvik, Grofova, Hammond, Feqer and Deniau, 1979) and by anterograde transport of tritiated amino acids in cat (Nomura, Mizuno and Sugimoto, 1980).

Thalamus.

Tritiated leucine and tritiated proline injected into the centre median-parafascicular (CM-PF) complex of the thalamus in cat and in rat stain the ipsilateral subthalamic nucleus, particularly at the rostral pole, and outline the

rostral borders of the nucleus. Less labelling is observed in the middle part of the nucleus and it is absent in the caudal pole. Injection of HRP into the subthalamic nucleus results in retrograde labelling of cells in the CM-PF complex (Sugimoto, Hattori, Mizuno, Itoh, and Sato, 1983). Light and electron microscopic study of material treated with tritiated amino acids indicates that the thalamo-subthalamic terminals contain round vesicles and make asymmetric synaptic contacts (Sugimoto et al, 1983).

Other sources.

Catecholamine-containing axons and varicosities have been found throughout the subthalamic nucleus in rat (Brown, Makman, Wolfson, Dworkin, Warner and Katzman, 1979), and appear to contain dopamine. In addition, flourescent cell bodies within the caudal subthalamic nucleus, spectrally characterized as dopaminergic, are aligned rostrocaudally with similar cells in the substantia nigra, pars reticulata. Dopamine-containing terminals and varicosities are found throughout the cat subthalamic nucleus. However, it has not been determined whether these terminals originate from the nigrostriatal pathway or from the dopaminergic cells found in the caudal subthalamic nucleus and substantia nigra, pars reticulata (Meibach and Katzman, 1979). Labelled cells in the substantia nigra appear after injection of HRP into the subthalamic nucleus. It should be noted that stained neurons are also seen in the locus coeruleus, suggesting a noradrenergic innervation of the subthalamic nucleus (Rinvik

et al., 1979). Serotoninergic input from the median raphe nucleus has been indicated both autoradiographically (Bobillier, Seguin, Petitjean, Salvert, Touret and Jouvet, 1976) and biochemically (Palkovits, Brownstein and Saavedra, 1976).

Efferentation

Globus Pallidus.

Early studies have shown that the medial pallidal segment is a major target for subthalamic efferents (Whittier and Mettler, 1949). A restricted projection from the subthalamic nucleus solely to the medial pallidal segment has recently been identified in which the efferent cells are located in the medial subthalamic nucleus and in the caudal third of the structure (Carpenter et al. 1981). The source appears to receive neither pallidal nor cortical input. Other studies have shown that the lateral pallidal segment also receives subthalamic innervation (Carpenter and Strominger, 1967; Nauta and Cole, 1978). Lesions placed in monkey subthalamic nucleus from a variety of stereotaxic approaches produce degenerating fibers which enter both the internal and external medullary laminae of the globus pallidus as well as both the medial and lateral pallidal segments; a small number of fibers course to the contralateral globus pallidus as well through the dorsal supraoptic commisure of Meynert (Carpenter and Strominger, 1967).

The subthalamopallidal projection in monkey is topologically organized (Nauta and Cole, 1978; Carpenter et

al., 1981). Autoradiographic studies show that the lateral part of the subthalamic nucleus projects to the body of the pallidal complex and the rostromedial part of the subthalamic nucleus projects to the rostral and medial parts of the globus pallidus, including the infracommissural area bordering the substantia innominata (Nauta and Cole, 1978). This projection terminates in discrete bands in monkey but is uniformly distributed in cat. Carpenter et al. (1981) found a more complex correspondence based on retrograde transport of HRP to the subthalamic nucleus after injections into both pallidal segments. Their results, shown in Figure 3, indicate that a) neurons in the caudal two-thirds of the subthalamic nucleus project to the medial pallidal segment, b) neurons in the medial region of the middle half of the nucleus project to the rostral lateral pallidal segment, and c) neurons located centrally in the rostral two-thirds project to the central portion of the lateral pallidal segment. Further, these authors reported an inverse dorsoventral relationship between the location of cells of origin in the subthalamic nucleus and their targets in the lateral pallidal segment. Carpenter (1984) suggested that little if any of the the lateral region of the subthalamic nucleus projects to any part of the globus pallidus.

The existence of some reciprocity in the pallido-subthalamo-pallidal loop has been demonstrated at the electron microscopic level (van der Kooy et al., 1981). HRP injected into rat globus pallidus, the homologue of the

Figure 3. Efferents of the subthalamic nucleus in monkey (modified from Carpenter, et al, 1981a). The plane of section is horizontal. CN, caudate nucleus. Put, putamen. LPS, lateral pallidal segment with a rostral region (heavy stippling) and a central region (hatched). MPS, medial pallidal segment. Fx, fornix. III, third ventricle. IC, internal capsule. MTT, mammillothalamic tract. OT, optic tract. STN, subthalamic nucleus. RN, red nucleus. The matched patterns in the globus pallidus and subthalamic nucleus correspond to the topologically organized pallidal terminations of subthalamic efferents.

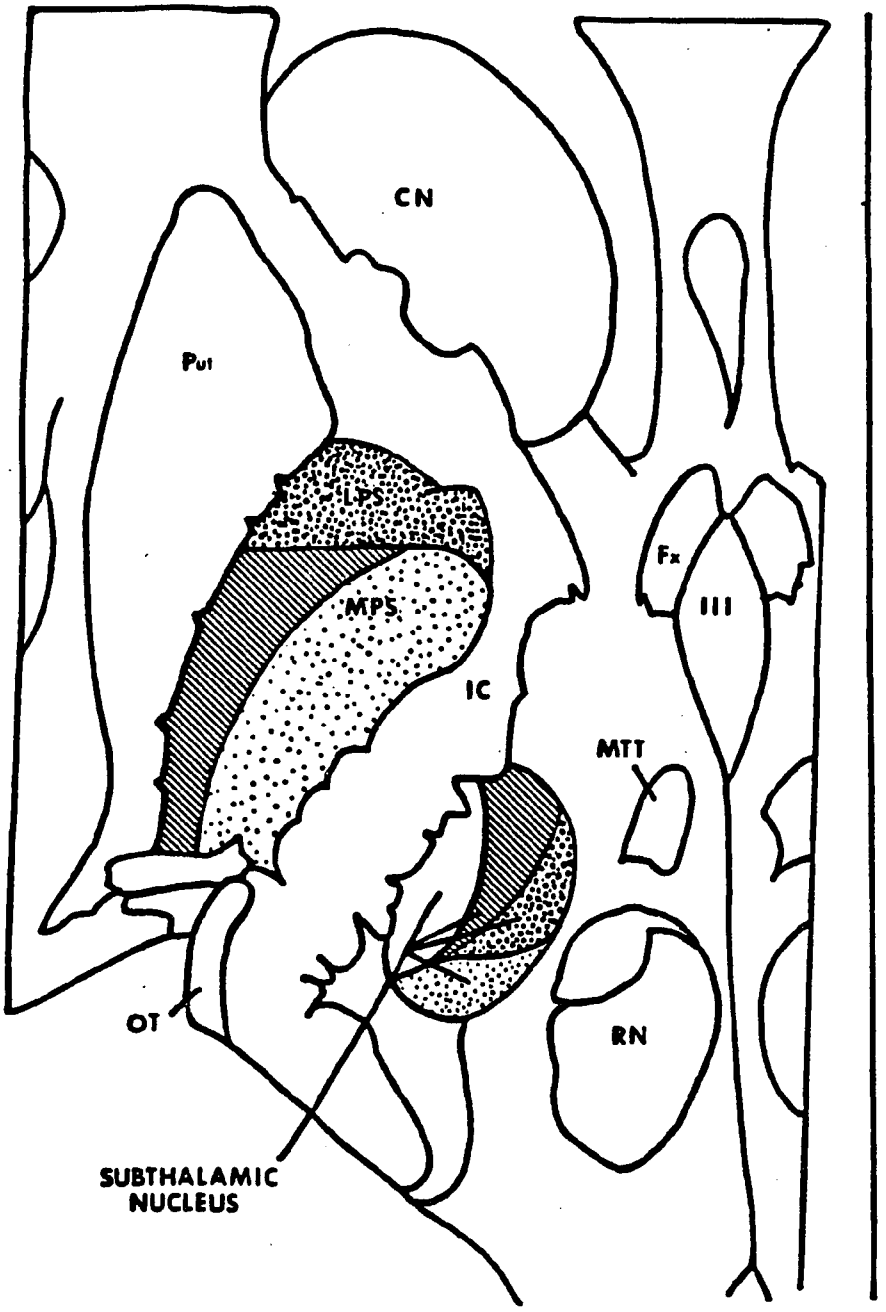
CN
Put
LP
MPS
IC
Fx
III
MTT
RN
OT
SUBTHALAMIC
NUCLEUS

lateral pallidal segment in primate, produces labelling of terminals forming symmetrical axosomatic and axodendriticsynapses on cells also labelled with HRP retrogradely. The anterograde labelling is abolished by prior kainic acid injection into the globus pallidus. Identification of a topological relationship, if one exists, is difficult because of the small size of the subthalamic nucleus in rat.

Larsen and Sutin (1978) found that stimulation of the subthalamic nucleus inhibits electrical activity in the feline entopeduncular nucleus, the homologue of the medial pallidal segment in primate. The target cells are predominantly those which project to the lateral habenular nucleus rather than to the VA nucleus of the thalamus.

Substantia Nigra

Both anatomical and physiological evidence point to a subthalamic projection to the substantia nigra. Whittier and Mettler (1949), found that a lesion placed in the subthalamic nucleus produced fine degeneration in the substantia nigra of the macaque, particularly following destruction of the ventrocaudal subthalamic nucleus. Injection of tritiated amino acids into the subthalamic nucleus in monkey produces prominent labelling of the substantia nigra. Fibers are seen to enter the substantia nigra either directly from the medial region of the subthalamic nucleus or after coursing with fibers which lie between the cerebral peduncle and the substantia nigra. The

subthalamic terminals do not impinge upon pigmented neurons of the pars compacta; the projection is directed toward the pars reticulata (Nauta and Cole, 1978). This finding is supported by Ricardo's (1980) autoradiographic study in rat. However, in this animal, HRP injections into the substantia nigra, both pars compacta and pars reticulata, produce retrograde labelling in the subthalamic nucleus (Kanazawa et al., 1976; Ricardo, 1980) indicating a possible subthalamic projection to both regions of the substantia nigra.

Electrophysiological evidence obtained in rat (Deniau, Hammond, Chevalier and Feger, 1978) indicates that those subthalamic cells which send axons to the globus pallidus and/or to the entopeduncular nucleus send an axonal branch to the substantia nigra was well. Chang et al. (1984) also observed axonal branching in their HRP and electron microscopic analysis of rat subthalamic efferents, with the terminals in the substantia nigra containing small oval vesicles and forming asymmetric synapses with dendrites.

In an electrophysiological study of the subthalamonigral projection, an excitatory response was found predominantly in the pars reticulata; however, the observers maintain that the projection is massive and includes the pars compacta as well (Hammond, Deniau, Rizk and Feger, 1978). This finding poses a problem in that a subthalamic efferent to the substantia nigra has been identified, in rat at least, as one branch of an output to the pallidum which is known to be inhibitory (Deniau et

al., 1978; Hammond and Yelnik, 1983; van der Kooy and Hattori, 1980). The problem of differential subthalamic effect on target elements may be species specific since the projection of the subthalamic nucleus to the globus pallidus in primate is much greater than that to the substantia nigra; it is still possible that different populations of cells within the subthalamic nucleus project to the two structures (Rouzaire-DuBois et al., 1984).

Cerebral Cortex.

When HRP is injected into the cerebral cortex in rat, retrogradely labels cells in the lateral and most rostral areas of the subthalamic nucleus are observed (Jackson and Crossman, 1981). As indicated previously, the lateral regions of the nucleus are also the areas which receive cortical afferents.

Pedunculopontine Nucleus

A projection from the subthalamic nucleus to the pedunculopontine nucleus has been reported (Jackson and Crossman, 1981; Nauta and Cole, 1978). The ipsilateral projection, which originates in the lateral subthalamic nucleus and terminates in the pars compacta of the pedunculopontine nucleus, is less in magnitude than the comparable projection to the substantia nigra (Nauta and Cole, 1978).

Other

Injection of triated amino acids into the subthalamic nuclei of Rhesus monkeys and of cats demonstrated a

projection to the putamen (Nauta and Cole, 1978). Some fibers from the subthalamic nucleus also enter the external capsule. Injection of HRP into the subthalamic nucleus produces a small number of labelled axons in the VA and VL nuclei of the thalamus (Nauta and Cole, 1978).

Summary

The subthalamic nucleus is a lens-shaped structure which receives major inputs from the lateral pallidal segment and from the cerebral cortex, as well as minor afferents from the CM-PF complex of the thalamus and pedunculopontine nucleus. These projections onto the subthalamic nucleus, summarized in Figure 4, are organized so that the major inputs from the cortex and lateral pallidal segment are to the lateral part of the structure while the other, minor inputs are more medially located. In addition, the nucleus receives monoaminergic innervation from the substantia nigra, locus coeruleus and dorsal raphe nucleus.

The subthalamic nucleus has major efferent projections to the medial globus pallidus and to the substantia nigra. Smaller numbers of subthalamic fibers project to the lateral pallidal segment, cerebral cortex, thalamus and the pendunculopontine nucleus. Outputs to the pallidum and to the substantia nigra are branches of axons from the same neuron in rat (Deniau et al, 1978). The major projection targets of the subthalamic nucleus and of the striatum are the same (Rouzaire-duBois et al., 1983). Thus, as Figure 4

shows, the subthalamic nucleus is in a position to influence the output of the basal ganglia through its pallidal and nigral efferents as well as through its smaller but direct efferents to the cortex and the pedunculopontine nucleus.

Figure 4. Connectivity diagram of the subthalamic nucleus. Cx, cortex. S, striatum. LPS, lateral pallidal segment. MPS, medial pallidal segment. Cm-Pf, centre median-parafascicular complex of the thalamus. Va-Vl, ventral anterior and ventrolateral nuclei of the thalamus. PPN, pedunculopontine nucleus. SNr, substantia nigra, pars reticulata. SNc, substantia nigra, pars compacta. LC, locus coeruleus. RN, raphe nuclei.

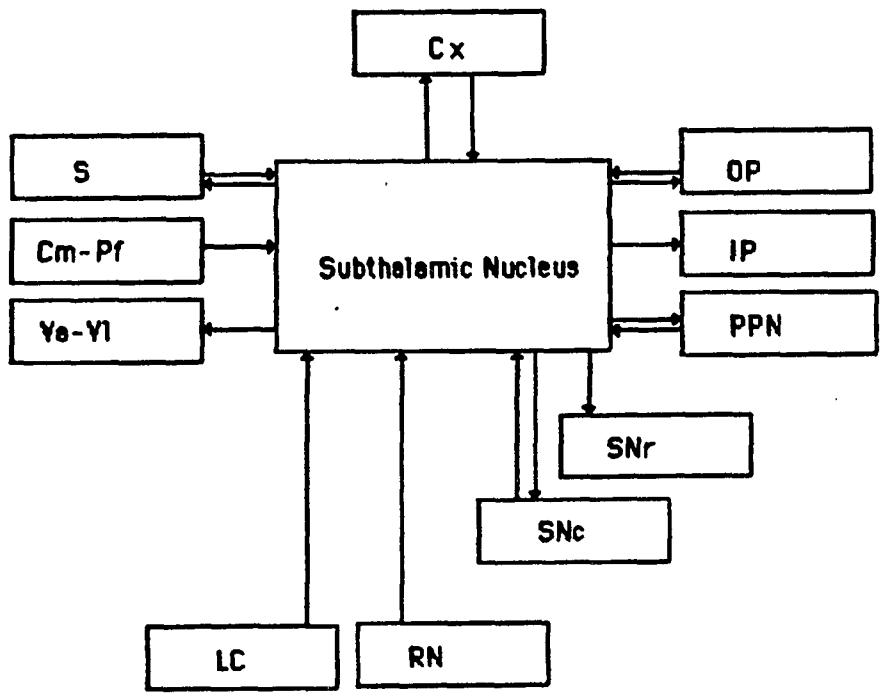
Cx
S
Cm-Pf
Ve-Vl
Subthalamic Nucleus
OP
IP
PPN
SNr
SNc
LC
RN

CHAPTER II

Materials and Methods

Subjects

Eleven monkeys (Macaca mulatta) served as subjects and were sacrificed as follows: 0 weeks (n=2), 1 week (n=2), 4 weeks (n=2), 8 weeks (n=3), 16 weeks (n=1), and 17 weeks (n=1). Four of the animals were derived from timed pregnancies and were delivered either spontaneously or by Caesarean section at 168-174 days of gestational age. Thisprecaution was taken because monkeys may be of different gestational ages at birth. In a quantitative comparison of structural change as a function of time, deviation from the mean of 168 days may be critical, particularly at the youngest ages. Table 2 summarizes the information on individual animals.

Perfusion

Each animal was deeply anesthetized by an intraperitoneal injection of 40 mg/kg of Nembutal (Sodium Pentobarbital). The axillary arteries were tied off, the abdominal aorta was visualized behind the left kidney, cannulated toward the heart and tied distally to the cannula. The perfusates, injected under pressure (80 mm Hg), included 300 units/kg of heparin, 0.2 ml/kg of a 3% solution of sodium nitrite, and 5 ml of normal saline. The inferior vena cava was isolated and cut for drainage.

The fixative mixture employed depended on whether the brains were to be processed for light or electron

Table 2

Information on Individual Monkeys

Animal Number	Sex	Post A. (weeks)	Gest.A. (days)	Weight at Post.A.	Microscopy	
					Light	Electron
1020	F	00	E168	475g	x	x
869	M	00	?	500g	x	
1018	M	01	E168	450g	x	x
851	M	01	?	380g	x	
1010	M	04	E168	400g	x	
846	F	04	?	600g	x	
1016	F	08	E174	600g		x
1011	F	08	?	570g	x	
847	M	08	?	666g	x	
1006	M	16	?	?	x	
874	F	17	?	900g	x	

Post.A., postnatal age.

Gest.A., gestational age.

microscopy. In the former case, a 5% solution of formalin followed a wash with normal saline; whereas in the latter instance, the final perfusate was a solution of 1% pure formaldehyde obtained from paraformaldehyde, 1% purified glutaraldehyde and 0.002% calcium chloride in 0.12M phosphate buffer. A total of 1600 ml/kg body weight was used with the first 80% given under pressure and the remainder as a drip.

Light Microscopy

In each case, after the perfusion was completed, the monkey's head was mounted in a stereotaxic apparatus and the skull and dura removed. The frontal lobes were cut in a coronal plane with a blade mounted in an electrode carrier. This cut determined the future plane of section. In order to ascertain the percentage of tissue shrinkage which results from processing, two pins, set 5 mm apart, were inserted rostrally in a horizontal stereotaxic plane through one occipital lobe perpendicular to the plane of the frontal cut. The brains were left in fixative for one week prior to embedding, at which time the pins were removed.

Histological Procedures

The brains were dehydrated in increasing grades of ethyl alcohol and embedded in celloidin. The blocks were mounted on a Leitz Wetzlar sliding microtome, and were carefully oriented so that the previous cut through the frontal lobe was parallel to the plane of section. All sections were cut at a microtome setting of 40 micrometers,

and stored in 70% alcohol. Every tenth section was stained with a 1% aqueous solution of cresyl violet, mounted with Permount and coverslipped. The inscribed identification of each slide was covered; all slides were coded using a table of random numbers.

Shrinkage Determination

The holes left upon removal of the calibration pins were clearly discernible in the mounted sections. These were projected onto graph paper and drawn. An inidividual linear shrinkage correction factor was obtained by dividing 5 mm, the distance between the pins inserted into the occipital lobe, by the mean inter-hole distance. The square and cube of this quotient gave the areal and volumetric shrinkage factors respectively. Application of correction factors was necessary in order to refer measurements to tissue in its condition before processing since it is known that the amount of shrinkage varies from specimen to specimen (Gottlieb, Pasik and Pasik, 1985). Correction factors for each animal are shown in Appendix 1.

Magnification Determination

In order to insure reliability in measurement, the linear magnification constant was ascertained for each of the objective lenses used in the light microscopic study. In all cases, the image was observed through a 10X eyepiece and projected through a drawing tube with an additional 1.8X magnification. Calibration with a Zeiss stage micrometer was repeated daily throughout the study and, when necessary, the

microscope height was adjusted so that the image viewed through the 2.5X objective was always magnified 50 times and the image observed through the 100X oil immersion objective was always magnified 1855 times.

Volume Estimation

In order to determine changes in the volume of the subthalamic nucleus with age, a series of drawings was made of sections from that structure. For each of eight monkeys, every twentieth section throughout the nucleus was viewed with a configuration which produced a total magnification of 50X. The subthalamic nucleus was projected and traced on 10 x 10/cm graph paper. The position of the midline was included in the drawing for future reference on possible rotation of the nucleus during development. A total of 14 nuclei were drawn representing both right and left structures in six animals, and right nuclei only in the two monkeys whose left hemispheres were used for electron microscopy.

The area of each drawn nucleus was measured using a Numonics Corporation Graphics Calculator. This instrument converts a movement of the tracing arm into digital information with a resolution of 0.25 mm. The measured area was divided by the areal magnification factor ($50^2 = 2500$).

The volume of the subthalamic nucleus at each age was determined by the application of Simpson's Rule for the estimation of the volume of irregular solids (Tuttle and Satterly, 1926). The structure was divided into an even

number (n) of slabs by an odd number (n-1) of equally spaced (d) parallel cuts. If the area of the nucleus at each intercepted plane was denoted by A1, A2, ...An-1, then the volume of the structure could be estimated by the expression:

$$1/3\ d\ [(A1+An-1)+4(A2+A4+...+An-2)+2(A3+A5+...+An-3)].$$

Since d is the product of section thickness and the number (20) of sections between samples, a possible source of error existed in the use of the nominal section thickness in this calculation. To determine true thickness, each section through the subthalamic nucleus was examined with a 100X oil immersion objective (N.A. 1.25). The planes between which any point in the field was in focus were noted on the micrometer scale of the microscope fine focussing knob. The mean section thickness for each animal was calculated from these values and is shown in Appendix 2. All volumes were adjusted by the application of the individual volumetric shrinkage factor.

A mean nuclear volume was estimated for each age. For one animal each at 0 and 1 weeks of age, only one hemisphere was available; the other hemisphere was used for electron microscopy. In these cases, the obtained values were summed twice in computing the grand mean volume. This procedure was justified because no significant hemispheric differences between subthalamic nuclei were found in those instances in which two nuclei were measured.

Figure 5. Selection of Sample Fields. Each numbered field measures 5 mm on a side and represents the upper right square of a rectangular region 10 x 20 mm. The aggregate of the sample fields is approximately 1/8 of the total area of the section. Each field is equivalent to 10,000 um^2. The scales on the right and bottom represent the x and y coordinates of the microscope stage, which were used to locate the fields.

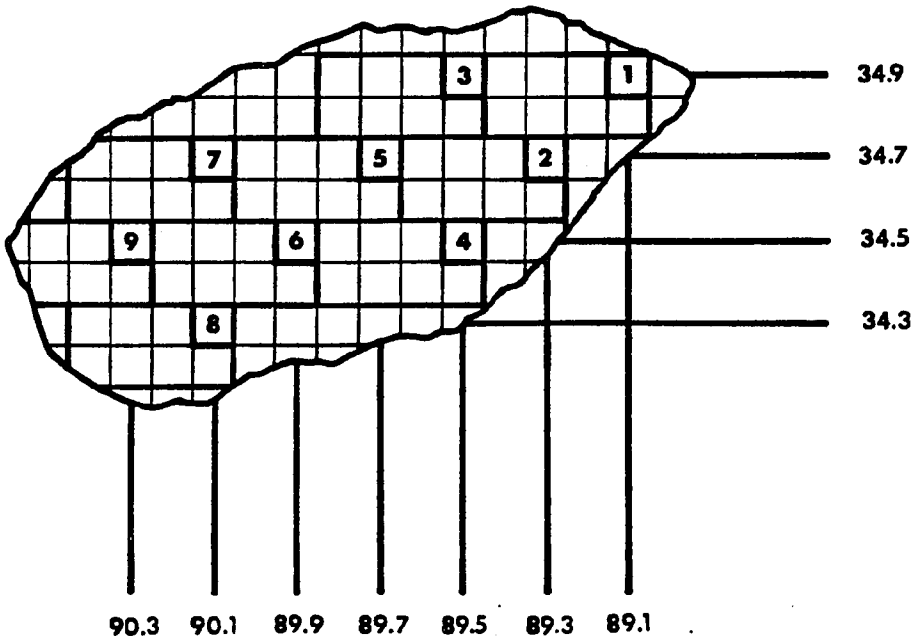
3
1
7
5
2
9
6
4
8
34.9
34.7
34.5
34.3
90.3
90.1
89.9
89.7
89.5
89.3
89.1

Cell Measurements

Figure 5 displays a template cut from 10 by 10/cm graph paper which was used to identify square sample fields. This template was superimposed on tracings of each of the right subthalamic nuclei which were used for the volume measurement study. The fields were numbered and their locations identified with the x-y coordinates of the microscope stage. Each field was viewed through a 100X Neofluar oil immersion objective (N.A. 1.0), and projected through a drawing tube onto a sheet which contained an outline exactly corresponding to a 100 x 100 micrometer field. Tracings were made of all projected cells with clear nucleoli which fell entirely within the confines of the outline and of those which overlapped the upper or right borders. The cross sectional area of the neuronal somata and of their nuclei were measured using the graphics calculator. The measurements were corrected by the areal shrinkage factor and magnification constant before analysis.

Possible regional differences in cell size were evaluated by dividing the subthalamic nucleus of each monkey into four regions. The method of division, described in detail in Appendix 3, involved the determination of the longest chord which divided the largest section into halves of equal area ($\pm$ 2%). A line perpendicular to this chord was placed so as to divide the structure into equal halves in the second dimension.

Cell Densities

The number of neurons per cubic millimeter was obtained for each field sampled. The thickness of the section used to determine volume was adjusted by adding the diameter of the largest of fifteen nucleoli sampled per slide (Abercrombie, 1946) (see Appendix 2). This correction was needed because some of the counting elements, the nucleoli, could occasionally be cut at the surface of the section. Where that occurred, the volume which encompassed the nucleolus included part of the neighboring tissue as well as the section in which it was counted. Without this correction, the number of nucleoli per unit volume would have been overestimated.

Cell Totals

Changes in cell density as a function of age are easy to misinterpret. Decreases in density may reflect a decrease in cell number, an increase in structural volume or both. Therefore, the total number of cells in the right subthalamic nucleus was estimated for each monkey for whom cell density measures were derived, on the basis of the volume of the right nucleus, corrected for shrinkage, multiplied by the mean cell density.

Statistical Analyses

The means and standard deviations of somal and nuclear areas were computed for each monkey. Separate one-way analyses of variance were performed, with age as the

independent variable, and cell somal size or cell nuclear size as the dependent variables.

Regional differences in cell size were evaluated at each age by computer assisted cluster analyses. Cluster analysis is a procedure by which elements are grouped on the basis of similarity. In short, the computer algorithm divides the neurons arbitrarily into two groups and determines the mean of each group. The initial grouping has no effect on the outcome of the analysis but simply provides a starting point from which further clusters may be derived. Each cell is compared with the means and placed in the cluster whose mean is closer. After all cells are reassigned, the means of the new clusters are calculated. Cells are again compared with the group means and placed in the cluster whose mean is closer. This process is iterated until all cells are in the group whose mean is closer and no further reassignment is possible. At this point, a t-test is performed on the means of the resultant clusters.

For each monkey, cluster analysis yielded two populations which formed the basis for further analysis. Differences between mean nuclear areas as well as between somal densities were tested as a function of the somal cluster. Subsequent to the division of the subthalamic nucleus into quadrants, analyses of variance were also performed on somal areas and somal densities as a function of quadrant.

Electron Microscopy

After perfusion, the heads of the monkeys were stored in fixative overnight. Subsequently, the calvaria and dura were removed and the head was mounted in a stereotaxic instrument. Sequential 2 mm coronal slices were cut in the stereotaxic plane and placed in cold fixative. In the two youngest specimens, the right hemisphere was not sliced since it was used for light microscopy (see above).

Embedding

Six to ten blocks of tissue were microdissected from the subthalamic nucleus of each brain. These blocks, which were about 1 cubic mm in maximum size, were collected into fixative and washed three times with 0.12M phosphate buffer. They were postfixed in a solution of 2% osmium tetroxide, 7% glucose and 0.002% calcium chloride in 0.12M phosphate buffer. The tissue was subsequently dehydrated with increasing grades of ethanol and with propylene oxide. It was stored in a mixture of 50% Epon-Araldite and 50% propylene oxide for two hours and then in pure Epon-Araldite overnight. Blocks were placed in Beem capsules in fresh Epon-Araldite and polymerized.

One micrometer sections were cut on an LKB IV Ultra-microtome, mounted on a glass slide, stained with toluidine blue, surveyed with a light microscope and areas for thin sectioning selected. Silver sections, approximately 80 nm thick, were collected onto 300-mesh copper grids, stained with a 5% aqueous solution of uranyl acetate and

counterstained with a solution of 0.2% lead acetate and 0.6% sodium hydroxide.

Calibration of the Electron Microscope

The true magnifications obtained with the electron microscope were determined by photographing a carbon grating replica of known periodicity (Ernest F. Fullam Inc., Schenectady, N.Y.) through each of three specimen holders at nominal settings of 6,000X and 10,000X. The results of this calibration, which are shown in Appendix 4, were applied such that the final print magnifications of the electron micrographs were precisely 18,000X or 25,000X respectively.

Grids were viewed at low magnification using an Hitachi HU-12A electron microscope. Sections which were free of knife marks, holes and compression were selected for photographing. Samples were chosen from windows completely covered with tissue. Care was taken to exclude material from sections which appeared to be sequentially cut.

Two groups of electron micrographs were taken. The first, at a nominal magnification of 6000X, was used to determine the proportion of neuropil present after exclusion of neuronal and glial somata, myelinated axons and capillaries. The areas selected for photographing were chosen without bias at a magnification and illumination low enough to prevent identification of profiles. The second group, taken at a nominal 10,000X, was used for the measurement of synaptic profiles. In this case, while the

tissue was scanned at lower magnification, regions were chosen to maximize representation of neuropil.

Photographs were taken from at least three blocks of tissue for each monkey. A maximum of eight micrographs per block was taken at each magnification. The number of pictures obtained at each age is shown in Appendix 5. All photographs were coded and randomly ordered for measurement.

Measurements of Electron Micrographs

Each micrograph printed exactly at 18,000X was marked using a template which delineated an area of 191 mm x 170 mm. The sole criterion for placement of the template was that the micrograph number be excluded. When corrected for magnification, the demarcated area represented 100 square micrometers of tissue. The regions occupied by neuronal and glial somata, blood vessels and myelinated axons were subtracted from 100 micrometers. This yielded the amount of net neuropil for the print. Coded data were entered into the CUNY computer by means of the Wylbur program. When data were decoded and sorted by animal, using the Statistical Analysis System (SAS), both net neuropil and total tissue were summed across prints and a ratio of net neuropil to total tissue determined separately for each monkey.

Measurement of Synapses

On each micrograph printed at a magnification of exactly 25,000X, a template was used to mark an area of 204 by 153 mm corrresponding to 50 square micrometers of neuropil. The small areas which contained somata, glia and

myelinated fibers were excluded. Synaptic profiles were identified on the basis of membrane thickenings even in the absence of a clear cleft, as occurred in tangential sections, and were numbered on coded micrographs. In addition, a judgement was made by the observer as to the maturity of the contact. If two or more synaptic vesicles adhered to the presynaptic membrane, the contact was identified as mature; all others were called immature. Similar arbitrary criteria have been used by other investigators in the past (Glees and Sheppard, 1964; Hamori and Dyachkova, 1964). All micrographs were examined by a second observer. In the event of disagreement between the observers, a third investigator made the final assignment. This situation occurred in 18% of the cases regarding the classification of a contact as synaptic, and in 31% of the instances concerning the degree of synaptic maturity. All judgements were made independently and without knowledge of the source of the material.

The lengths of profiles were measured with a graphics calculator serially interfaced to an Apple II computer. A custom made program was made available for data entry and analysis. A single correction factor changed the measurements, taken in centimeters, to micrometers and divided this by the print magnification. A coded identification number was entered; when all measurements were completed, decoding information was input into the computer including the number and age of the monkey and the

area of neuropil present in each print. This program then segregated profile data by animal as well as to summed neuropil areas across prints.

Data Analysis

Sample variability.

For each monkey, a special algorithm was available to group the micrographs randomly into four sets. The area fraction occupied by synaptic profiles was determined for each set. The fraction was the quotient of total area of the synaptic profile and total area of the tissue which contained them. The total area of synaptic profiles was obtained by summation of profile lengths multiplied by a constant of 35 nm representing the sum of the thicknesses of the presynaptic and postsynaptic membranes, and of the interneuronal cleft (Peters, Palay, and Webster, 1976). The total area of tissue which contained the profiles was obtained by summation of the net neuropil areas adjusted with the proportion of neuropil to total tissue obtained earlier. The mean area fraction of the four groups and standard deviation were calculated and where the coefficient of variation was greater than 0.3, additional micrographs were added to the sample. These values are shown in Appendix 5.

Stereological procedure.

For the sterological analysis, synaptic profiles are defined as the one dimensional element appearing in the electron micrographs; synaptic plaques are the two dimensional elements derived from the stereologic

reconstruction of synaptic profiles. For each monkey, synaptic profiles were sorted and grouped by size in the maximum number of classes which resulted in a continuous distribution. If the interval containing the largest profiles is "a", that containing the next largest "b", and that with the smallest "n", only in group "a" are all synaptic profiles pure members of the synaptic plaque of which the largest profile represents a cut through its diameter, Da. All other intervals contain a mixed population of profiles, some of which belong to the interval in which they appear, and some others are eccentric cuts from larger diameter synaptic plaques. Coupland's stereologic method is based on the assumption that the elements to be measured are circular, and permits the attribution of synaptic profiles to the classes of plaques of which they are true members (Coupland, 1968). The procedure, discussed at greater length by Holstein (1983), is as follows:

While the profiles within interval "a" are a pure population cut from the largest synaptic plaques, the actual number of plaques of diameter D_a is greater than that counted because the plaques may have been cut further away producing profiles smaller than those included within interval "a". The actual number, N_a, is calculated by dividing the number counted in the interval, n_a, by y_a which is the probability that a plaque of diameter D_a would be

sectioned so as to produce a profile whose diameter fell within interval "a".

$$N_t = \frac{N_a}{y_a}$$

The value of Y_a is obtained by application of the Pythagorean theorem (Coupland, 1968; Holstein, 1983).

The number of profiles of diameter D_a counted in interval "b" is determined in the same manner. That number is subtracted from interval "b" and added to interval "a". Interval "b" now has a pure but incomplete population of profiles cut from synaptic plaque with a diameter D_b. The number of profiles remaining within interval "b" is divided by y_b, the probability that a plaque with diameter D_b be sectioned so as to produce a profile whose length falls within the limits of interval "b", yielding N_b for interval "b".

This same procedure is followed for each of the other intervals, that is, the proportion of profiles measured which belong to larger intervals is determined. These are subtracted from the interval into which they had been placed and added to the intervals of which they are true members. Because this process is based on the proportion of elements which should be in each class, it also produces an estimate of the number of elements which were too small to have been measured.

Density calculation.

The density of synaptic plaques within each class of plaques was computed. Density is the quotient of plaque number and volume of the tissue which contains them. This volume is the product of section thickness and the sample area. Section thickness was increased by addition of the diameter of the largest synaptic plaque in each class (Abercrombie, 1946). As a result of this manipulation, it was necessary to compute separately the density of synaptic plaques for each class. Finally, the partial densities were summed to give the total density of synapses for the subthalamic nucleus for each monkey.

Synapse totals.

The total number of synapses in the subthalamic nucleus of each monkey was estimated. For the neonate and one week old monkeys, the right hemisphere had been used for light microscopy and therefore for volume estimation whereas the left hemisphere was used for electron microscopy. In these cases, synaptic density was multiplied by the estimated volume of the right subthalamic nucleus. For the other animals, where light microscopy had not been performed, synapse totals were derived by multiplying synaptic density by the mean volume of all hemispheres measured by light microscopy for that age.

Chapter III

Results

Light Microscopy

Qualitative Observations

At all ages examined, as well as in the adult monkey (Figure 1), the subthalamic nucleus is sharply demarcated by fiber bundles on its dorsal, lateral and ventral surfaces. The medial limits of the structure are less clearly defined and, in some sections, represent a point of uncertainty. Occasionally, cells of the subthalamic nucleus appear to blend into the hypothalamus or into the nuclei of the fields of Forel.

When viewed with a low power objective, the central and lateral regions of each nucleus appear to be loosely filled with moderately large cells, whereas the medial and peripheral areas are densely packed with smaller cells (Figure 1, bottom).

At higher magnification, the cells, well stained with cresyl violet, show easily discernible somal and nuclear limits. Frequently, the latter are invaginated; nucleoli are heavily stained.

Quantitative Analysis

Volume estimation.

The volumes of the subthalamic nuclei for eight monkeys, corrected for shrinkage, are graphed in Figure 6 as a function of age. These include both right and left nuclei in two eight-week old monkeys, and in one monkey at

Figure 6. Estimated Volumes of Subthalamic Nuclei in Infant Monkeys. Each point represents a single nucleus except the solid symbol at eight weeks which includes two nuclei of almost identical values. At each age, nuclei of individual animals are indicated by either solid or open symbols. The open symbol at 0 weeks and the solid symbol at 1 week correspond to values derived from timed pregnancies. The solid line connects the means obtained for each age.

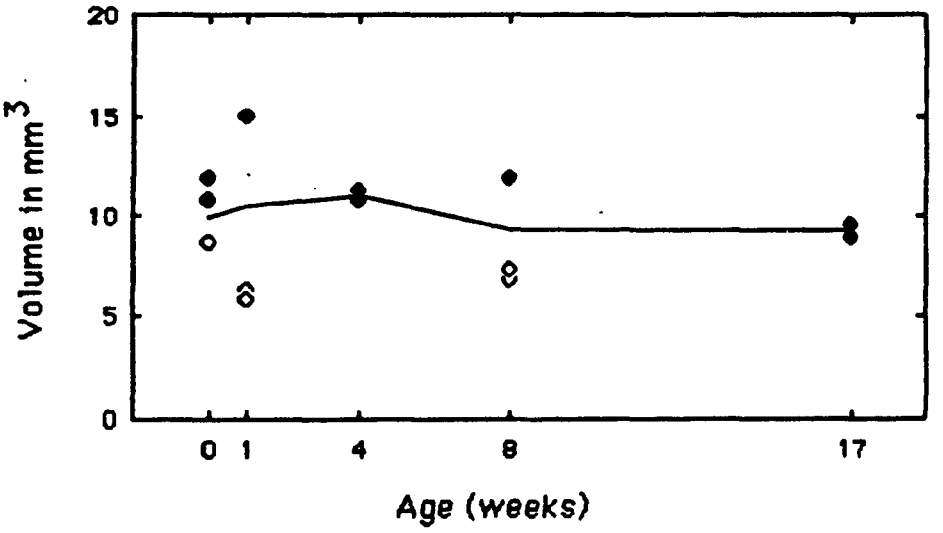
20
15
10
5
0
Volume in mm3
0 1 4 8 17
Age (weeks)

each other age. A single subthalamic nucleus was measured, in addition, in a neonate and one week old monkey, both of whom were delivered at 168 days of conceptual age (E168). As illustrated in Figure 6, where two brains were available for measurement at 0, 1, and 8 weeks, intersubject variability was high. A mean estimated volume was calculated at each age. Because only one hemisphere was available for one neonate and one week old monkey, the estimated volumes for the two youngest animals were weighted by doubling the value of the single measurement. It is apparent that the mean volume of the subthalamic nucleus thus obtained does not change significantly from birth to 17 weeks.

Both right and left subthalamic nuclei were available for analysis of laterality differences in volume in at least one animal at each age. These differences, listed in Table 3, range between 1% and 9% but their directions vary such that neither the right nor the left subthalamic nucleus is consistently larger.

Cross sectional cell area.

Figure 7 depicts the size frequency histograms of somal areas for the five ages examined. The 0 and 1 week old monkeys were derived from timed pregnancies. The total number of cells measured ranges beween 390 in the neonate and 743 in the one week old monkey. The histograms show quasi-normal distributions at all ages. Means, standard

Table 3

Hemispheric Differences in Volume of the Subthalamic Nucleus

Age (weeks)	Animal #	Hemisphere	Volume (mm^3)
00	869	R	10.840
		L	11.867
01	851	R	6.279
		L	5.801
04	846	R	10.760
		L	11.223
08	847	R	6.834
		L	7.251
08	1011	R	11.937
		L	11.798
17	874	R	8.919
		L	9.497

Figure 7. Size Frequency Histograms for Subthalamic Nucleus Neurons. The number of cells measured at each age was: 390 at 0 weeks; 743 at 1 week; 692 at 4 weeks; 637 at 8 weeks; 518 at 17 weeks. Note that the distributions are quasi-normal and that there is a shift toward smaller sizes with time.

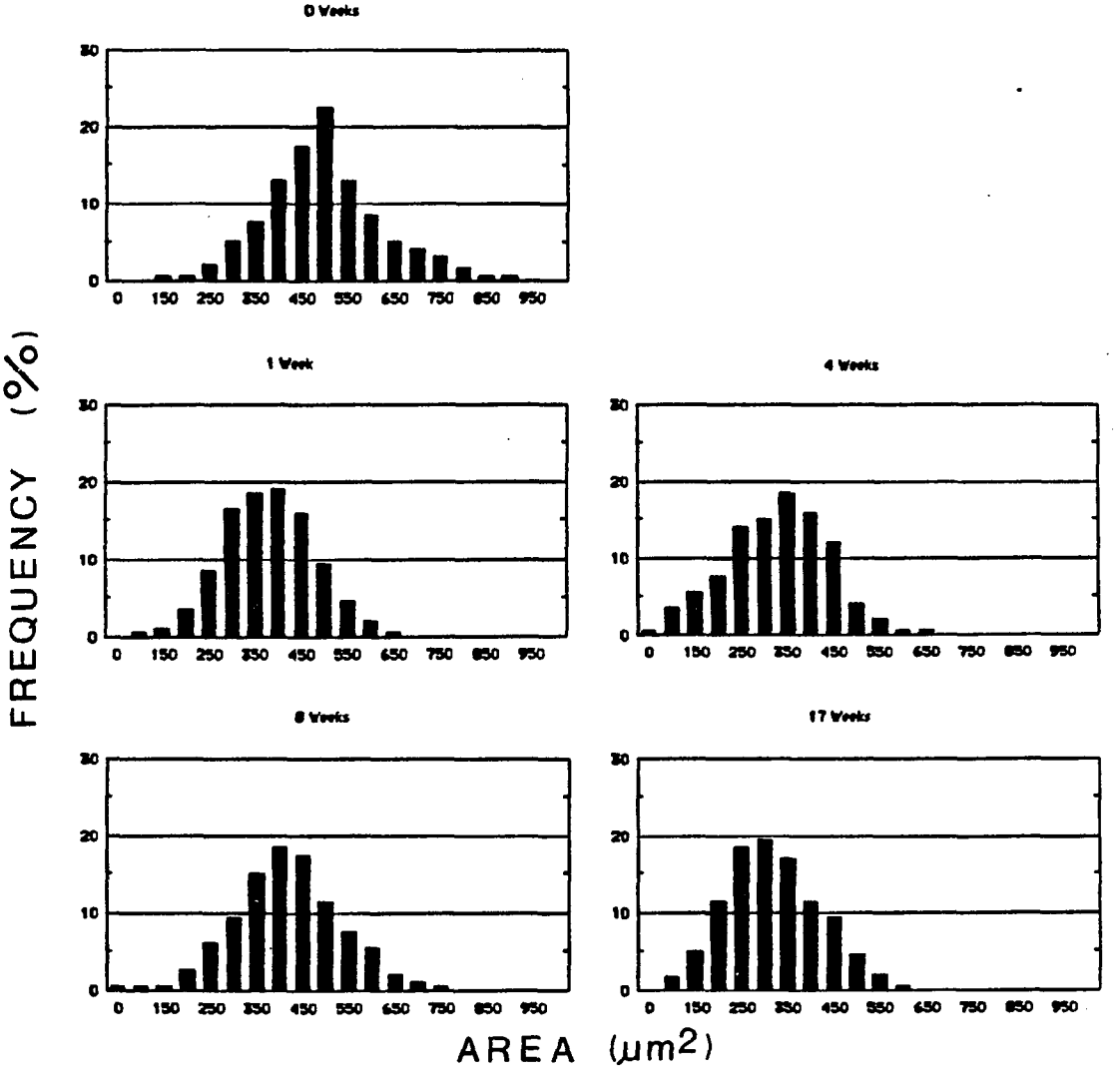
0 Weeks
1 Week
4 Weeks
8 Weeks
17 Weeks
FREQUENCY (%)
AREA (μm2)
0
10
20
30
0 150 250 350 450 550 650 750 850 950

deviations, skewedness and kurtosis of these distributions are given in Appendix 6.

Variations in the mean of these distributions are better seen in Figure 8. There is a decrease in mean somal size during the period of study, so that the value at 17 weeks is only 67% of that at birth. The greatest proportion of this decrease occurs within the first month. In a one way Analysis of Variance performed on somal areas as a function of age, a significant difference among ages is found ($F(4,2972)=198.7$, $p<0.05$). Pairwise comparisons are significant between all combinations of ages except for the 4 and 17 week old monkeys (Tukey, Duncan and Least Significant Difference tests, ($p<0.05$). There is no significant correlation between mean somal area and volume of the subthalamic nucleus.

In view of the qualitative observation of regional differences in cell size, cluster analysis was performed on somal areas as a function of age. This analysis produced two populations at each age whose variances differed significantly ($p<0.01$) and which were maximally separated from each other. The range of values for somal areas, the means and standard deviations of each cluster and the number of cells sampled are shown in Table 4.

To facilitate discussion of the results of cluster analysis, sample fields in the cluster with the larger mean cell sizes are designated magnocellular, whereas fields in the second cluster are named parvocellular. Figure 8,

Figure 8. Mean Cross Sectional Cell and Nuclear Areas.
Top: mean cell area of the total population (solid diamond) at five postnatal ages. N for each age is given in legend of Figure 7. The standard errors of the mean range from 3.7 at 1 week to 5.7 at birth. Separate graphs are also given for mean areas of neurons in parvocellular (solid square) and magnocellular (open diamond) regions.
Bottom: mean nuclear areas of the total population of the same neurons as above. Standard errors range between 1.2 and 2.5.

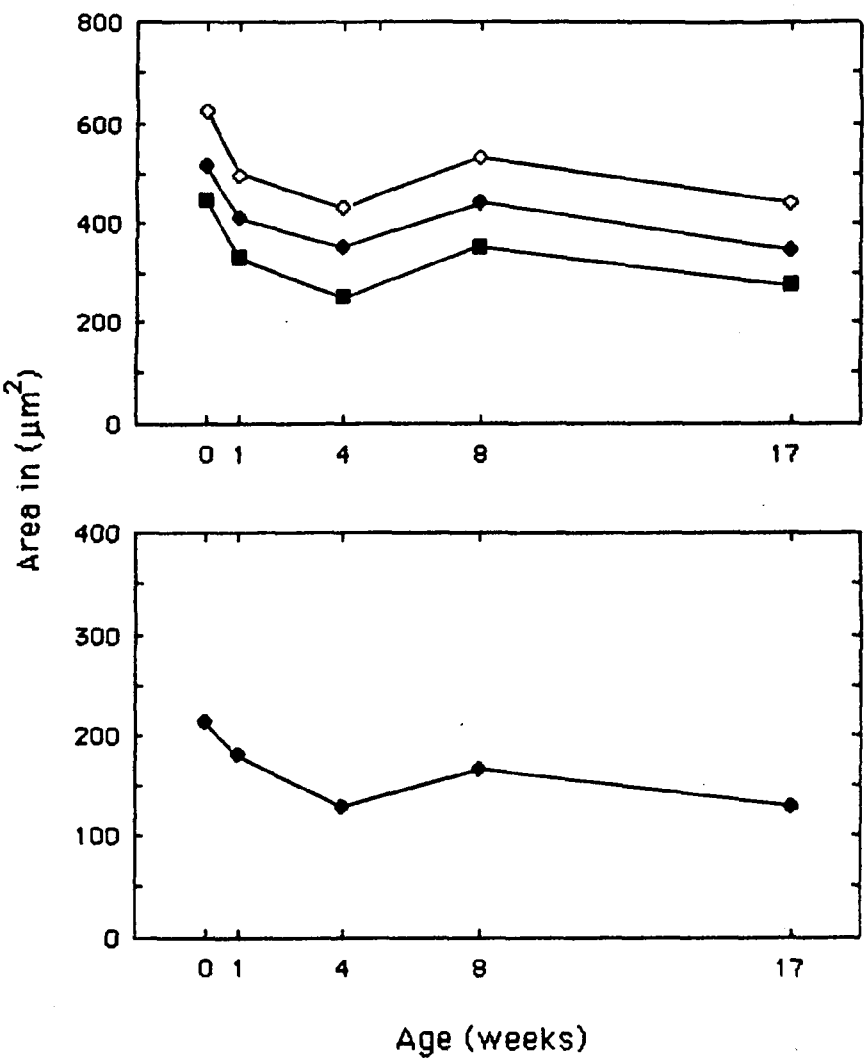
800
600
400
200
0
0 1 4 8 17
400
300
200
100
0
0 1 4 8 17
Area in (µm²)
Age (weeks)

Table 4

Somal areas segregated by cluster analysis

Age (weeks)	Total Cells Measured	Number of Cells in Two Clusters	Area Range (um^2)	Mean Area (um^2)	S.D.
00	390	240	175-532	444	68
		150	534-914	622	76
01	743	389	105-412	332	56
		354	413-842	492	64
04	690	300	72-340	252	68
		390	341-689	430	64
08	636	316	83-440	352	70
		320	443-864	531	76
17	518	299	80-355	274	54
		219	356-627	437	62

top, shows the mean somal cross sectional areas of the two regions as a function of age. It is apparent that the patterns of change in somal area in the magnocellular and parvocellular sections are highly similar and therefore parallel to the total. In both, there is a decline in the area of cells between birth and 17 weeks and in both this decrease occurs predominantly within the first month. The regional separations by size and age are illustrated in Figure 9-13.

In the subthalamic nucleus of the neonatal monkey, shown in Figure 9, the medial portions of the two sections examined contain small cells. These cells are unevenly distributed throughout the remaining areas of the two sections. However, the region close to the dorsomedial surface is predominantly parvocellular in the more caudal section. At one week, the nucleus, (Figure 10) shows more clearly a pattern of parvocellular predominance in the medial regions. In addition, the entire dorsal surface of the most anterior region contains small cells, as do portions close to the periphery in the other sections. This includes the entire lateral border of the most caudal section. At four weeks (Figure 11), the most medial regions of the two anterior sections and the dorsal surface of the more rostral section are parvocellular. As was the case with the one week old monkey, there are small parvocellular areas on the lateral borders of the nucleus. At eight weeks, the subthalamic nucleus shows more strongly the

Figure 9. Segregation of parvocellular (stippled) and magnocellular regions in the subthalamic nucleus of a newborn monkey (#1020) based on cluster analysis. Vertical line on the left represents the orientation of the midline. C and M indicate caudal and medial respectively. Distance between sections: 1.07 mm (corrected for shinkage).

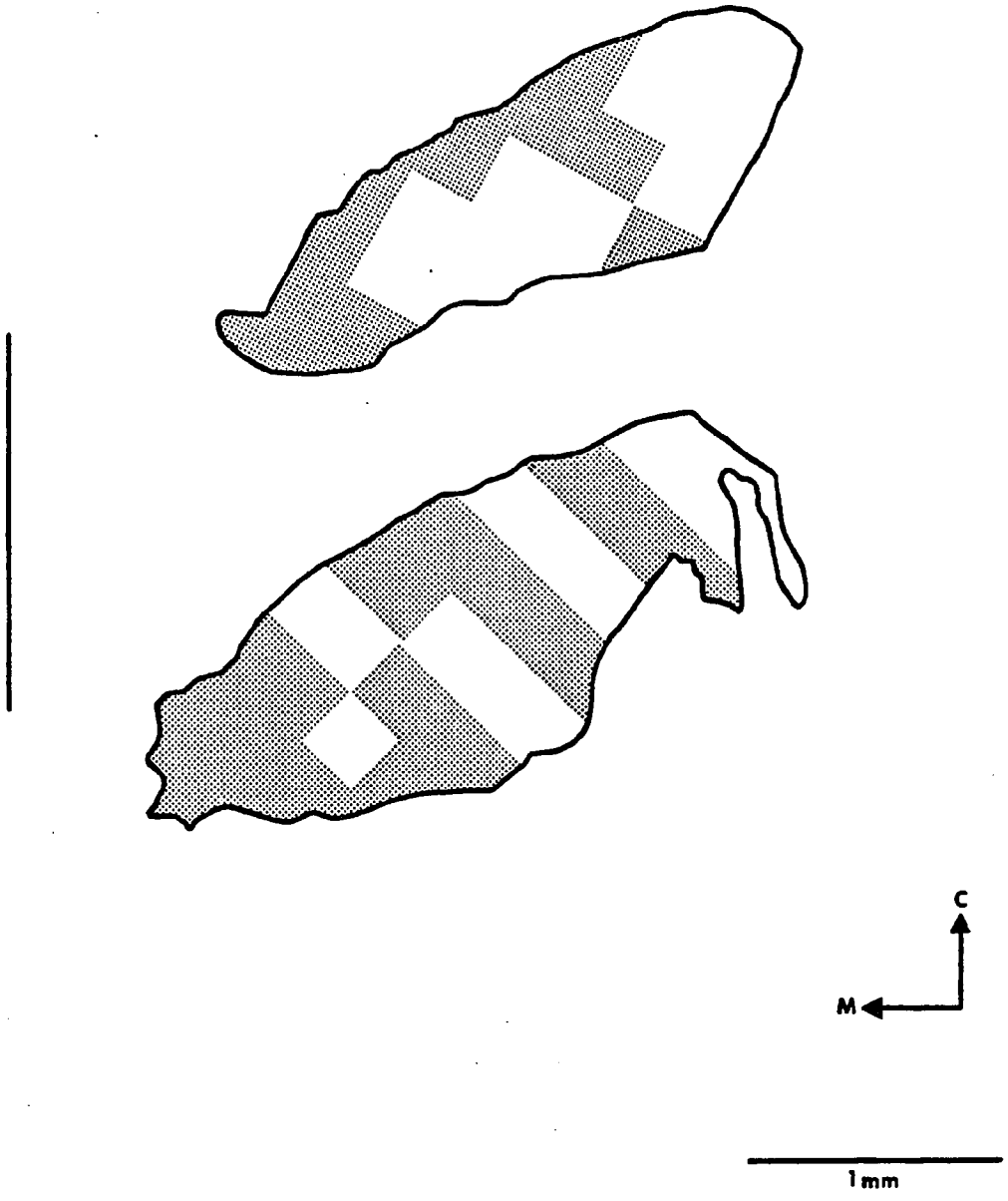
C
M
1mm

Figure 10. One week old monkey (#1018). Notation as in Figure 9. Distance between sections: 0.98 mm (corrected for shrinkage).

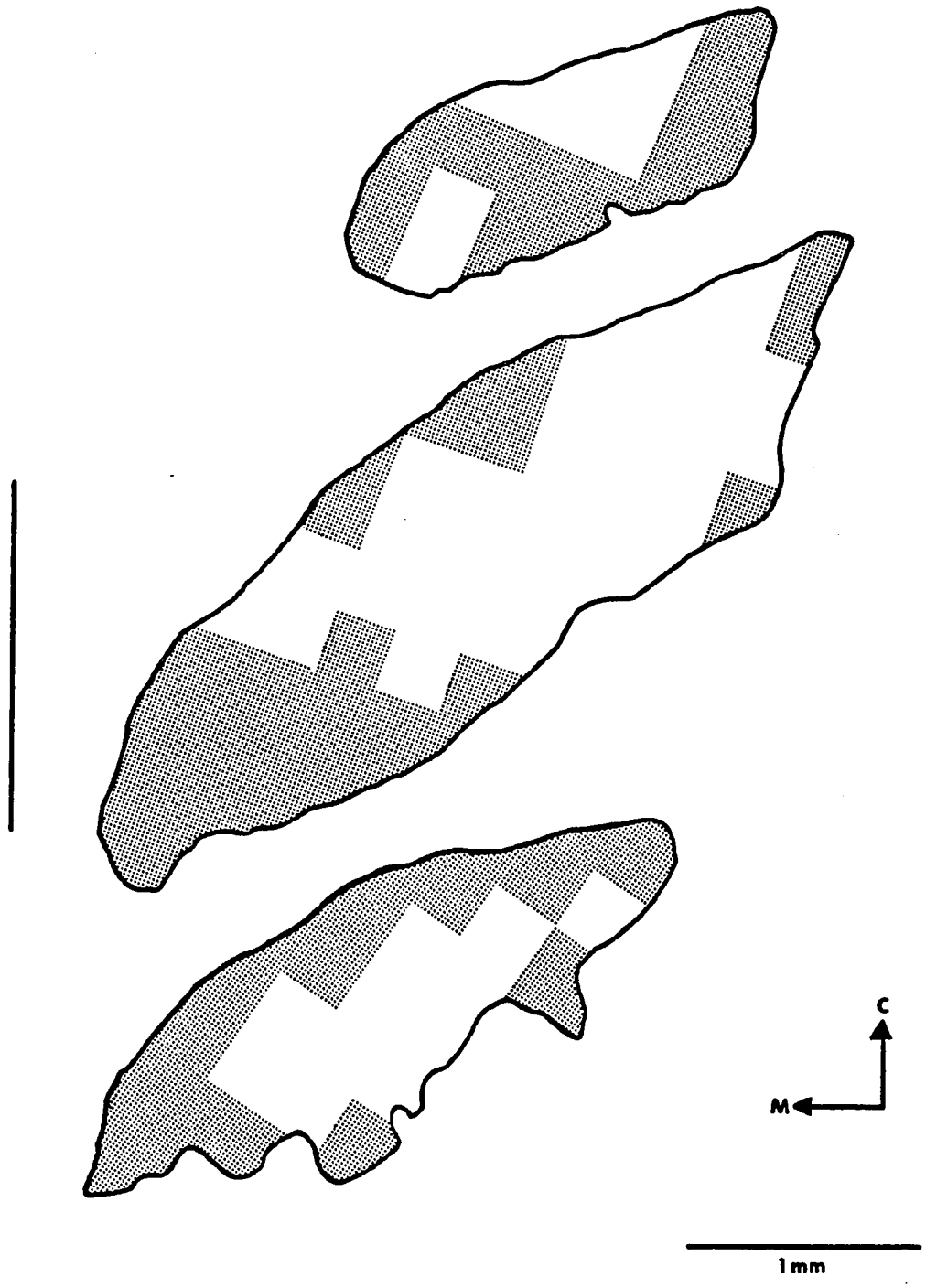
C
M
1mm

Figure 11. Four week old monkey (#846). Notation as in Figure 9. Distance between sections: 0.91 mm (corrected for shrinkage).

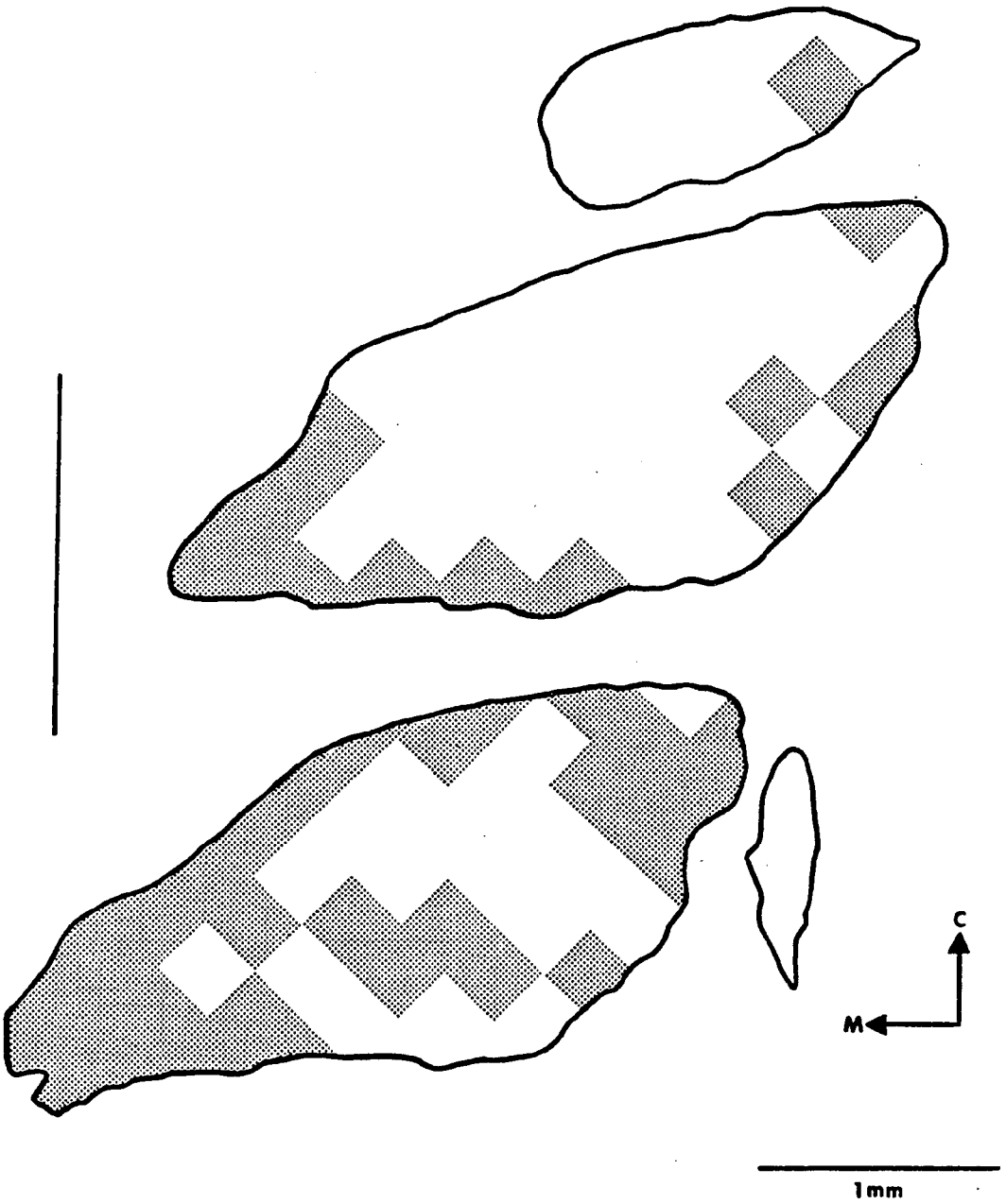
C
M
1mm

predominance of small cells in the most medial areas as well as on the borders of the structure. As Figure 12 illustrates, again there is a small parvocellular area on the lateral surface of the two most posterior sections. The subthalamic nucleus of the 17-week old monkey is illustrated in Figure 13. The anterior section is almost entirely filled with small cells. The second section shows the familiar pattern of parvocellular predominance in the medial region; however, the medial area has a mixed population in the third section. In the most caudal section, the dorsomedial area is parvocellular as is the lateral surface.

Thus, a pattern appears across ages, of small cells in the medial regions and close to the borders of the nucleus. In addition, the parvocellular areas probably form a cap on the most rostral and caudal poles of the subthalamic nucleus. For purposes of further analysis, each nucleus was divided into quadrants according to predetermined criteria (See Methods section). Across sections, a determination was made of the fraction of each quadrant which contained small cells. These areal fractions are listed in Table 5. An Analysis of Variance shows the differences between quadrants to be significant ($F(3,4)=11.06$, $p<0.05$). Subsequent analyses (Tukey, Duncan, Scheffe tests) confirm the significance of the gradient which is apparent in Table 5. The smallest cells are in the dorsomedial quadrants and the largest in the ventrolateral quadrants. Further comparisons were made of mean somal size in the dorsal and ventral

Figure 12. Eight week old monkey (#1011). Notation as in Figure 9. Distance between sections: 0.90 mm (corrected for shrinkage).

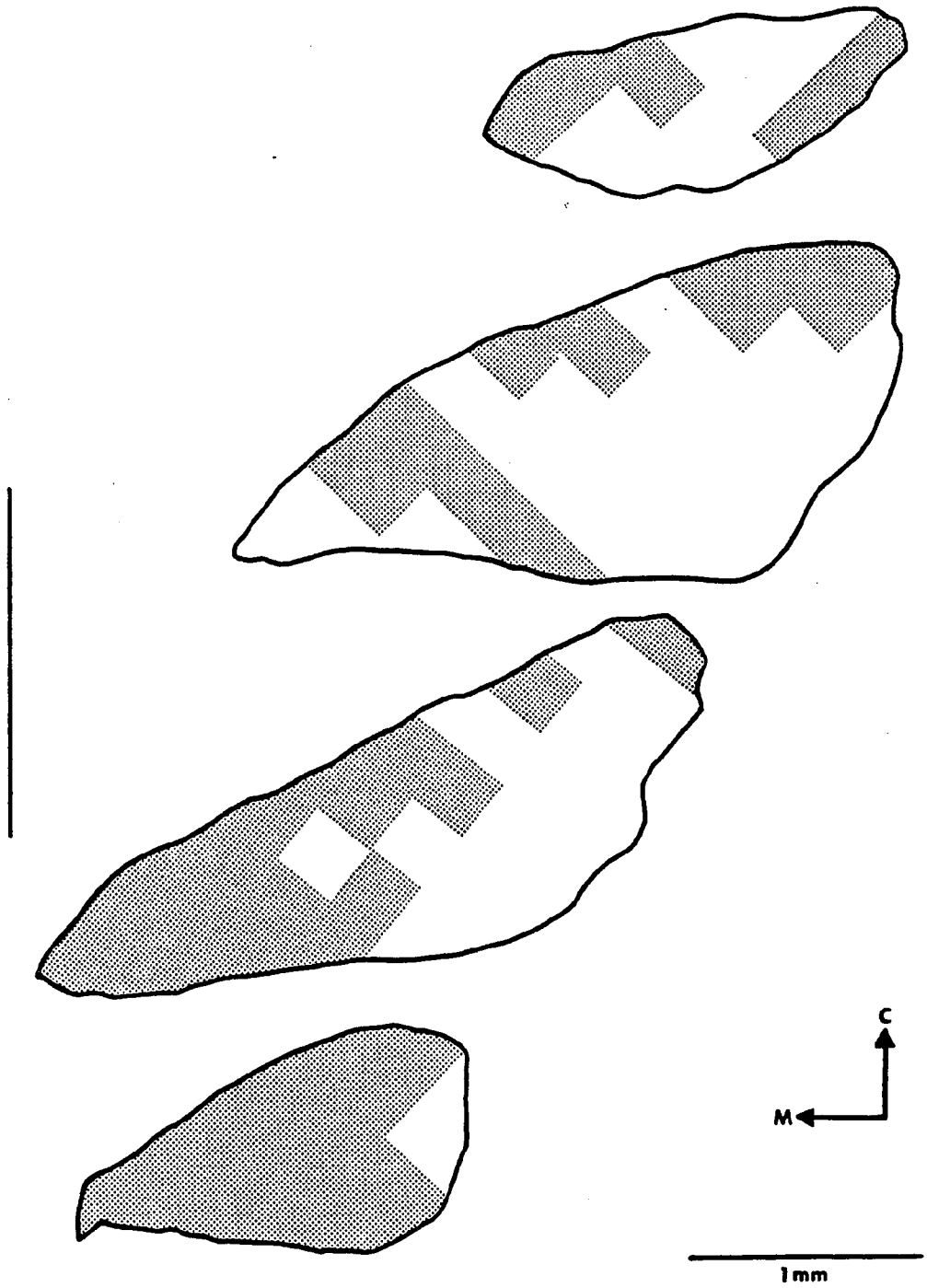
C
M
1mm

Figure 13. Seventeen week old monkey (#874). Notation as in Figure 9. Distance between sections: 0.81 mm (corrected for shrinkage).

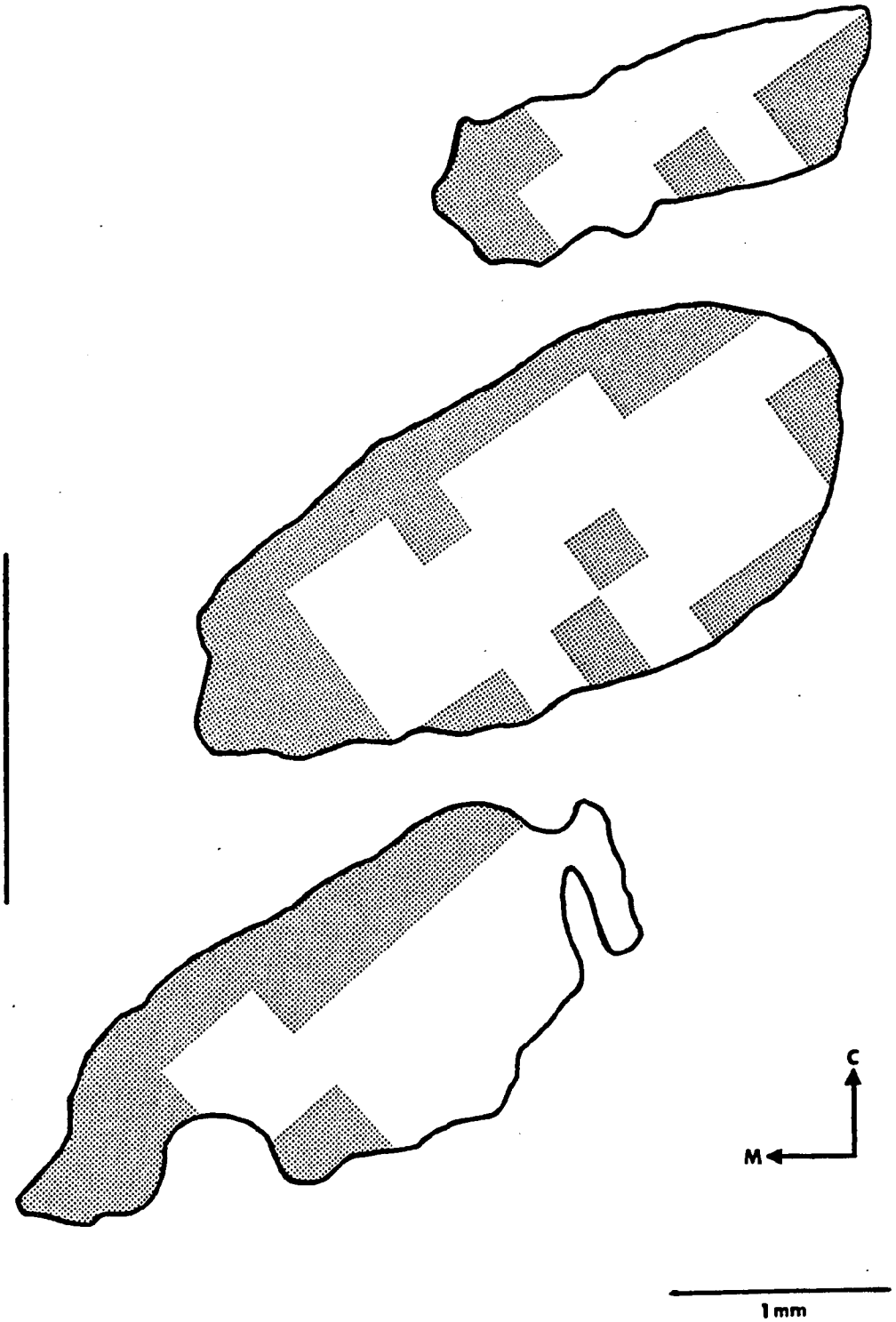
C
M
1 mm

Table 5

Percentage of Each Quadrant Occupied by Small Cells

Age (weeks)	Medial Region		Lateral Region	
	Dorsal	Ventral	Dorsal	Ventral
0	68.20	55.17	50.68	34.06
1	63.49	64.48	36.73	37.14
4	45.65	44.57	27.21	31.39
8	65.84	40.48	43.22	26.35
17	75.36	55.81	49.21	19.34
$\bar{X}$	63.70	52.10	41.41	29.66
S.D.	11.03	9.59	9.66	7.00

halves of the subthalamic nuclei as well as of the medial and lateral halves of the structure. Both comparisons yielded significant differences between halves ($p<0.05$). These may reflect the magnitude of the difference between the parvocellular dorsomedial and magnocellular ventrolateral quadrants.

The volumes of parvocellular and magnocellular segments were compared at each age. Initially there is a slight predominance of parvocellular regions. At four weeks, the magnocellular regions are larger. However, the differences are minor. An overall comparison shows no significant differences, leading to the conclusion that the two segments have about an equal share of the total structure. In fact, the mean volume (N=5) of the parvocellular region is 5.1 cubic millimeters (S.D.=1.4) whereas that of the magnocellular segment is 5.9 cubic millimeters (S.D.=1.5).

Cell nuclear area.

The changes in nuclear size as a function of age are found in Figure 8 bottom. Mean cell nuclear area is largest at birth and decreases in size so that by 17 weeks it is only 61% of the neonatal value. Similar to the reduction observed in the mean somal area, the decrease occurs mostly in the first month. When nuclei are separated into groups by cluster analysis of their corresponding somata an Analysis of Variance shows that the nuclei of the cells in the parvocellular regions are significantly smaller than those in the magnocellular areas ($F(1,4)=162.6$, $p<0.05$).

Although patterns of change in somal and nuclear areas are quite similar, (compare Figure 8 top and bottom) and correlate significantly at each age ($p<0.01$) (Table 6), the perikaryon/nucleus ratio increases steadily after the first week from a low of 1.2 to 1.7 at 17 weeks.

Cell density.

The number of cells per cubic millimeter in each sample field was calculated for each monkey. The number of fields ranged from 67 in the newborn to 95 in the four-week old. A mean somal density was determined for each subthalamic nucleus as a whole and, separately, for magnocellular and parvocellular regions. The general shapes of the three functions are similar and, as illustrated in Figure 14 top, show an overall increase from birth to 17 weeks. The regional patterns are not identical, however. The density increases in both magnocellular and parvocellular areas in the first four weeks. By the seventeenth week, however, the density value has returned to within 0.4% of the level at birth in the magnocellular regions. In contrast, the number of cells per cubic millimeter is even greater in the parvocellular regions at 17 weeks than it was at four weeks. This value represents an increase of 21% in regional density from the value in the neonate. Consistently, at each age, there is higher density in the parvocellular region. The differences between regions are significant ($F(1,4)=277.73$, $p<0.05$).

Table 6

Correlation between Somal and Nuclear Areas

Age (weeks)	Number	Correlation Coefficient (r)
0	390	0.41
1	743	0.57
4	692	0.63
8	637	0.59
17	519	0.67

Figure 14. Mean Neuronal Density (top) and Total Number of Neurons (bottom) as a function of age.

Top: mean neuronal density for the total cell population of the subthalamic nucleus (solid diamond) and for separate magnocellular (open diamond) and parvocellular (solid square) regions. Standard errors of the means ranged from 331 to 491.

Bottom: total number of neurons. Symbols as above. The increase during the first week may be artefactual (see text).

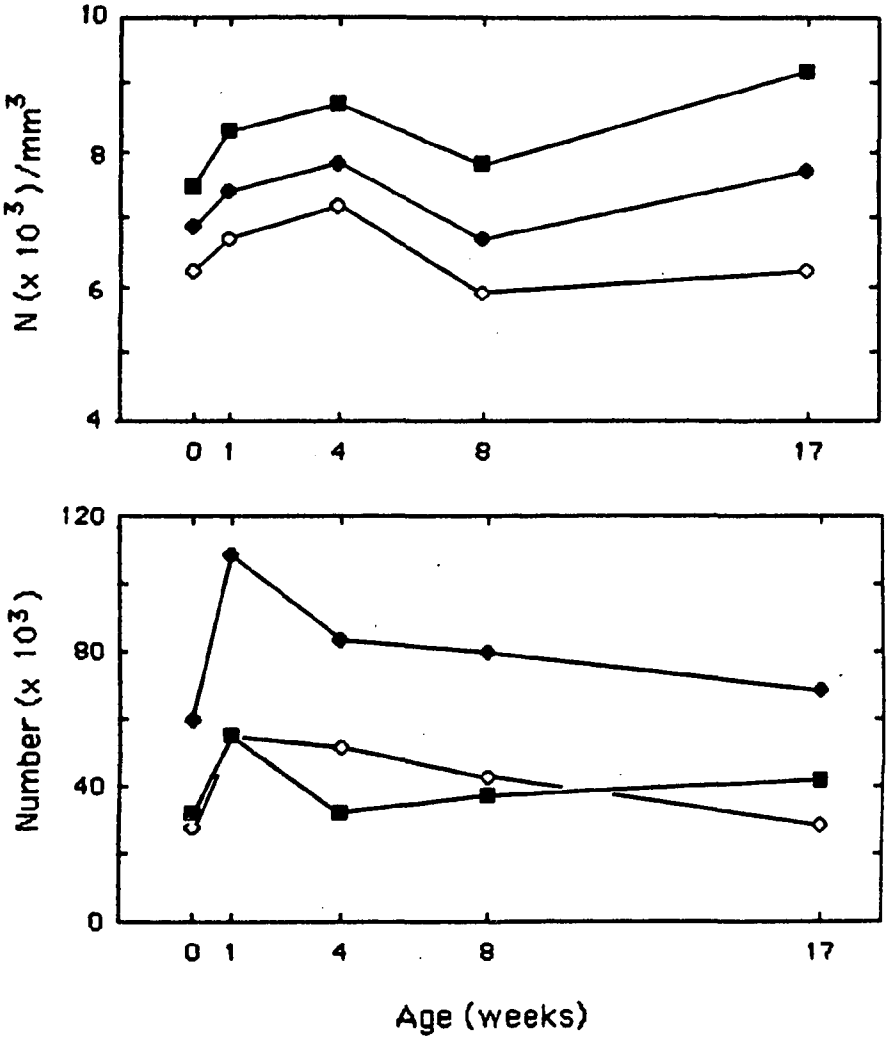
10
8
6
4
N (x 10³)/mm³
0 1 4 8 17
120
80
40
0
Number (x 10³)
0 1 4 8 17
Age (weeks)

Total cell number.

The estimated total number of cells in the right subthalamic nucleus (Figure 14 bottom) was smallest in the neonate (67,000) and greatest in the one week old monkey (111,000). The values decreased from one to seventeen weeks. Further, the estimated total numbers of cells in the magnocellular and parvocellular regions, apparently peak at one week and decline thereafter. This is noted in both segments but stabilization is attained in the parvocellular region within the first month whereas the decline continues throughout the entire period of study in the magnocellular component. It should be noted that the unexpected increase in cell numbers during the first week is not accompanied by any evidence of mitosis and could, therefore, be due to an artefact created by the selection of the counting element (see Discussion).

Electron Microscopy

Qualitative Observations

Neuronal somata.

Portions of cell somata and nuclei were included in electron micrographs of fields selected for the determination of the percentage of neuropil within the subthalamic nucleus. Figure 15, taken from a one week old monkey, shows the deeply invaginated nuclear envelope characteristic of subthalamic neurons. Ribosomes, which fill the nuclear invagination, are found throughout the

Figure 15. Electron micrograph of a portion of the cell body of a subthalamic neuron from a one week old monkey (#1018). The invaginations of the nuclear envelope (asterisks) are filled with ribosomes (X18,000).

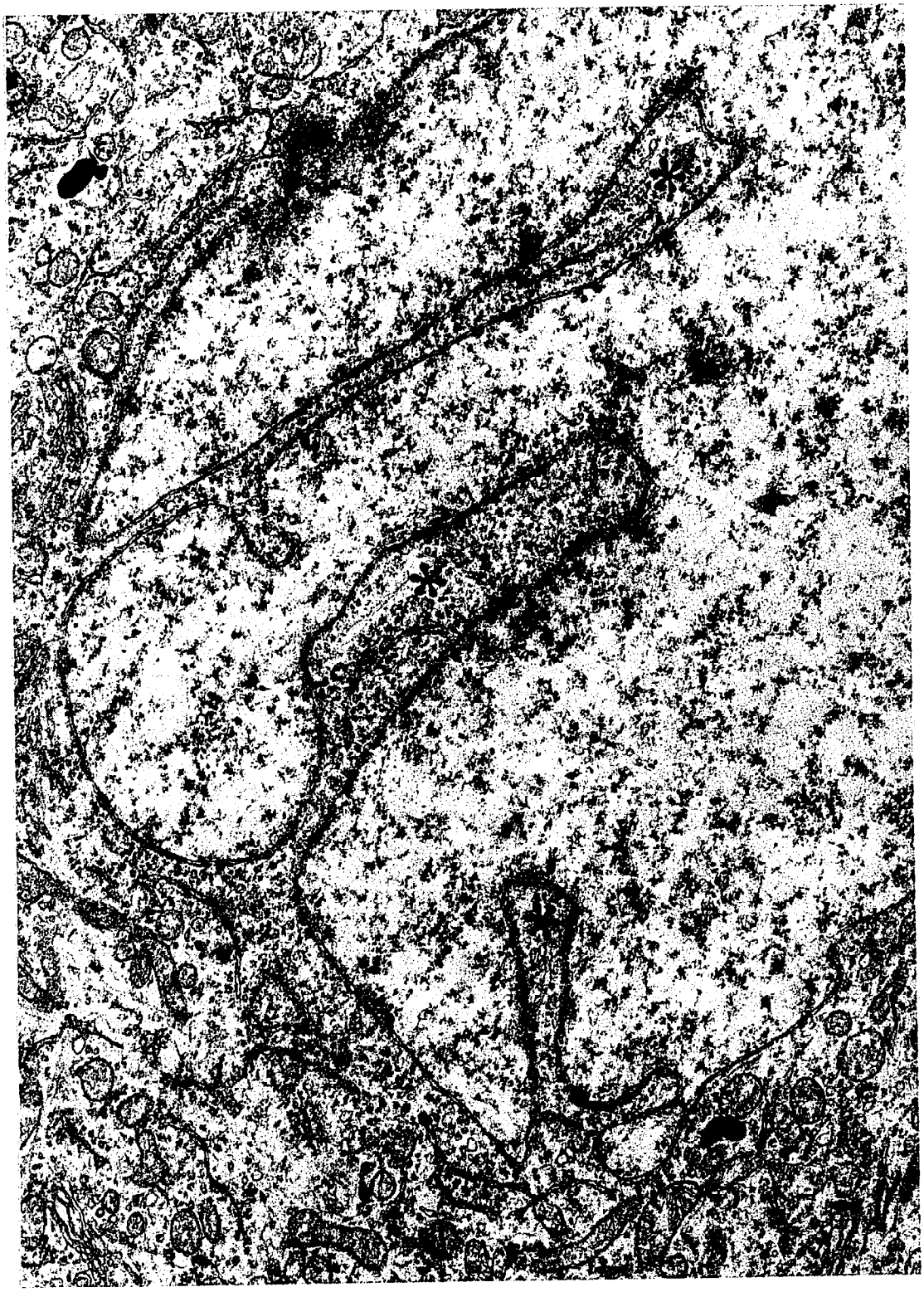

somal matrix, as well, most commonly in the form of polyribosomes or ribosomal rosettes. These either lie adjacent to the endoplasmic reticulum or are scattered freely throughout the cytoplasm.

The perikaryon has abundant mitochondria and Golgi apparatus in most of the cells observed (Figure .15). Granulated endoplasmic reticulum is typically in the form of single strands, although stacks occasionally are seen. In addition, subthalamic neurons contain many lysosomes.

Dendrites.

Dendrites of subthalamic neurons share many of the characteristics of the perikaryal cytoplasm. In Figure 16, taken from a 16-week old monkey, the emerging dendrite contains many of the same organelles as the cell body from which it arises. Figure 17 shows a more distal, tapering dendrite from the same monkey. In addition to abundant mitochondria, it contains strands of rough endoplasmic reticulum, polyribosomes and lysosomes. These organelles appear to be relatively confined to the thicker, more proximal portions of the dendrite. The thinner portion, seen at the lower left of the micrograph, contains parallel strands of microtubules. While the dendritic spines apparent in this micrograph are short and thick, subthalamic neuropil contains dendrites with long, thin spines as well.

In micrographs of neuropil from the neonatal monkey, dendritic growth cones were identified. In Figure 18, the characteristic pale cytoplasm and swollen appearence of the

Figure 16. Part of a neuron from the subthalamic nucleus of a 16-week old monkey (#1006). The emerging dendrite (D) arises from a cell body which contains numerous organelles. Part of the nucleus (N) is shown as well. (X18,000).

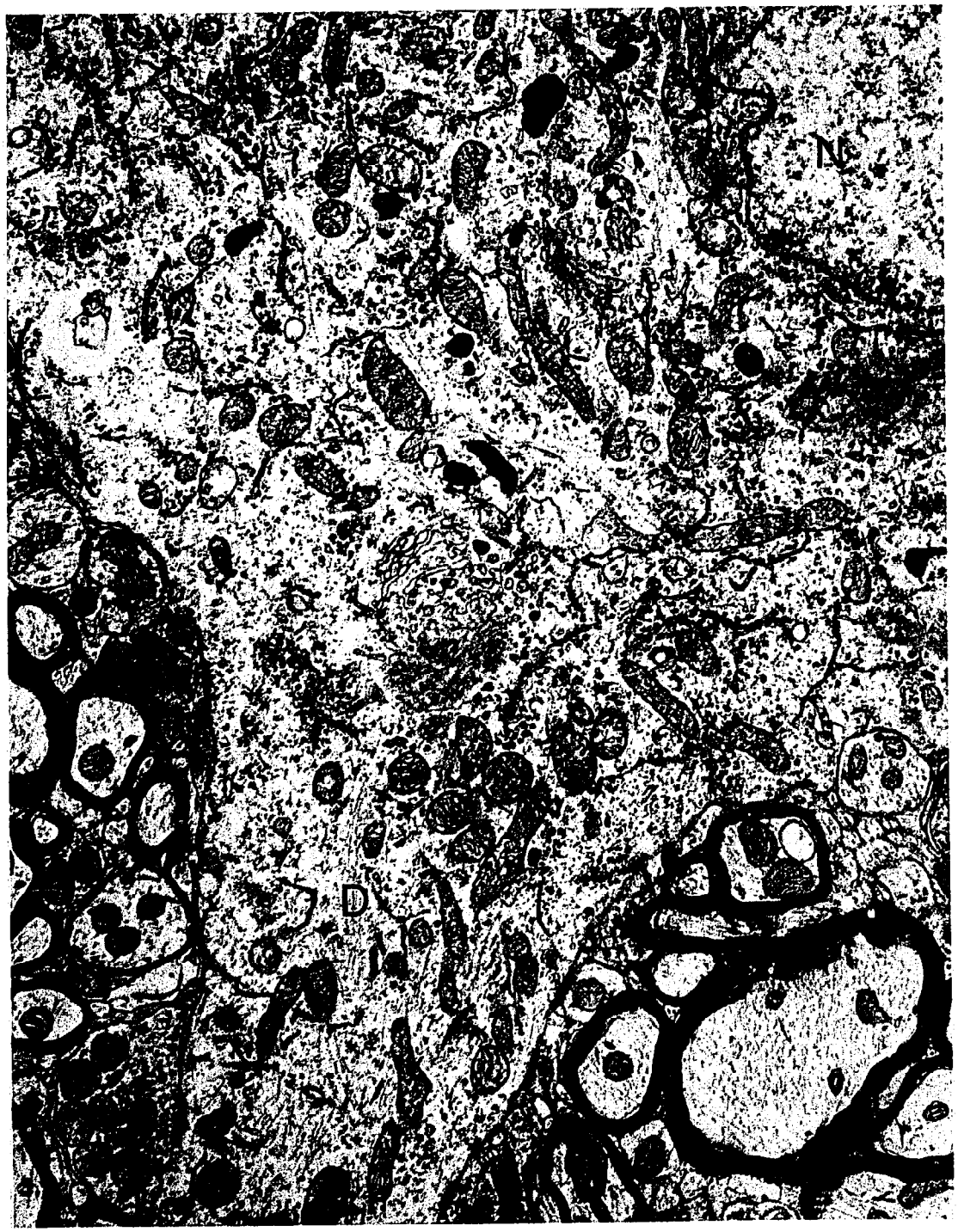
N
D
N

Figure 17. An emerging dendrite of a subthalamic nucleus neuron of a 16-week old monkey (#1006). Both mature (arrowheads) and immature (arrows) synapses are present. There are two spines (s), the upper one containing a multivesicular body. The large vesicle opening into the extracellular space (curved arrow) may represent an addition of membrane to the dendrite (X25,000).

Figure 18. Growth cones (C) in the neuropil of the newborn monkey (#1020), probably of dendritic origin, characterized by a pale matrix, containing smooth endoplasmic reticulum, enlarged cisterns, coated vesicles and an occasional mitochondrion.

Top: a cross section of a cone in contact with an axonal profile.

Bottom: a longitudinal section of a growth cone. (X30,000).

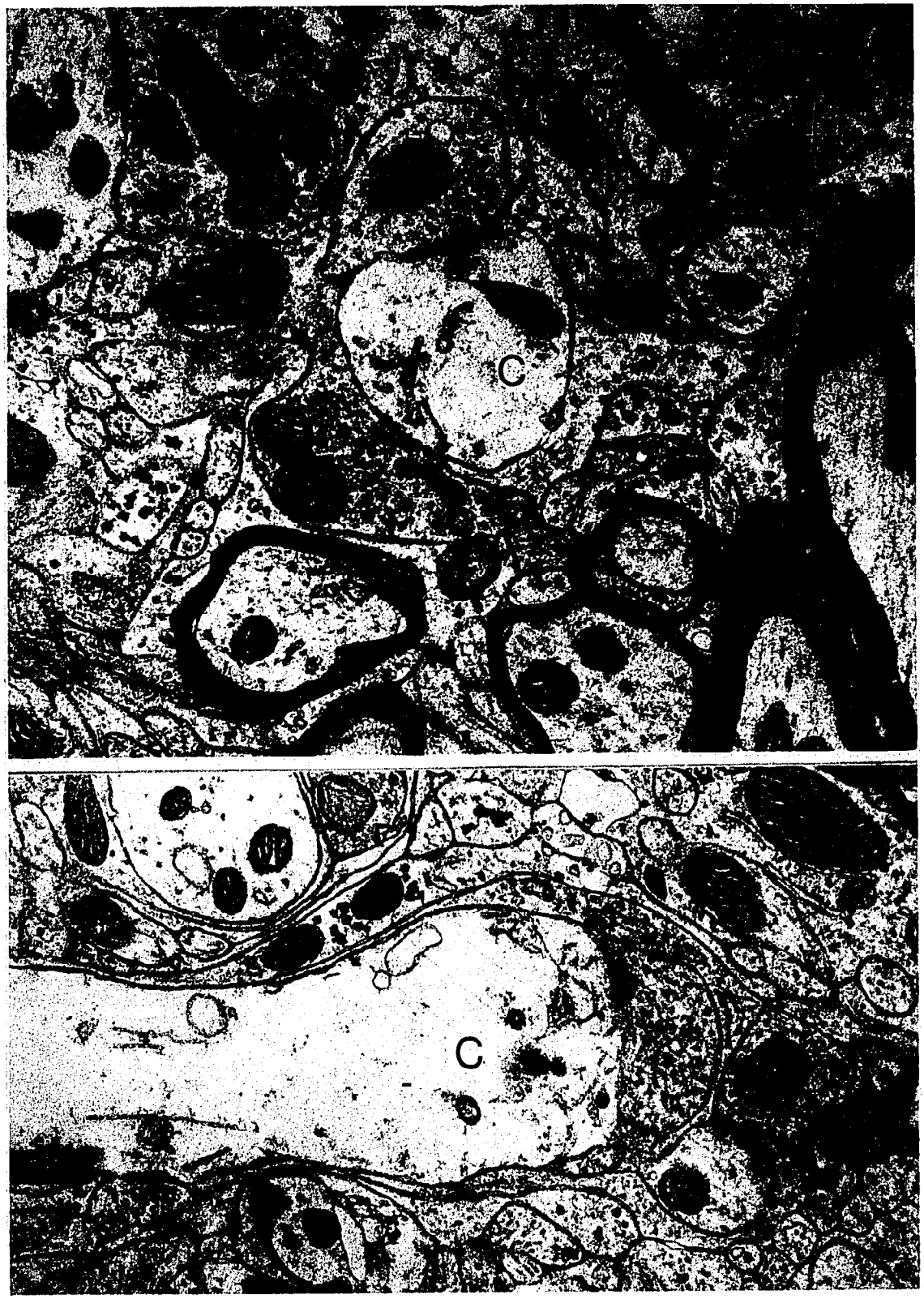
C
C

cones are shown in cross-section (top) and longitudinally (bottom).

Axons.

Many myelinated axons are observed within the subthalamic nucleus. The differences between axons are best determined by analysis of their numerous terminal boutons. These appear to be of at least two types: one, that is more commonly seen, is characterized by the presence of flat or pleomorphic synaptic vesicles; the other, less frequently observed, contains many round vesicles. Examples of both types of terminal are clearly identifiable in Figures 19-23, which are representative samples of neuropil, randomly selected from the subthalamic nucleus of each monkey used in the electron microscopic study.

Axonal degeneration is evident in micrographs taken of neuropil from the older monkeys. In the first micrograph, (Figure 24 top), taken from the 16-week old monkey, a vesicle filled terminal includes a region of hyper-filamentosis. The electron dense terminal in Figure 24 middle, from the same animal, is surrounded by astroglial processes. Both normal myelinated axons, as well as two axons in the process of degeneration, are shown in Figure 24 bottom, a micrograph of neuropil from the four-week old monkey.

Synapses.

A variety of synapses are observed in electron micrographs of the subthalamic nucleus. Contacts differ

Figure 19. Representative electron micrograph of randomly selected neuropil from the subthalamic nucleus of a newborn monkey (#1020). Notation as in Figure 15. Mature synapses include two contacts between a single dendrite (D) and axon terminals containing pleomorphic vesicles. A probably degenerating element (d) is seen at the lower left corner of the micrograph (X25,000).

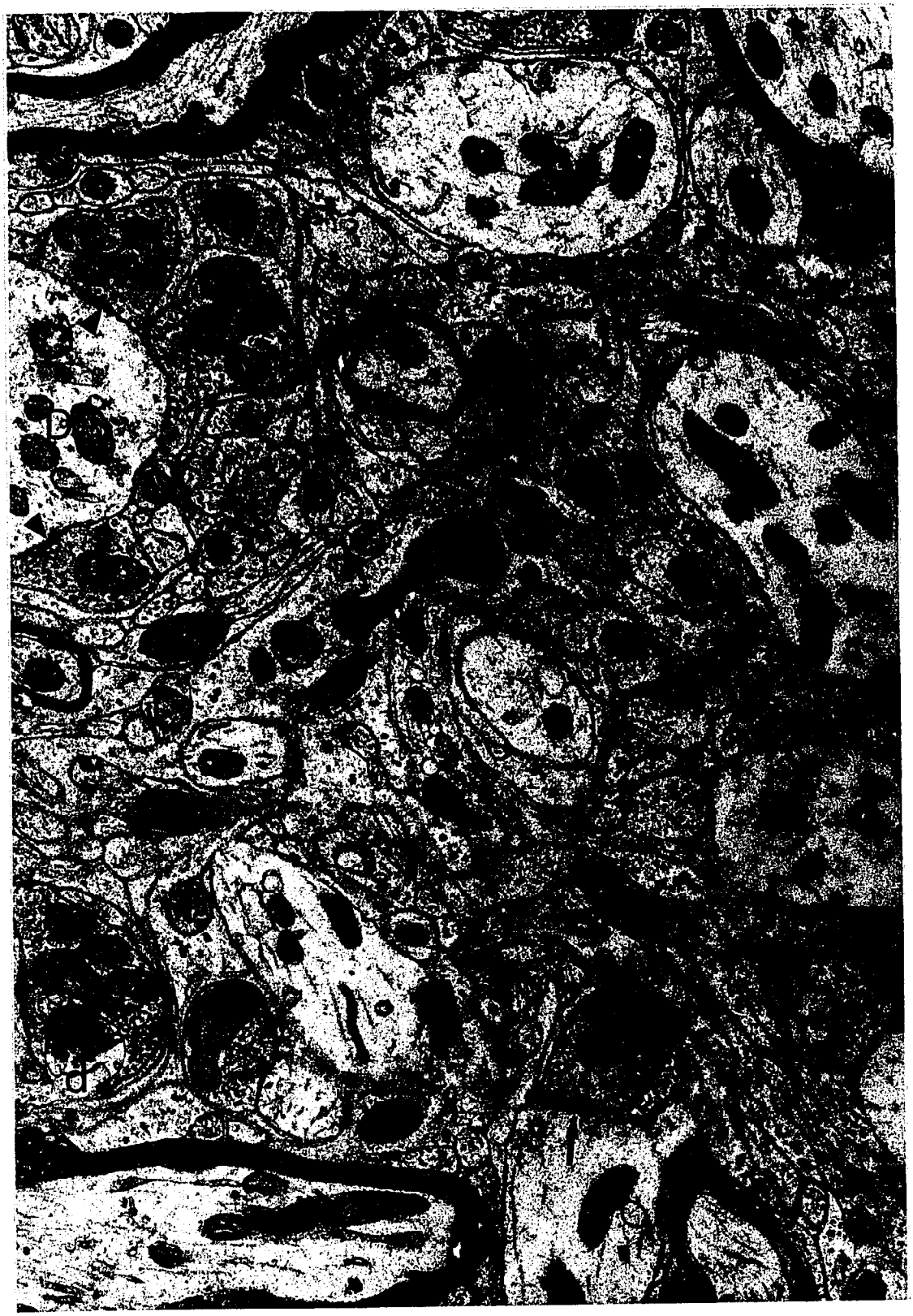
D
d

Figure 20. Electron micrograph of randomly selected neuropil from the subthalamic nucleus of a one week old monkey (#1018). Notation as in Figure 15. Both round vesicle (R) and pleomorphic vesicle (P) containing terminal boutons are shown, as are contacts with dendritic spines (s). There are signs of immaturity which include the presence of a degenerating element (d) and an axon with few myelin wrappings adjacent to a more heavily myelinated axon (MA). (X25,000).

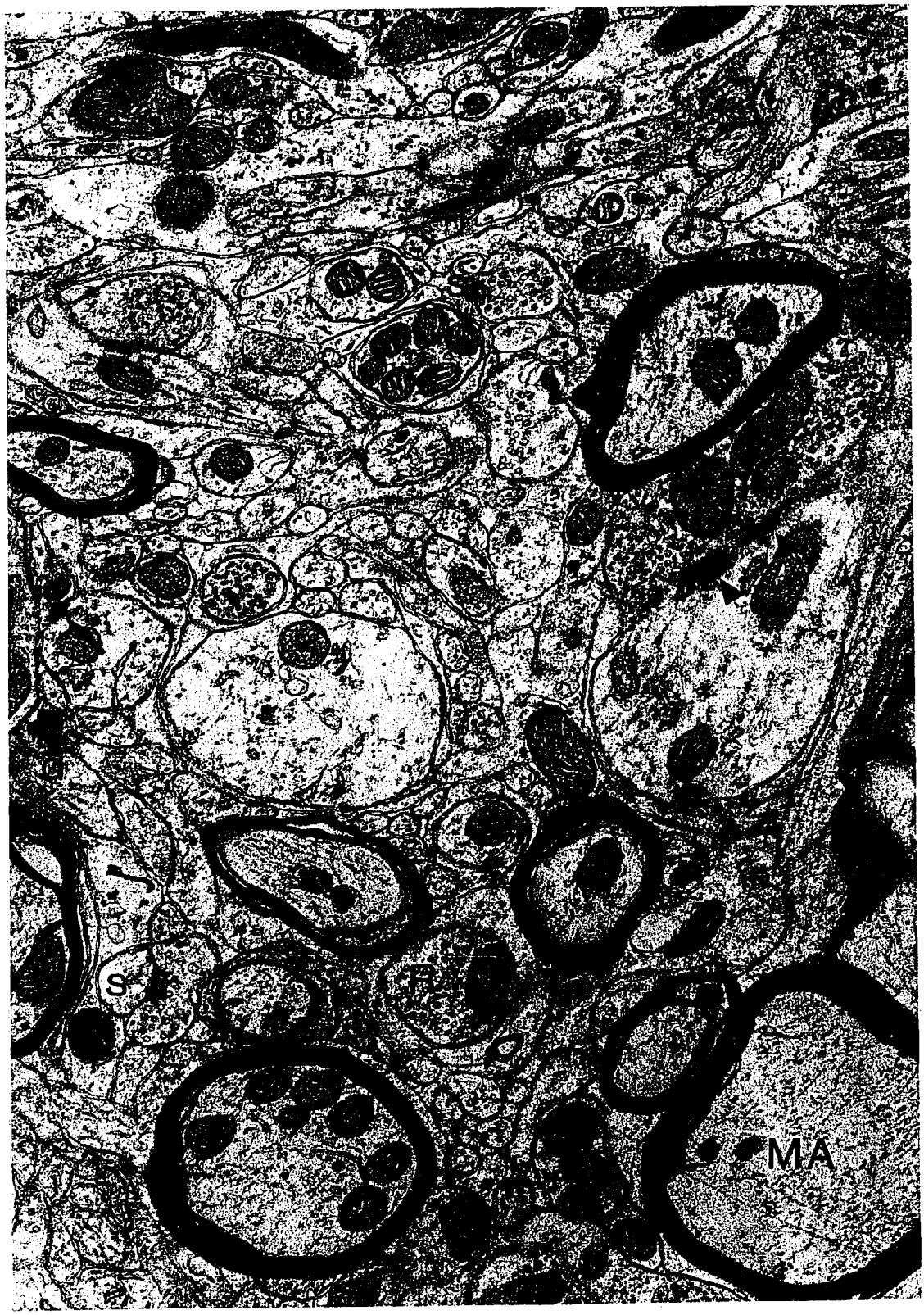
S
MA

Figure 21. Electron micrograph of neuropil randomly selected from the subthalamic nucleus of a four-week old monkey (#1010). Notation as in Figure 15. Of particular note is a mature synaptic contact between two vesicle containing elements (open arrow) and a multiple contact by a single presynaptic terminal. (X25,000).

Figure 22. Electron micrograph of randomly selected subthalamic neuropil of an eight-week old monkey (#1016). Notation as in Figure 15. A round vesicle containing element is forming a synapse with a more sparsely filled vesicle containing profile (open arrow). Also present is an axon terminal containing dense core vesicles (dv). (X25,000).

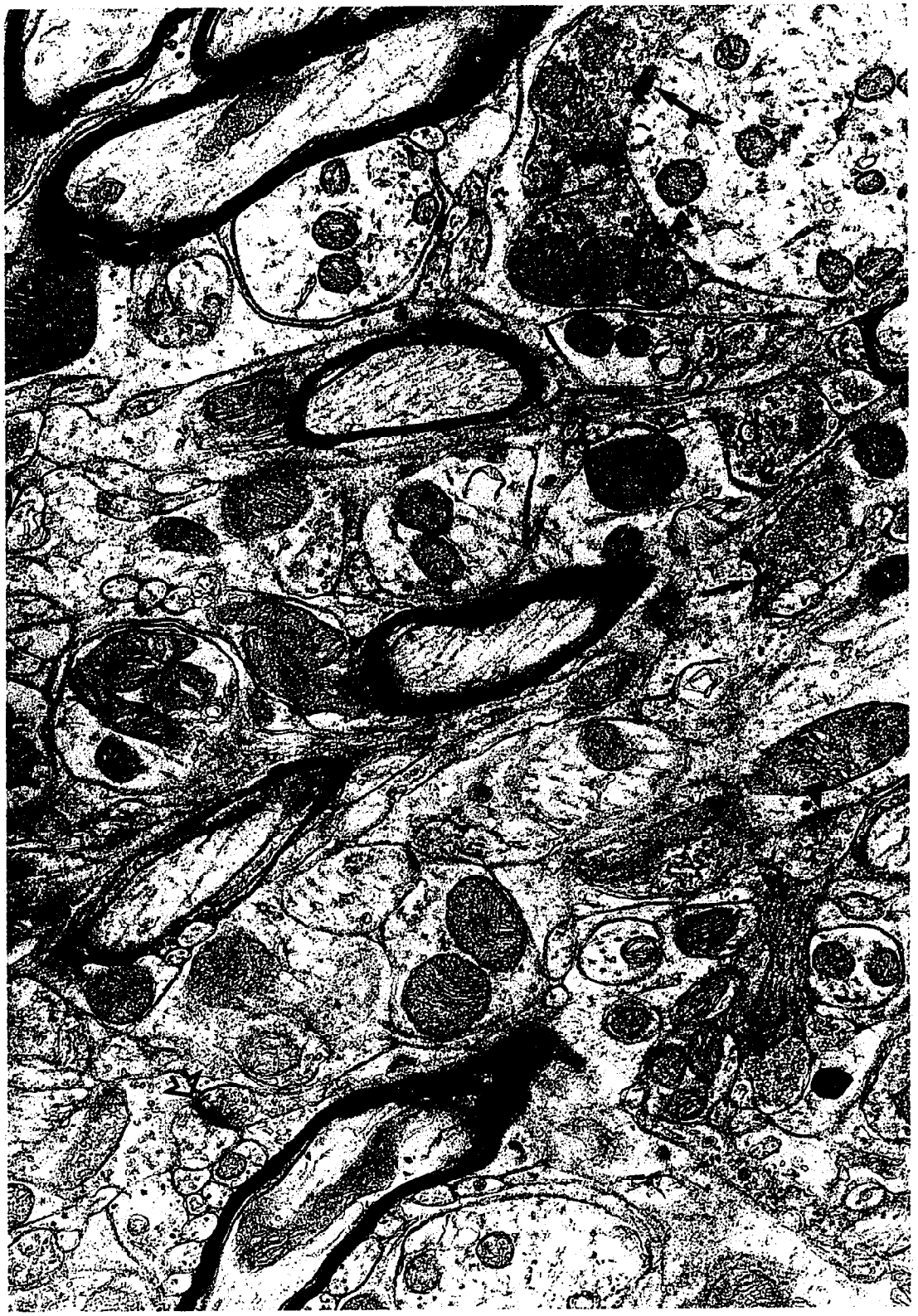

Figure 23. Electron micrograph of randomly selected subthalamic neuropil from a sixteen-week old monkey (#1006). Notation is as in Figure 15. The varicose dendrite has multiple synapses. These include a mature contact by a small round vesicle containing terminal (R) as well as an immature synapse by a very large terminal filled with pleomorphic vesicles (P). (X25,000).

Figure 24. Examples of axonal degeneration. Top: a vesicle filled terminal has a region of hyperfilamentosis (arrow).

Middle: an electron dense terminal is engulfed by an astrocytic process (arrow). Both top and middle electron micrographs are taken from the subthalamic nucleus of a sixteen-week old monkey (#1006).

Bottom: two myelinated axons in the process of degeneration (asterisks) from a four-week old animal (#1010). (X30,000).

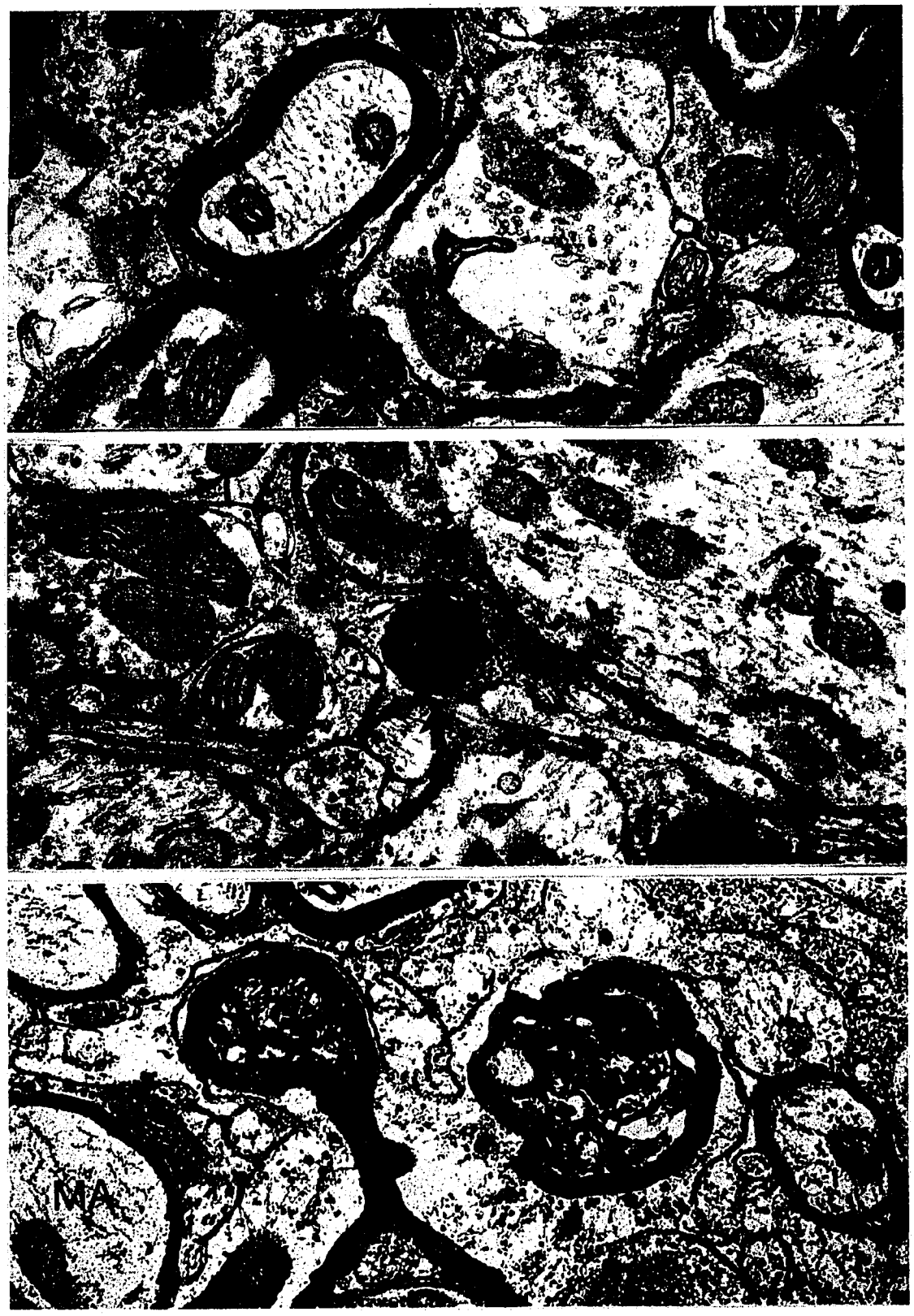
MA

with regard to the symmetry of the membrane thickenings, the maturity of the synapses, the shape of the vesicles in the presynaptic boutons, and the elements involved in the contact. Both axosomatic and axodendritic synapses are present. The latter include contacts with the shaft of the dendrite as well as with dendritic spines. Examples of axodendritic and axospinous contacts are shown in Figure 17. Particularly noteworthy are synapses between vesicle containing profiles. These, indicated in Figures 21 and 22 by open arrows, are seen only in the 4, 8, and 16 week old monkeys.

Quantitative Analysis

Neuropil Measurements.

The percentage of tissue remaining after subtraction of areas occupied by blood vessels, myelinated axons and glial and neuronal somata is graphed in Figure 25 top. There is a monotonic decline of 25% from birth to 16 weeks. The greatest proportion of that decline occurs within the first postnatal week.

Changes in total neuropil volume (percent neuropil times total nuclear volume) as a function of age do not parallel those of the proportion of the subthalamic nucleus occupied by neuropil. In fact, there is an increase in neuropil volume at 1 week and then a rather precipitous decline of 46% during the ensuing two months with stabilization thereafter (Figure 25 bottom).

Figure 25. Amount of Neuropil as a Function of Age.
Top: relative area of neuropil in random sections after subtraction of areas occupied by glial and neuronal somata, myelinated axons and blood vessels.
Bottom: estimated volume of neuropil obtained from the data above and the estimated total volume of the nucleus (see Figure 6). The two values derived from opposite hemispheres of the same animal at 0 and 1 week. For the remaining ages, a mean nuclear volume was used.

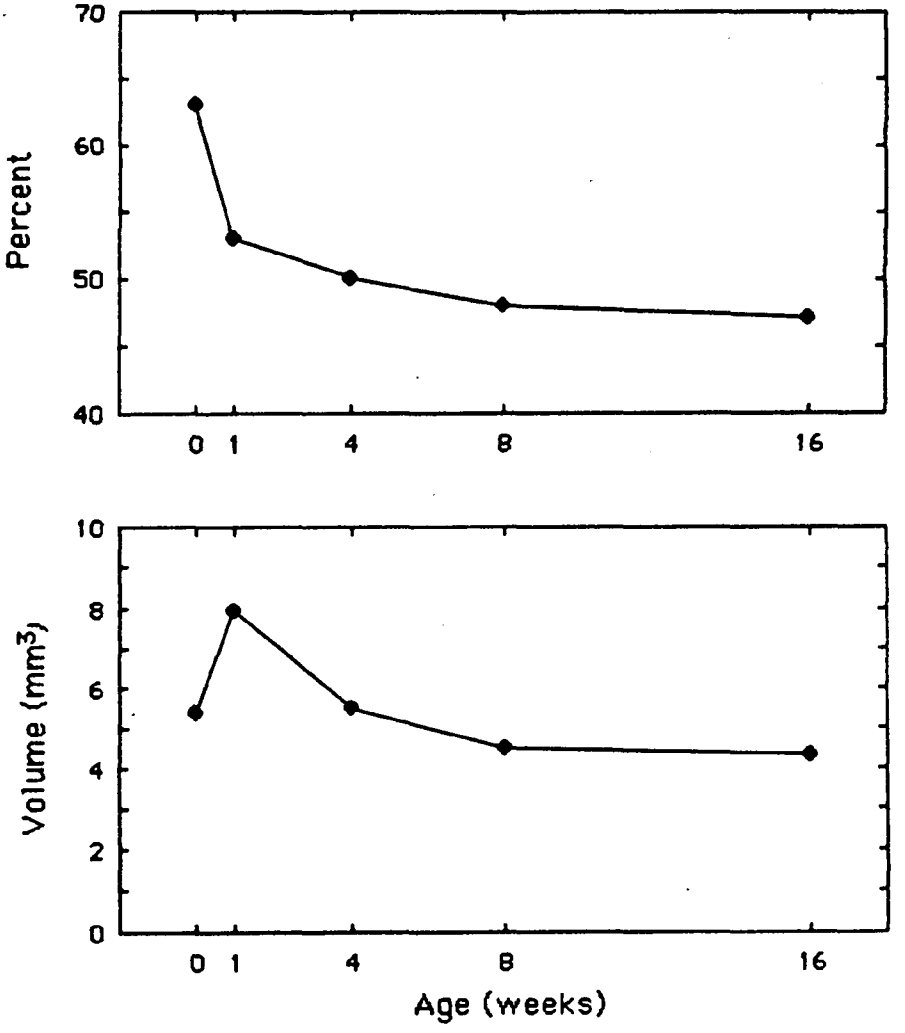
70
60
50
40
Percent
0 1 4 8 16
10
8
6
4
2
0
Volume (mm3)
0 1 4 8 16
Age (weeks)

Size Distribution of synaptic plaques.

The size distribution of synaptic plaques was reconstructed from measurements of synaptic profiles appearing in electron micrographs. In order to control for intra-animal sample variability, a special algorithm was applied which grouped the micrographs from each monkey randomly into four sets (see Methods section).

A distribution of synaptic plaque diameters was produced for each of the five monkeys by application of the Coupland method of stereological analysis. The size distribution of synaptic plaques was based on division of the data into seven categories. This was the maximum number of groups which produced a full distribution for four of the five animals thereby facilitating comparison between them. In the fifth animal, which was the newborn, this condition could not be met. Several size intervals were tested, none of which produced a full distribution for the newborn monkey; this was not accomplished even when three intervals were used. However, for the sake of comparison, eight categories were used for this animal. Figure 26 shows that whereas there is overlap in the distribution of profiles and synaptic plaques, there are more large-diameter plaques than there are profiles of the same size. This finding was expected because the stereologic method permits correct attribution of eccentrically cut small profiles to the larger size categories of which they are true members. Negative numbers in the smaller diameter intervals represent

Figure 26. Histograms of synaptic profiles (open bars) and synaptic plaques (hatched bars). Class width: 0.125 micrometers. The number of profiles measured ranged from 91 to 134. Note the expected shift to the right of the plaques distribution obtained by the Coupland Stereologic method. The negative values in the smallest class, present at 0, 4, and 16 weeks, represent plaques which were too small to be identified. The mean size of synaptic plaques ranges from 0.27 micrometers at 0 and 4 weeks to 0.33 micrometers at 16 weeks.

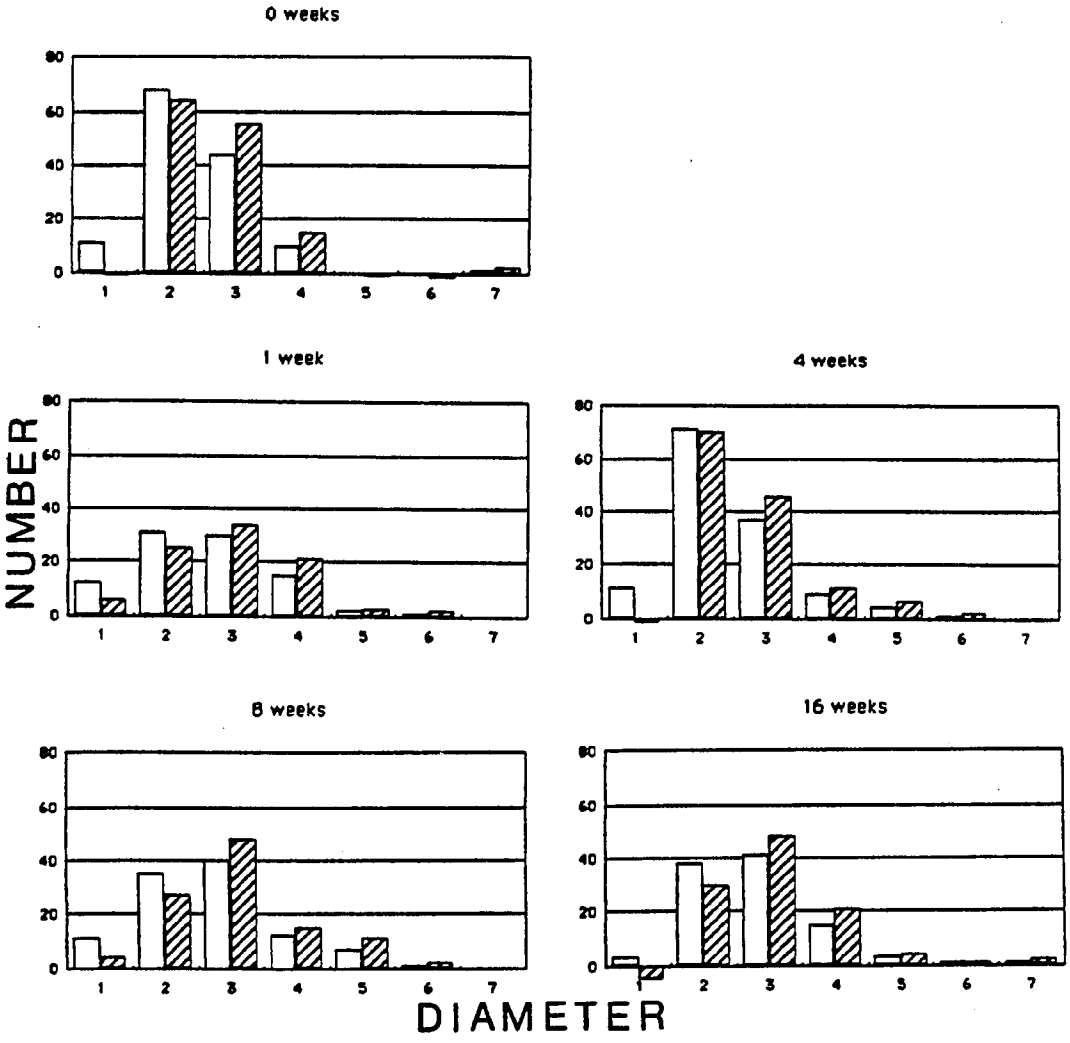
0 weeks
1 week
4 weeks
8 weeks
16 weeks
NUMBER
DIAMETER
0
20
40
60
80
1
2
3
4
5
6
7

elements too small to be identified. There are some cases, however, as in the 1 and 8 week old animals, in which there are no negative remainders probably because the profiles belong to higher diameter plaques within that interval and were therefore recognized.

At all ages, the largest number of plaques falls between 0.1 and 0.4 micrometers in diameter. The mean diameters, range between 0.27 micrometers at birth and 0.33 micrometers at 16 weeks, the maximum occurring at the latter age. In all cases, the standard error of the mean was 0.01.

Synaptic density.

The computerized application of the Coupland stereologic method produced a calculation of the density of synaptic plaques per cubic millimeter of neuropil. This value was obtained by computation of the partial densities for each size interval adjusted by the corresponding Abercrombie correction factor (Abercrombie, 1948). The partial densities were summed yielding the total synaptic density for the neuropil at each age. The synaptic density for the entire subthalamic nucleus was given as the productof the latter value and the percentage of neuropil previously determined. These results are plotted in Figure 27, top, which shows an overall decline during the period of study.

Total Number of Synapses.

The decline in synaptic density noted above may be misleading since it may only reflect a dilution effect due

Figure 27. Synapses in the Subthalamic Nucleus as a Function of Age.

Top: synaptic density (number of synapses per unit volume of tissue).

Middle: total number of synapses (synaptic density times total volume of nucleus) indicated by solid diamond, and of mature (open diamonds) and immature (solid squares) contacts. The values of mature and immature at 4 weeks overlap.

Bottom: cumulative area of synaptic plaques (total number of synapses times mean area of synaptic plaques).

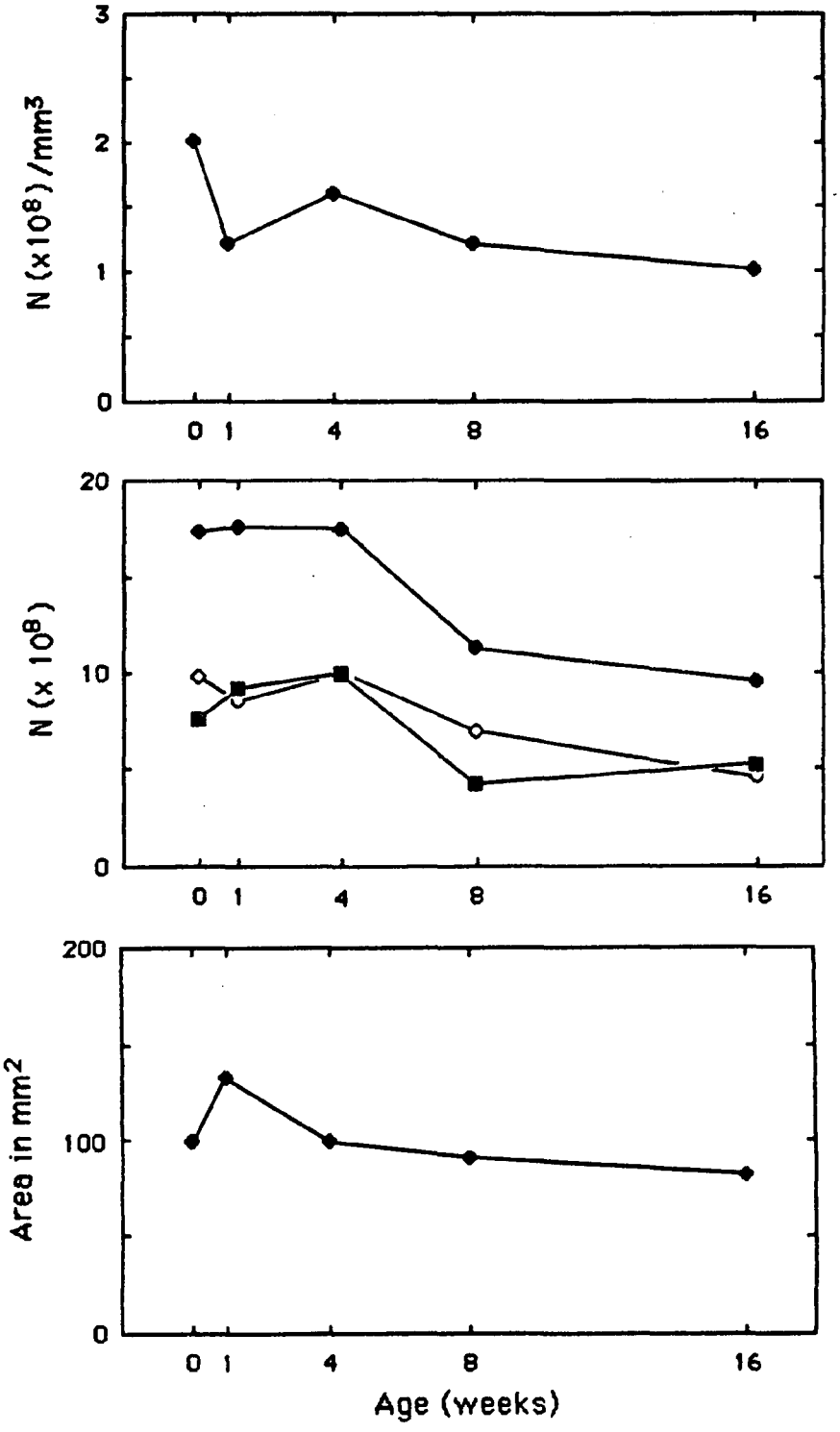
3
2
1
0
N (x10⁸) /mm³
0 1 4 8 16
20
10
0
N (x 10⁸)
0 1 4 8 16
200
100
0
Area in mm²
0 1 4 8 16
Age (weeks)

to total growth of the structure. This qualification may be obviated by estimating the total number of synapses in the entire nucleus obtained by the product of synaptic density and subthalamic nucleus volume. As Figure 27 middle shows, the total number of synaptic plaques within the subthalamic nucleus is stable during the first postnatal month. There is a marked decline in the second month and a lesser but continuing decrease in the number of synaptic plaques thereafter, so that by 16 weeks the value is only 55% of that at birth. It is possible that the number of plaques does not reach asymptote within the period of study. There is a highly significant negative correlation between age and the total number of synapses ($r=0.93$, $p<0.01$).

When synaptic plaques are divided into two subpopulations of mature and immature synapses (see Methods section), the levels at 16 weeks are 46% of the neonate for the mature contacts, and 68% for the immature synapses. From birth to 16 weeks, as Figure 27 middle illustrates, there is an overall elimination of synaptic plaques, the greatest proportion of which occurs in the second month but continues at a slower rate thereafter.

Cumulative area of synaptic plaques.

The total area of synaptic contacts is graphed in Figure 27 bottom as a function of age. It is apparent that the cumulative area of plaques peaks in the 1 week old monkey. There is a sharp drop in the area of plaques in the subsequent 3 weeks and a monotonic decline thereafter,

reaching a 62% level of the peak value at 16 weeks. The decline in cumulative plaque area does not appear to have ceased during the period of study.

Chapter IV

Discussion

The present study demonstrates that substantial changes in the neuronal architecture of the macaque subthalamic nucleus which take place during the first four postnatal months are detectable at both the light microscopic and ultrastructural levels. In addition, statistically significant and anatomically meaningful regional differences are found in the size and distribution of subthalamic neurons at all ages examined. These results must be viewed in light of the limited number of animals available for the investigation. In total, subthalamic nuclei were obtained from eleven monkeys. Nuclei from two monkeys each were available at three of the five ages for which volumes were estimated, but data were accumulated from only one animal at each age for measurements of somal area and lengths of synaptic profiles. Both the limited availability and prohibitive cost of infant macaques made it impossible to increase the number of subjects. This was particularly true with the youngest ages which require subjects derived from timed pregnancies. Such a limitation has been characteristic of most developmental studies in monkeys (Rakic, 1977; Gottlieb, et al, 1985; Holstein, Pasik and Pasik, 1985). The intrasubject consistency is assured, however, by the sampling methods used to obtain the data on both soma and synapses. On the former, despite the small number of monkeys, the cell sample size was large enough to

find statistically significant differences in cell somal and cell nuclear size both as a function of age and as a result of location within the structure. On the synapses, the number of profiles measured for each monkey was increased until the predetermined criterion of intrasubject variability was reached.

In order to facilitate the following discussion, Table 7 gives a summary of the main changes in the monkey subthalamic nucleus during the first four postnatal months. These are: 1) minimal alterations in the nuclear volume; 2) overall decreases in somal and cell nuclear sizes; 3) a regional differentiation into a magnocellular area and a parvocellular segment; 4) an overall decline in total cell numbers; and 5) a marked synapse elimination.

Volume of the Subthalamic Nucleus in Development

The volumes of the subthalamic nuclei estimated in this study, varied between approximately 6 and 15 cubic mm. At the ages where volumes were estimated for two monkeys each, the intersubject variability was particularly high at one week. Although the mean volumes did not change much, when only the animals derived from dated pregnancies are considered, there appears to be an initial increase during the first week followed by a progressive decrease. In any event, the values at birth and at 17 weeks are quite similar. A few such measurements can be found in the literature on adult monkeys but results are difficult to compare with the present findings because no correction

Table 7

Summary of Main Findings

	Postnatal Weeks 0-1	1-4	4-8	8-17	% Birth Value at 4 Months
Mean Volume:	-	-	D	-	92
Mean Somal Area					
Total:	D	D	I	D	67
Magnocellular Area:	D	D	I	D	70
Parvocellular Area:	D	D	I	D	62
Cell Nuclear Area:	D	D	I	D	61
Cell Density					
Total:	i	-	D	I	112
Magnocellular Area:	i	-	d	I	121
Parvocelluar Area:	i	i	D	-	100
Number of Cells					
Total:	I	D	-	D	116
Magnocellular Area:	I	-	D	D	104
Parvocellular Area:	I	D	I	i	126
Neuropil Percentage:	-	d	-	-	75
Neuropil Volume:	I	D	D	-	80
Number of Synapses					
Total:	-	-	D	D	55
Mature Synapses:	D	I	D	D	46
Immature Synapses:	I	i	D	I	68
Cumulative Synaptic Area	I	D	d	d	82

I = Increase of > 10% i= Increase of >5% and =< 10%
D = Decrease of > 10% d= Decrease of >5% and =< 10%
- = No Change

for shrinkage is given in those studies (Carpenter and Carpenter, 1951; von Bonin and Shariff, 1951).

Alterations in subthalamic nucleus volume, such as those found in the present investigation, may be due to changes in the number and size of neurons and their processes as well as of non-neuronal elements such as glia, myelin and blood vessels. During the interval in which the volume increases, the mean cell size in both the magnocellular and parvocellular regions decreases substantially, as does the percentage of neuropil within the nucleus (Table 7). Therefore, volumetric change during this period must be attributed to the growth of non-neuronal elements such as blood vessels and glia as well as to an increase in myelination.

It is interesting to compare volumetric changes in the subthalamic nucleus with those of other brain structures during the same postnatal period. For example, volumes of the lateral geniculate nuclei (LGNd) and of striate cortex were measured in infant monkeys, some of which were used in the present study (Gottlieb et al., 1985). The striate cortex increases in volume from birth to, and perhaps beyond, the study interval of 17 weeks. Of particular interest is the comparison with the LGN which, being also of diencephalic origin, is essentially of sensory rather than motor nature. The pattern of change in the LGNd is more like that of the subthalamic nucleus in that a small increase is followed by a slight decline. However, unlike

the case of the subthalamic nucleus, the overall volume of the LGNd is larger at 17 weeks than it was at birth. The greatest proportion of volumetric change in the LGNd occurs in the parvocellular laminae; the magnocellular layers are essentially stable from birth to 17 weeks (Gottlieb, et al, 1985). Regional volumetric differences similarly exist within the subthalamic nucleus, although in this structure the magnocellular and parvocellular regions are less clearly demarcated anatomically than are the LGNd laminae. In the current study, the volumes of the two regions of the subthalamic nucleus are approximately equal in both the neonate and seventeen week old monkeys, but at the intermediate ages, the magnocellular volume is larger. The late decline in the volume of the magnocellular region may be due to the substantial loss of large cells during the third and fourth postnatal months, whereas the number of cells in the parvocellular areas is virtually stable during this interval. The difference in pattern of volumetric changes between the subthalamic nucleus and the LGNd may reflect either the importance of sensory experience in the shaping of the LGNd during the early postnatal period or the relative maturity of the subthalamic nucleus during this interval.

Somal and Cell Nuclear Sizes in Development

Between 390 and 743 cells were measured at ages 0, 1, 4, 8, and 17 weeks, using one monkey at each age. The 0 and 1 week old monkeys were derived from timed pregnancies. The

number of cells was sufficient to demonstrate significant differences in mean cell size both as a function of age as well as location within the nucleus. The mean cell size declines in both the parvocellular and magnocellular regions during the period of study, the greatest decrease occurring during the first month. On the average, cells in the 17-week old monkey are one third smaller than those in the newborn monkey. In the study of somal size in the lateral geniculate nucleus, which uses some of the infant monkeys in this investigation, increases in somal area are found in both the magnocellular and parvocellular regions (Gottlieb et al, 1985). However, whereas somal size continues to increase in the magnocellular region, by 17 weeks it subsides to close to the neonatal value in the parvocellular region.

The finding of decreases in somal area of subthalamic neurons during the early postnatal period is consistent in both regions of the nucleus and contrasts with developmental changes in somal area of lateral geniculate neurons in some of the same animals. It is possible that this decrease in neuronal area is a function of the relative maturity of this motor structure at birth. It is known that even among the structures which modulate the output of the neostriatum, the maturation of the subthalamic nucleus precedes that of the globus pallidus and substantia nigra (Richter, 1965). Finally, in a comparison of cell size in visual and motor cortices in rabbit, for example, cells in motor cortex were

found to approximate adult values at birth, whereas cells in visual cortex did not reach mature size until 10 days later (Vrensen, deGroot and Nunes-Cardozo, 1977). Finally, the increase in the perikaryon/nucleus ratio as a function of age, found in the present study, may indicate a slowing of, nuclear activity over time in parallel with the stabilization of growth.

Regional Differentiation of the Subthalamic Nucleus

At all ages, there is a gradient in the distribution of somal size such that the smallest cells are in the dorso-medial quadrant of the nucleus and the largest in the ventrolateral area. These results reflect the existence of at least two populations of cells which are defined by both size and location, and derive from a cluster analysis for the determination of significant differences in such populations within the subthalamic nucleus. Cluster analysis is a powerful statistical method which groups objects into classes on the basis of similarity with regard to some attribute, here somal size, and tests for significant differences between the groups (Engleman and Hartigan, 1983). The detection of two populations of cells whose sizes are significantly different, is of interest only insofar as they have anatomical and/or physiological relevance. When, as a result of the clustering, the sample fields are segregated on the basis of mean somal size, the groupings become of anatomical interest. In this study, across ages, the parvocellular fields are largely medial and

peripheral whereas the magnocellular fields are predominantly confined to the core of the structure.

The existence of anatomically separate subpopulations of cells within the subthalamic nucleus raises the question whether they perform physiologically different functions as well. It is clear that there are regional differences in afferentation and efferentation which may be important in this regard. In monkey, the major inputs into the subthalamic nucleus are not distributed uniformly. Those from the cerebral cortex (Hartman-von Monakow et al., 1979), and the lateral pallidal segment (Carpenter et al, 1981; DeLong, Crutcher, and Georgopoulos, 1985) terminate in the lateral, and probably magnocellular, region of the nucleus. And in cat and rat, the input from the centre median-parafascicular complex of the thalamus predominates in the rostral portion of the nucleus (Sugimoto, et al. 1983) which is found to be essentially parvocellular in the present study. Furthermore, restricted efferent regions of some specificity have also been noted, (Carpenter, et al, 1981a; Jackson and Crossman, 1981b), the rostromedial (parvocellular) segment of the nucleus projecting mostly to the lateral pallidal segment.

From the earliest descriptions of subthalamic morphology, observers have indicated that the medial portion of the nucleus contains small cells (Whittier and Mettler, 1949). The present study shows that not only are medial cells significantly smaller than those in the more lateral

portions of the subthalamic nucleus, but also that they are part of a more widespread parvocellular population. Some students of the subthalamic nucleus claim, however, that there is only one cell type within the structure (Yelnik and Percheron, 1979). These investigators assert, on the basis of observations in Golgi impregnated material, that quantitative descriptions of differences in cell type are artefacts of the orientation of the neurons measured within the nucleus. When neurons and their dendritic fields are orthogonally rotated, a single type is seen. In order to assess the validity of this criticism, we have measured subthalamic neurons in two adult macaques according to the same protocol described in the Methods section. In one monkey, the brain was sectioned coronally and measurements made of cells in the right subthalamic nucleus. In the second monkey, one hemisphere was cut in the sagittal plane and the other half in the horizontal plane. Cluster analysis was performed separately on the somal measurements for each animal and, in each case, two populations of cells differing significantly in size were found (unpublished observations). In the adult monkey, the results from the developmental series are replicated. The medial segment of the nucleus is parvocellular, independent of orientation of the section, as is much of the periphery. Further, the core of the structure is magnocellular. It is possible that in the Golgi study (Yelnik and Percheron, 1979), the authors dealt with a particular population of cells which, due to

the known capriciousness of the technique, were predominantly impregnated. Support for this interpretation is given by the report of more than one cell type based on axonal length (Rafols and Fox, 1976). It is especially noteworthy that the groupings produced by cluster analysis persist across ages and independently of the angle of sectioning of the brain.

Neuronal Density and Total Number

The changes in neuronal density during the first two months are characterized by a peak at four weeks which remains valid even if the increase noted in the first week were due to an artefact in the counting process (see below). After the second month, the overall density increases again but only at the expense of the parvocellular region, the magnocellular component showing early stabilization. At all ages, somal density is greater in the parvocellular region. During the first two months, there are approximately 25% more cells per cubic millimeter in the parvocellular regions than in the magnocellular areas. This proportion increases during the subsequent two months, so that the 17-week old monkey has nearly 50% more neurons per cubic millimeter in the parvocellular than in the magnocellular regions.

The results for the estimated total number of neurons were unexpected regarding the rather sharp increase noted during the first week. If genuine, this finding would indicate a certain degree of postnatal neurogenesis. Such

phenomenon has not been observed previously in the monkey brain (Rakic, 1985), and the absence of mitosis after careful review of the present material casts doubt on the validity of the observation. It is possible that not all the nucleoli, which served as counting elements (see Methods section), have reached a clearly differentiated stage during the first week and therefore a number of them may not have been counted. In fact, there is some evidence that a similar finding in the monkey lateral geniculate (Pasik, Pasik, and Holstein, 1984) could involve such an explanation (Pasik, personal communication, 1985). After the first week, there is a steady decline of the cell population that stabilizes in the parvocellular region after the first month, but continues, probably beyond the period of study, in the magnocellular division.

Prestige (1974) points out two problems in counting cells. The first of these is that of defining the cell population. This is certainly critical when attempting to count cells with characteristics which are not easily identifiable anatomically, as for example, cells with particular electrophysiological characteristics. However, in all cases, to reduce possible bias, it is essential that strict criteria be defined before counting and that the criteria be rigorously adhered to. In the present study, all cells which fell within the sample area and which had nucleoli were counted. It should be noted that, as pointed out above, the use of the nucleolus as the counting element

may have resulted in an underestimation of cell numbers in the subthalamic nucleus of the neonatal monkey.

A further problem in insuring accuracy is that of counting each element only once. Here, sections were selected for sampling at nominal intervals of 800 micrometers. No element measured had a diameter of that magnitude. Further, to avoid overestimating the density of the cells within the sample fields, the Abercrombie method was used (Abercrombie, 1946). This correction was needed because some of the counting elements, the nucleoli, could occasionally be cut at the surface of the section. Where that occurs, the volume which encompasses the nucleolus includes part of the neighboring tissue as well as the section in which it is counted. Without adjusting the sampled section thickness by twice the radius of the nucleolus, the nucleolar density, which is equivalent to cell density, would be overestimated.

Synapses in the Developing Subthalamic Nucleus

The present study utilized a stereologic method for the quantitative analysis of synaptic contacts. This approach was deemed necessary because otherwise in any given sample of synaptic profiles cut from a mixed population of synaptic plaques, the relative proportion of the largest plaques are underestimated. Indeed, shorter profiles may represent multiple eccentric cuts from larger synaptic plaques. If the mean diameter of the profiles is calculated, it will be less than the mean diameter of the synaptic plaques because

it will be derived from the the more numerous eccentric sections rather than from the synaptic plaques themselves. The Coupland method of stereologic analysis (Coupland, 1968) as used in this investigation, results in the grouping of synaptic profiles on the basis of size and the subsequent correct attribution of these profiles to the size interval of synaptic plaques of which they are true members. With this procedure, it is found that most synaptic plaques in the developing subthalamic nucleus have a diameter of 0.4 micrometers or less. Although the mean values do not increase monotonically, the smallest synaptic diameter is found in the neonate and the largest in the 16-week old monkey.

A major finding of the present study is the marked drop in the number of synapses in the subthalamic nucleus. The decline in synapse number is precipitous during the second month and continues at a lesser rate thereafter. The result is that the number at 16 weeks is only half that seen at birth. Whereas both mature synapses, which show vesicles adherent to the presynaptic membrane, and immature synapses are eliminated, the patterns of change differ. Immature synapses sharply decline between four and eight weeks and then increase slightly thereafter. Mature synapses, on the other hand, show the steepest decrease after four weeks, a trend which continues, possibly beyond the period of study. The total area of synaptic plaques within the subthalamic nucleus similarly declines after the first postnatal week.

Synapse elimination during the early postnatal period has also been found in the lateral geniculate nucleus of macaques (Holstein et al, 1985). In a quantitative electron microscopic study which included as subjects the three youngest monkeys used in the present analysis of the subthalamic nucleus, significant elimination of synapses made by retinal terminals was evident in both the magnocellular and parvocellular geniculate laminae. The effect was maximal in the parvocellular region but the steepest decline occurrred during the first month after birth. It appears that the loss of synaptic contacts takes place in motor structures later than in sensory systems suggesting a longer period of reorganization (plasticity?) in nuclei related to the control of movement. It should be noted that microdissection of the subthalamic nucleus was undertaken without regard to possible regional differences in the structure, and consequently it was not possible to determine whether there were differences in relative elimination of synapses in the magnocellular and parvocellular areas of this nucleus.

Both synaptogenesis and synapse elimination during development have been found in the central nervous systems of many species, including man. For example, in kitten, synapse density increases in the caudate nucleus during the first postnatal month; the greatest proportion of this occurs during the first week of life (Adinolfi, 1977). In macaque, a comparison of one week old and adult neostriatum

shows both an increase in the density of synapses and elimination of axodendritic synapses in favor of axospinous contacts (DiFiglia, et al, 1979). In human visual and frontal cortex, two periods of age-related change in synapse density are found, the first of which, between birth and two years of age, is characterized by synaptogenesis; the second consists of synapse elimination which continues into adulthood (Huttenlocher, DeCourten, Garey, and van der Loos, 1982). Synapse elimination has also been reported in kitten spinal cord (Ronnevi and Conradi, 1974), in cat visual system (Cragg, 1975), rabbit visual and motor cortex (Vrensen, deGroot, and Nunez-Cardozo; 1977) as well as in lateral geniculate nucleus (Holstein, et al, 1985) and visual cortex in the macaque (O'Kusky and Colonnier, 1982).

Postnatal reorganization of neuronal circuitry may result from factors which include neuronal death, synaptogenesis, and synapse elimination. Where the last is found, as in the subthalamic nucleus of infant macaques, it may reflect the loss of presynaptic and/or postsynaptic neurons, a reduction in the number of axons innervating a target cell, or a reduction in the number of contacts by a given axon, whether this be by the lessening of the numbers of boutons and/or the synapses a given bouton makes. Examination of electron micrographs used in the present study has produced evidence of reorganization within the neuropil of the infant monkey, several examples of which are illustrated in the Results section. In the youngest animal,

there are dendritic growth cones which indicate enlargement of the receptive surfaces of subthalamic neurons. In the older monkeys, there are several signs that the loss of efferent elements is in progress. Among these are myelinated axons containing degenerating material, axonal terminals with regions of hyperfilamentosis, and electron dense terminals surrounded by astroglia. The amount of axonal degeneration encountered, however, is too small to account for a 50% loss of synapses. This finding has been frequently reported (Rakic, 1985; Holstein, 1985) and, at least in the prenatal material, attributed to the quick removal of the products of degeneration. A more plausible explanation for the results in the postnatal period of the monkey subthalamic nucleus is that of the retraction and disappearance of the contact within the presynapatic terminal. In any event, synapse elimination is clearly one mechanism by which the initial redundancy of contacts within the subthalamic nucleus is reduced to permit more discrete afferent control of this structure.

Development of Movement and Changes in Morphology of the Subthalamic Nucleus

The first four postnatal weeks are a period of rapid change in both the development of movement in the infant macaque (Hines, 1942) and in the morphology of the subthalamic nucleus, one of the diencephalic structures involved in movement. During this interval, a number of reflexes achieve a mature form. Among these are placing,

stepping and righting reflexes. By the seventeenth week, the temporal limit of this study, the infant monkey moves, in many ways, as does the adult. For example, it has achieved the mature form of vertical and horizontal movement, of jumping, and of galloping. Further, it is able to perform spontaneous movements, such as picking up objects, in an adult fashion.

Clearly, the development of movement in the infant rhesus monkey is not solely dependent on the development of the subthalamic nucleus. However, it is now known that the subthalamic nucleus has the anatomical connections which would allow it to modulate the outflow of the basal ganglia system. Insofar as the maturation of movement is dependent on the maturity of this sytem, the stage of subthalamic development may play an important role. It can be hypothesized, therefore, that the alterations in volume, somal size and number, and, in particular, the synapse elimination found in this study reflect an underlying morphological reconstruction important to the development of movement control in monkey.

Future Research

The present results should be extended by replication of this study with a greater number of infant monkeys, particularly those of known gestational age. It would be especially useful to measure subthalamic volumes and cell sizes in a greater number of monkeys from which tissue is also prepared for electron microscopy. In other animals, in

a similar developmental series, cluster analyses could be repeated in both the horizontal and sagittal planes of section.

In the past, microdissection of tissue for electron microscopy was not undertaken with a view to possible regional differences in the structure. A future course of research could be directed to ultrastructural differences in the two regions during development and in the fully mature monkey as well. In addition, it may prove fruitful to determine the origin and distribution of boutons in the developing subthalamic nucleus, both within the nucleus as a whole as well as locally in the magnocellular and parvocellular regions.

Finally, where cost and availability make such research in monkey prohibitive, similar studies may be undertaken in other species. Some insight might be gained into the existence and role of regional differences in the subthalamic nucleus within the motor sytem.

Appendix 1

Linear, Areal, and Volumetric Correction Factors

Age	Animal Number	Slide	Distance (d)	Shrinkage Factors Linear (5/d)	Areal $(5/d)^2$	Volumetric $(5/d)^3$
00	869	all	3.827	1.306	1.707	2.230
00	1020	all	3.215	1.555	2.419	3.762
01	851	all	4.283	1.617	1.363	1.591
01	1018	402	3.552	1.455	2.177	3.080
04	846	all	3.911	1.279	1.635	2.090
08	847	all	4.091	1.222	1.494	1.826
08	1011	all	3.745	1.335	1.782	2.377
17	874	all	3.934	1.271	1.616	2.053

Appendix 2

Thickness of Light Microscopic Sections

Age	Animal Number	Slide	Section Thickness	Nucleolar Diameter (in um)	Adjusted Thickness
00	1020	509	41.3		
00	1020	519	32.2	2.8	35.0
00	1020	529	31.3	2.2	33.5
00	1020	539	32.8	2.6	35.4
00	869	491	35		
00	869	501	34		
00	869	511	36.5		
00	869	521	35		
00	869	531	36.5		
00	869	541	31		
00	869	551	34.5		
01	1018	392	32.3		
01	1018	402	38.8	2.9	41.7
01	1018	412	31.7		
01	1018	422	36	2.6	38.6
01	1018	432	27.6		
01	1018	442	35.2	2.3	37.5
01	851	552	31		
01	851	562	32		
01	851	572	35.5		
01	851	582	29.5		
01	851	592	35		
01	851	602	30.5		
01	851	612	31		
04	846	592	30.4		
04	846	601	50	2.5	52.5
04	846	611	31.6		
04	846	621	32.5	2.5	35
04	846	631	33.8		
04	846	641	37.8	2.3	40.1
04	846	651	33.6		

Appendix 2 (continued)

08	1011	750	29.2	2.6	31.8
08	1011	760	26		
08	1011	770	33.5	2.7	36.2
08	1011	780	33.8		
08	1011	790	37.5	2.7	40.2
08	1011	800	42		
08	847	571	35.7		
08	847	581	34.2		
08	847	591	35.8		
08	847	601	42.3		
08	847	611	33.2		
08	847	621	34.5		
08	847	631	32.5		
17	874	661	29.8	2.3	32.1
17	874	671	34.2		
17	874	681	34	2.5	36.5
17	874	691	27.2		
17	874	701	33.2	2.1	35.3
17	874	711	31.8		
17	874	721	32	2.5	34.5

Nucleolar diameter and the resultant adjusted section thickness (Abercrombie, 1946) were used in slides utilized for cell density determination. These slides and all the others served for volume estimation of the subthalamic nucleus.

Appendix 3

Division of Subthalamic Nucleus into Quadrants

For each monkey, the longest chord which divided the largest section of subthalamic nucleus into two segments of equal area (± 2%) was selected as follows:

A first line was selected by eye. The ventral half of the nucleus was measured. If this area was equal to one half of the total area of this section of subthalamic nucleus, ± 2%, it was accepted as the longest chord.

If the error was greater than 2%, three additional chords were drawn. Each of these was adjusted so as to divide the nucleus into two segments of equal area. They included a line parallel to the initial chord, one in which the medial endpoint differed from the initial estimate, and one in which the lateral end point was changed. The longest of these three lines was chosen.

A line was drawn perpendicular to the determined longest chord to divide the structure into two segments of equal area, ± 2%, in the medio-lateral plane. For each monkey, this chord and its perpendicular were superimposed on the other sections with reference to midline and adjusted so as to produce equal medial and lateral segments as well as equal dorsal and ventral segments. The total areas (A) of each quadrant were measured. The areas designated parvocellular by cluster analysis were similarly measured

and summed across sections by quadrant. The area fraction (a/A) was determined separately for the dorsomedial, ventromedial, dorsolateral and ventrolateral quadrants.

Appendix 4. Calibration of the Electron Microscope

Holder Number	Magnification			
	Expected	Observed	Factor	Print
1	6,000X	6,780X	2.62	10,000X
1	10,000X	10,246X	2.44	25,000X
2	6,000X	6,793X	2.65	18,000X
2	10,000X	10,122X	2.47	25,000X
4	6,000X	6,870X	2.62	18,000X
4	10,000X	10,246X	2.44	25,000X

Appendix 5

Number of synaptic profiles measured.

Age	Number of Pictures	Number of Profiles	Coefficient of Variation
00	24	134	0.168
01	24	91	0.164
04	30	133	0.235
08	26	106	0.231
16	29	102	0.065

Coefficient of Variation refers to the mean area fraction of synaptic profiles present in four randomly grouped sets of pictures per animal divided by the corresponding standard deviation.

Appendix 6

Characteristics of Distributions of Somal Areas

Age	N	X	SD	SEM	Skewness	Kurtosis
00	390	512	112	6	.3	.6
01	743	408	100	4	.3	.4
04	690	353	112	4	-.2	-.1
08	636	442	118	5	.0	.8
17	518	343	100	4	.2	-.1

References

Abercrombie, M. (1946). Estimation of nuclear population from microtome sections. Anatomical Record, 94, 239-247.

Adinolfi, A. M. (1977). The postnatal development of the caudate nucleus: A Golgi and electron microscopic study of kittens. Brain Research, 133, 251-266.

Adinolfi, A. M., Levine, M.S., & Hull, C. D. (1980). Early postnatal development of entopeduncular neurons and their neostriatal connections. Experimental Neurology, 70, 463-474.

Altman, J. & Dittmer, D. (1964). Biological data books. Washington: Federation of American Societies for Experimental Biology.

Armstrong-James, M. & Johnson, R. (1970). Quantitative studies of postnatal changes in synapses in rat superficial motor cerebral cortex. Zeitschrift fur Zellforschung und mikroskopische Anatomie, 110, 559-568.

Auer, J. (1956). Terminal degeneration in the diencephalon after ablation of frontal cortex in cat. Journal of Anatomy (London), 90, 30-41.

Beckstead, R. (1983). A reciprocal axonal connection between the subthalamic nucleus and the neostriatum in cat. Brain Research, 275, 137-142.

Bobillier, P., Seguin, S., Petitjean, F., Salvert, D., Touret, M. & Jouvet, M. (1976). The raphe nuclei of the cat brain stem: a topographic atlas of their efferent projections as revealed by autoradiography. Brain Research, 113, 449-486.

Brand, S. and Rakic, P. (1979). Genesis of the primate neostriatum: [^{3}H] Thymidine autoradiographic analysis of the time of neuron origin in the rhesus monkey. Neuroscience, 4, 767-778.

Brown, L. L., Makman, M. H., Wolfson, L. I., Dvorkin, B., Warner, C., & Katzman, R. (1979). A direct role of dopamine in the rat subthalamic nucleus and an adjacent intrapeduncular area. Science, 206, 1416-1418.

Carpenter, M. B. (1984). Interconnections between the corpus striatum and brain stem nuclei. Advances in Behavioral Biology, 27, 1-67.

Carpenter, M. B., Batton, R. R., Carleton, S. C. & Keller, J. T. (1981a). Interconnections and organization of pallidal and subthalamic nucleus neurons in the monkey. The Journal of Comparative Neurology, 197, 579-603.

Carpenter, M. B., Carleton, S. C., Keller, J. T., & Conte, P. (1981b). Connections of the subthalamic nucleus in the monkey. Brain Research, 224, 1-29.

Carpenter, M. B., & Carpenter, C. S. (1951). Analysis of somatotopic relations of the corpus Luysi in man and monkey. The Journal of Comparative Neurology, 95, 349-370.

Carpenter, M. B., Fraser, R. A., & Shriver, J. E. (1968). The organization of pallidosubthalamic fibers in the monkey. Brain Research, 11, 522-559.

Carpenter, M. B. & Strominger, N. L. (1967). Efferent fibers of the subthalamic nucleus in monkey. American Journal of Anatomy, 121, 41-72.

Carter, D. A. & Fibiger, H. C. (1978). The projections of the entopeduncular nucleus and globus pallidus in rat as demoncstrated by auto-radiography and horseradish peroxidase histochemistry. The Journal of Comparative Neurology, 177, 113-124.

Chang, H. T., Kita, H., & Kitai, S. T. (1983). The fine structure of the rat subthalamic nucleus: an electron microscopic study. The Journal of Comparative Neurology, 221, 113-123.

Chang, H. T., Kita, H., & Kitai, S. T. (1984). The ultrastructural morphology of the subthalamic-nigral axon terminals intracellularly labeled with horseradish peroxidase. Brain Research, 299, 182-185.

Coupland, R. (1968). Determining sizes and distribution of sizes of spherical bodies such as chromaffin granules in tissue sections. Nature, 217, 384-388.

Courville, C. (1971). Birth and brain damage. Pasadena: Margaret Farnsworth Courville.

Cragg, B. G. (1974). Plasticity of synapses. British Medical Bulletin, 30, 141-144.

Dekaban, A. (1970). Neurology of early childhood. Baltimore: The William and Wilkins Co.

Del Cerro, M. P., & Snider, R. S. (1968). Studies on the developing cerebellum. The Journal of Comparative Neurology, 133, 341-362.

DeLong, M., Crutcher, M., and Georgopoulos, A. (1985). Primate globus pallidus and subthalamic nucleus: functional organization. Journal Of Neurophysiology, 53, 530-543.

Deniau, J. M. , Hammond, C., Chevalier, G., & Feger, J. (1978). Evidence for branched subthalamic nucleus projections to substantia nigra, entopeduncular nucleus and globus pallidus. Neuroscience Letters, 9, 117-121.

DeVito, J. L. & Smith, O. A. (1964). Subcortical projections of the prefrontal lobe of the monkey. The Journal of Comparative Neurology, 123, 413-424.

DiFiglia, M., Pasik, P., & Pasik, T. (1980). Early post-natal development of the monkey neostriatum: a Golgi and ultrastructural study. Journal of Comparative Neurology, 190, 303-331.

DiFiglia, M., Pasik, T., & Pasik, P. (1979). Developmental aspects of neostriatal organization in monkeys. Applied Neurophysiology, 42, 81-83.

Engleman, L. and Hartigan, J. A. (1983). K-means clustering. In Dixon, W. J. (Ed.) BMDP statistical software. Berkeley: University of California Press, 464-473.

Feger, J. (1981). Electrophysiological studies of GABAergic neurons in the basal ganglia: nigro-collicular, nigro-thalamic, and pallido-subthalamic neurons. In DiChiara, G..P. & Gessa, G. L. (Eds.) GABA and the basal ganglia, New York: Raven Press, 321-350.

Fisher, R., Levine, M.S., Hull, C.D., and Buchwald, N. (1982). Postnatal ontogeny of evoked neuronal responses in the substantia nigra of the cat. Developmental Brain Research, 3, 443-462.

Fonnum, F., Grofova, I., and Rinvik, E. (1978). Origin and distribution of glutamate decarboxylase in the nucleus subthalamicus of the cat. Brain Research, 153, 370-374.

Glees, P. & Shephard, B. (1964). Electron microscopical studies of the synapses in the developing chick spinal cord. Zeitschrift fur Zellforschung, 62, 356-326.

Gottlieb, M.D., Pasik, P., & Pasik, T. (1985). Early postnatal development of the monkey visual system. I. Growth of the lateral geniculate nucleus and striate cortex. Developmental Brain Research, 17, 53-62.

Gottlieb, M., Pasik, T., & Pasik, P. (1980). Developmental features of dorsal lateral geniculate nucleus in monkeys. Society of Neuroscience Abstracts, 6, 662.

Gruner, J. (1970). The maturation of human cerebral cortex: An electron microscopy study of post-mortem punctures in premature infants. Biology of the Neonate, 16, 243-255.

Hammond, C., Deniau, J. M., Rizk, A. & Feger, J. (1978). Electrophysiological demonstration of an excitatory subthalamonigral pathway in the rat. Brain Research, 151, 235-264.

Hammond, C., Deniau, J. M., Rouzaire-Dubois, B., & Feger, J. (1978) Peripheral input to the rat subthalamic nucleus, an electrophysiological study. Neuroscience Letters, 9, 171-176.

Hammond, C. & Yelnik, J. (1983). Intracellular labelling of subthalamic neurons with horseradish peroxidase: computer analysis of dendrites and characterization of axonal arborization. Neuroscience, 8, 781-790.

Hamori, J. & Dyachkova, L. (1964). Electron microscope studies on developmental differentiation of ciliary ganglion synapses in chicken. Acta Biologica (Hungarian Academy of Sciences), 15, 213-230.

Hamori, J. & Somogyi, J. (1983). Differentiation of cerebellar mossy fiber synapses in the rat: a quantitative electron microscope study. The Journal of Comparative Neurology, 220, 365-377.

Harlow, H. & Harlow, M. (1965). The affectional systems. In Schrier, A., Harlow, H. & Stollnitz, F. (Eds.), Behavior of nonhuman primates. New York: Academic Press, 287-334.

Hartman-von Monakow, K., Akert, K. & Kunzle, H. (1978). Projections of the precentral motor cortex and other cortical areas of the frontal lobe to the subthalamic nucleus in monkey. Experimental Brain Research, 33, 395-403.

Hassler, R., Usunoff, K. G., Romansky, K., & Christ, J. F. (1982). Electron microscopy of the subthalamic nucleus in the baboon. I. Synaptic organization of the subthalamic nucleus in the baboon. Journal fur Hirnforschung, 23, 597-611.

Hattori, T. & McGeer, P. (1973). Synaptogenesis in the corpus striatum of infant rat. Experimental Neurology, 38, 70-79.

Hines, M. (1942). The development and regression of reflexes, postures and progression in the young macaque. Contributions of Embryology, No. 196, 30, 153-209.

Holstein, G. R. (1983). Early postnatal development of retinogeniculate termination patterns in monkeys. Unpublished doctoral dissertation, City University of New York, New York.

Holstein, G. R., Pasik, P., & Pasik, T. (1985). Early postnatal development of the monkey visual system. II. Elimination of retinogeniculate synapses. Developmental Brain Research, 20, 15-31.

Hull, C. D., McAllister, J., Levine, M. S., & Adinolfi, A.M. (1981). Quantitative developmental studies of feline neostriatal spiny neurons. Developmental Brain Research, 1, 309-332.

Huttenlocher, P. R., deCourten, C., Garey, L., & Loos, H. van der, (1982). Synaptogenesis in human visual cortex - evidence for synapse elimination during normal development. Neuroscience Letters, 33, 247-252.

Iwahori, N. (1978). A Golgi study on the subthalamic nucleus of the cat. The Journal of Comparative Neurology, 1978, 182, 383-398.

Jackson, A. & Crossman, R. (1981a). Subthalamic nucleus efferent projection to the cerebral cortex. Neuroscience, 6, 7-2377.

Jackson, A. & Crossman, R. (1981b). Basal ganglia and other afferent projections to the peribrachial region in the rat: a study using retrograde and anterograde transport of horseradish peroxidase. Neuroscience, 6, 1537-1549.

Kanazawa, I., Marshall, G. R., & Kelly, J. S. (1976). Afferents to the rat substantia nigra studied with horseradish peroxidase, with special reference to fibers from the subthalamic nucleus. Brain Research, 1976, 115, 485-491.

Kita, H., Chang, H. T., & Kitai, S. T. (1983). The morphology of intracellularly labelled rat subthalamic neurons: A light microscopic analysis. The Journal of Comparative Neurology, 215, 215-245.

Kitai, S. T. & Deniau, J. M. (1981). Cortical inputs to the subthalamus: intracellular analysis. Brain Research, 214, 411-415.

Kooy, D., van der, & Hattori, T. (1980). Single subthalamic neurons project to both the globus pallidus and substantia nigra in rat. Journal of Comparative Neurology, 192, 751-768.

Kooy, D., van der, Hattori, T., Shannak, K. & Hornykiewicz, O. (1981). The pallido-subthalamic projection in rat: anatomical and biochemical studies. Brain Research, 204, 253-268.

Kunzle, H. & Akert, K. (1977). Efferent connections of cortical area 8 (frontal eye field) in Macaca fascicularis. A reinvestigation using the autoradiographic technique. The Journal of Comparative Neurology, 173, 147-164.

Larsen, K. D. & Sutin, J. (1978). Output organization of the feline entopeduncular and subthalamic nuclei. Brain Research, 157, 21-31.

Levine, M. S., Cherubini, E., Novack, G., Hull, C. D., & Buchwald, N. (1979). Development of responses of globus pallidus and entopeduncular neurons to stimulation of the caudate nucleus and precruciate cortex. Experimental Neurology, 66, 479-492.

Marsden, C. D. (1976). Dystonia: The spectrum of the disease. In M. D. Yahr, The basal ganglia, New York, Raven Press, 351-368.

Mason, W. (1965). Effects of age and stimulus characteristics on manipulatory responsiveness of monkeys raised in a restricted environment. Journal of Genetic Psychology, 99, 301-308.

McKenzie, J. S. (1984). Structure and function of the basal ganglia: a point of view. Advances in Behavioral Biology, 27, 545-555.

Meibach, R. C. & Katzman, R. (1979). Catecholaminergic innervation of the subthalamic nucleus: evidence for a rostral continuation of the A9 (substantia nigra) dopaminergic cell group. Brain Research, 173, 364-368.

Myers, R. E. (1975). Perinatal asphyxia: The neurologist's viewpoint. In Adamsons, K. & Fox, H. A. (Eds.), Preventability of perinatal injury. New York: Liss, 59-93.

Nauta, H. J. W. & Cole, M. (1978). Efferent projections of the subthalamic nucleus: an autoradiographic study in monkey and cat. The Journal of Comparative Neurology, 180, 1-16.

Nauta, W. & Mehler, W. (1966). Projections of the lentiform nucleus in monkey. Brain Research, 1, 3-42.

Nomura, S., Mizuno, N. & Sugimoto, T. (1980) Direct projections from the pedunculopontine tegmental nucleus to the subthalamic nucleus in the cat. Brain Research, 196, 223-227.

Ohye, C., Le Guyader, C., & Feger, J. (1976). Responses of the subthalamic and pallidal neurons to striatal stimulation: an extracellular study on awake monkeys. Brain Research, 11, 241-252.

O'Kusky, J. & Colonnier, M. (1982). Postnatal changes in the number of neurons and synapses in the visual cortex (area 17) of the macaque monkey: A stereological analysis in normal and monocularly deprived animals. The Journal of Comparative Neurology, 210, 291-306.

Palkovits, M., Brownstein, M., & Saavedra, J. (1974). Serotonin content of the brainstem nuclei in the rat. Brain Research, 80, 237-249.

Pasik, P., Pasik, T., & Holstein, G. (1984). Neuron counts and synapses/neuron ratios during postnatal development. Society for Neuroscience Abstracts, 10, 669.

Penney, J. B., Jr., & Young, A. B. (1983). Speculations on the functional anatomy of basal ganglia disorders. Annual Review of Neuroscience, 6, 73-94.

Peters, A., Palay, S., and Webster, H. (1976). The fine structure of the nervous system, Philadelphia: W. B. Saunders Company.

Petras, J. (1965). Some fiber connections of the precentral and post-central cortex with the basal ganglia, thalamus and subthalamus. Transactions of the American Neurolological Association, 90, 274-275.

Phelps, P., Adinolfi, A. M., & Levine, M. S. (1983). Development of the kitten substantia nigra: a rapid Golgi study of the early postnatal period. Developmental Brain Research, 10, 1-19.

Prestige, M. C. (1974). Axon and cell numbers in the developing nervous system. British Medical Bulletin, 30, 107-111.

Purpura, D. (1975) Physiological organization of the basal ganglia. In M. D. Yahr, The basal ganglia, New York, Raven Press, 91-114.

Rafols, J. A. & Fox, C. A. (1976). The neurons in the primate subthalamic nucleus: a Golgi and electron microscopic study. The Journal of Comparative Neurology, 168, 75-112.

Rakic, P. (1977). Genesis of the dorsal lateral geniculate nucleus in the rhesus monkey: site and time of origin, kinetics of proliferation, routes of migration and pattern of distribution of neurons. Journal of Comparative Neurology, 176, 23-53.

Rakic, P. (1985). Limits of neurogenesis in the primate. Science, 227, 1054-1056.

Rakic, P., & Riley, K. (1983). Regulation of axon number in primate optic nerve by prenatal binocular competition. Nature, 305, 135-137.

Ramon y Cajal, S. (1966). Studies on the diencephalon (E. Ramon-Moliner,Trans.). Springfield: Thomas. (Original work published 1914).

Ricardo, J. A. (1980). Efferent connections of the subthalamic region in the rat. I. The subthalamic nucleus of Luys. Brain Research, 202, 257-271.

Richter, E. (1965). Die Entwichlung des Globus Pallidus und des Corpus Subthalamicum. Berlin: Springer Verlag.

Rinvik, E., Grofova, I., Hammond, C., Feger, J., & Deniau, J. M. (1979). A study of the afferent connections to the subthalamic nucleus in the monkey and in the cat using the HRP technique. Advances in Neurology, 24, 53-70.

Romansky, K., Usunoff, K., Ivanov, D., & Galbov, G. (1979). Cortico-subthalamic projection in the cat: An electron microscopic study. Brain Research, 163, 319-322.

Ronnevi, L-O. & Conradi, S. (1974). Ultrastructural evidence for spontaneous elimination of synaptic terminals on spinal motoneurons in the kitten. Brain Research, 80, 335-339.

Rouzaire-Dubois, B., Hammond, C., Hamon, B., and Feger, J. (1980). Pharmacological blockade of the globus pallidus induced inhibitory response of subthalamic cells in the rat. Brain Research, 200, 321-330.

Rouzaire-Dubois, B., Hammond, C. Yelnik, J. & Feger, J. (1984). Anatomy and neurophysiology of the subthalamic efferent neurons. Advances in Behavioral Biology, 27, 205-234.

Simonds, P. (1974). The social primates. New York: Harper and Row.

Smith, J. (1974). Pediatric neuropathology. New York: McGraw-Hill.

Sugimoto, T., Hattori, T., Mizuno, N., Itoh, K., & Sato, M. (1983). Direct projections from the centre median-parafascicular complex to the subthalamic nucleus in the cat and rat. The Journal of Comparative Neurology, 214, 209-216.

Tanaka, D., Jr., Gorska, T., & Dutkiewicz, K. (1980). Corticostriate projection patterns and synaptic morphology in the puppy caudate nucleus. Experimental Neurology. 70, 98-108.

Tuttle, L. & Satterly, J. (1925). Theory of measurement. London: Longmans.

Usunoff, K. G., Hassler, R., Romansky, K. V., Wagner, A., & Christ, J. F. (1982). Electron microscopy of the subthalamic nucleus in the baboon. II. Experimental demonstration of pallido-subthalamic synapses. Journal fur Hirnforschung (Berlin), 23, 613-625.

Von Bonin, G., & Shariff, G. (1951). Extrapyramidal nuclei among mammals. The Journal of Comparative Neurology, 94 (3), 427-438.

Vrensen, G., De Groot, D., & Nunes-Cardozo, J. (1977). Postnatal development of neurons and synapses in the visual and motor cortex of rabbits: a quantitative light and electron microscopic study. Brain Research Bulletin, 2, 405-416.

Whittier, J. R. & Mettler, F. (1949). Studies on the subthalamic nucleus of the rhesus monkey. The Journal of Comparative Neurology, 10, 281-318.

Yelnik, J. & Percheron, G. (1979) Subthalamic neurons in primates: a quantitative and comparative analysis. Neuroscience, 4, 1717-1743.